
OUT-OF-PLANE BUCKLING BEHAVIOUR OF STEEL MEMBERS WITH ROTATION AND WARPING RESTRAINTS



Graz University of Technology

Technische Universität Graz

MASTERARBEIT

von

ZOLTÁN FEHÉR

Eingereicht an der
Fakultät für Bauingenieurwesen der
Technischen Universität Graz

Institut für Stahlbau

Betreuer:

Univ.-Prof. Dipl.-Ing. Dr.techn. Harald Unterweger

mitbetreuender Assistent:

Dipl.-Ing. Dr.techn. Andreas Taras

Graz, im Juni 2012

STATUTORY DECLARATION

I declare that I have authored this thesis independently, that I have not used other than the declared sources/resources, and that I have explicitly marked all material which has been quoted either literally or by content from the used sources.

.....

date

.....

(signature)

ABSTRACT

The present thesis deals with the numerical modelling and analysis - through parametric studies - of the out-of-plane buckling behaviour of steel members (columns, beams and beam-columns) under realistic, non-hinged support conditions. The studied members are loaded under compression (N) or compression and bending (N + M_y).

The main objective is the discussion of the out-of-plane flexural and lateral-torsional buckling resistance of steel members with I sections and additional rotational and/or warping restraints at the member ends. The most important design formulae that concern these failure modes in the structural steel design code Eurocode 3 (EC3) are derived for the case of “pin-ended” members, in which the rotation and the warping of the two ends is not restrained. In practical design, there are several situations in which the support conditions are quite different from this “standard case”. The applicability of the standard design rules – with modifications to these “realistic” boundary conditions - therefore had to be checked.

The aim of this work is therefore the study and analysis of the “realistic” buckling behaviour of members with rotation and/or warping fixations at the member ends by means of numerical (FEM) modelling by using the software ABAQUS.

The most important parts of the thesis are the presented comparisons between the GMNIA- (geometrically and materially non-linear analyses with imperfections) and LBA- (linear buckling analyses) results and the calculations according to the current EC3 design code. The comparison between the numerical results and the EC3 - rules for these cases shows new perspectives of code development (since in many cases the code is conservative), or shows limits of application of the code (in the cases where the code is “unconservative”).

In the comparisons with the EC3 - rules, the main focus is put on the “interaction formulae” of EN 1993-1-1 for members loaded under N + M_y. However, also the so-called “Overall” or “General Method”, which is an alternative approach in EC 3, is taken into account.

Additionally, the topic of the determination of the critical bifurcation bending moment M_{cr} and the corresponding slenderness $\bar{\lambda}_{LT}$ by means of simple hand formulae detected in the literature (with the “C₁” or “k_c” factors) is also treated extensively in this thesis.

The last two chapters contain small studies about the new design proposal for LT-buckling developed at Graz University of Technology and about the additional warping stresses at the restrained end sections, which are relevant for joint design.

KURZFASSUNG

Diese Masterarbeit behandelt die numerische Modellierung und Analyse des Stabilitätsverhaltens von Bauteilen aus Stahl (Stützen, Träger) aus der Ebene unter realen, nicht gelenkigen Auflagerbedingungen, mittels umfangreicher Parameterstudien. Die Bauteilbelastung umfasst dabei reine Normalkrafts- sowie Normalkrafts- und Biegebeanspruchung ($N + M_y$).

Das Hauptziel ist die Analyse der Traglast bei Biegeknickversagen aus der Ebene sowie bei Biegedrillknickversagen der Bauteile mit I-Querschnitt und zusätzlichen Rotations- und/oder Verwölbungsbehinderungen an deren Endquerschnitten. Die wichtigsten Bemessungsformeln im Eurocode 3 (EC3), die diese Stabilitätsfälle abdecken, wurden für den Fall mit beidseitiger gelenkiger Gabellagerung hergeleitet. Dabei sind die Rotation und die Verwölbung bei den Endquerschnitten nicht hinderlich. In der Praxis gibt es viele Fälle, in denen die Randbedingungen von diesem „Standardfall“ abweichen. Die Anwendbarkeit der EC3 Formeln für diese Fälle sollte daher überprüft werden.

Das Ziel dieser Arbeit ist demnach die Analyse des „realen“ Stabilitätsverhaltens von Bauteilen mit Rotations- und/oder Verwölbungsbehinderungen an den Endquerschnitten durch numerische (FEM) Modellierung mit dem Programm ABAQUS.

Die wichtigsten Teile der Masterarbeit sind die Vergleiche zwischen den GMNIA- (geometrisch und materiell nichtlineare Analyse mit Imperfektionen) und LBA- (lineare Beul- bzw. Knickanalyse) Ergebnissen und den Berechnungen nach der gültigen Bemessungsnorm EC3 für den Stahlbau. Die Vergleiche zwischen numerischen Ergebnissen und EC3-Regeln für diese Fälle zeigen neue Perspektiven der Normenweiterentwicklung auf (wenn die Norm konservativ ist), bzw. weisen auf die Grenzen der Anwendung der Norm hin (wenn die Norm „unkonservativ“ ist).

Bei den Vergleichen mit den EC3 - Regeln liegt der Schwerpunkt bei der „Interaktionsformel“ für Beanspruchungen aus Normalkraft N und Biegemoment M_y . Zusätzlich wird auch die sogenannte „Overall -“ oder „General Method“, welche im EC 3 als alternatives Nachweisformat enthalten ist, mit untersucht.

Das Thema der Berechnung des kritischen idealen Biegedrillknickmomentes M_{cr} und der zugehörigen Schlankheit $\bar{\lambda}_{LT}$ durch einfache Handformeln aus der Literatur (mit „ C_1 “ oder „ k_c “ Faktoren) wird auch umfassend behandelt.

Die zwei letzten Kapitel enthalten kleinere Studien über den neuen Bemessungsvorschlag für Abminderungskurven für das Biegedrillknicken, der an der TU Graz entwickelt wurde, sowie über die zusätzlich auftretenden Wölbnormalspannungen an den Bauteilenden mit Endeinspannungen, die für die Bemessung der Verbindungen von Bedeutung sind.

Acknowledgements

I would to express my gratitude to my thesis supervisor, Prof. Dr. Unterweger, who gave me the possibility to complete this thesis. It was a great honor for me to write this thesis at the Institute for Steel Structures of Graz University of Technology.

I am deeply indebted to my co-advisor, Dr. Andreas Taras, whose enduring patience, help – especially in the introduction to ABAQUS -, stimulating suggestions and encouragement helped me in all the time of work for and writing of this thesis.

I would like to thank the colleagues at the Institute for all their help, useful hints and the friendly and tolerant atmosphere.

My appreciation goes to my friend and fellow student, Simon Hafner for his creative comments and for the valuable discussions during the work.

I am very thankful to all my friends in Graz and in Hungary for their help and encouragement through these years.

Finally, I would like to give my special thanks to my parents, Ilona und László, my family and my girlfriend, Viktória. Their love, support, patience and encouragement helped me to fulfil my dream.

Table of contents

ABSTRACT.....	3
KURZFASSUNG.....	4
Acknowledgements.....	3
Table of contents.....	6
1. Introduction	8
1.1. Motivation and objective	8
1.2. Organization.....	12
2. Methodology	14
2.1. Basics of Finite Element Method.....	14
2.2. Types of calculations	15
2.3. Influences of structural parameters	16
2.4. ABAQUS models.....	18
3. Elastic critical moment M_{cr} (LBA)	21
3.1. Factors k and k_w	22
3.2. Factor C_1	22
3.3. Conclusions.....	39
4. Flexural Buckling (pure compression, GMNIA)	40
4.1. Elastic Bifurcation and Eurocode 3 Design Rules	40
4.2. GMNIA Buckling Curves	41
4.3. Conclusions.....	45
5. Lateral-Torsional Buckling (pure bending, GMNIA).....	46
5.1. GMNIA analyses for different cases of support conditions.....	49
5.2. GMNIA buckling curves for the support condition $k=0,7$ $k_w=0,7$	56
5.3. GMNIA analyses for cases with equal slenderness for LTB.....	64
5.4. Conclusions.....	65
6. Interaction concept for beam columns (compression and bending, GMNIA)	66
6.1. Interaction factor k_{LT}	68
6.2. Plotting the n-m interaction curves according to EC3	68
6.3. Input and output of GMNIA for beam-columns	69

6.4.	GMNIA analyses for beam-columns	71
6.5.	Conclusions.....	87
7.	Overall concept (compression and bending, GMNIA).....	88
7.1.	Background of the overall concept.....	88
7.2.	Plastic resistance for N+M according to EC3	91
7.3.	Plastic resistance according to MNA analyses.....	98
7.4.	Conclusions.....	102
8.	New Proposal for χ_{LT} for Hot-Rolled Sections.....	103
9.	Additional bimoment caused by warping fixation	109
10.	Summary and conclusions.....	115
10.1.	Outlook	117
11.	References	118

1. Introduction

1.1. Motivation and objective

The main topic of this thesis is the out-of-plane flexural and lateral-torsional buckling resistance of steel members with I sections and rotational and/or warping restraints at the member ends. The most important design formulae that concern this failure mode in the structural design code Eurocode 3 are derived for the case of “pin-ended” members, in which the rotation and the warping of the two end are not restrained. In the practical design, there are several situations in which the support conditions are quite different from this “standard case”.

In recent times – thanks to the improvement of computational science –numerical modelling techniques have provided a valid alternative to the classical experimental procedures used in the structural engineering science; thereby, the most common analysis method is the **Finite Element Method (FEM)**.

The **aim** of this work is the study and analysis –by means of the FEM- of the “realistic” buckling behaviour of members with rotation and/or warping fixations at the member ends through numerical modelling (Fig. 1).

The **comparison** between the numerical results and the EC3 rules for these cases can show new perspectives of code developments (if the code is conservative), or it can show limits of application of the code . (if the code is “unconservative”).

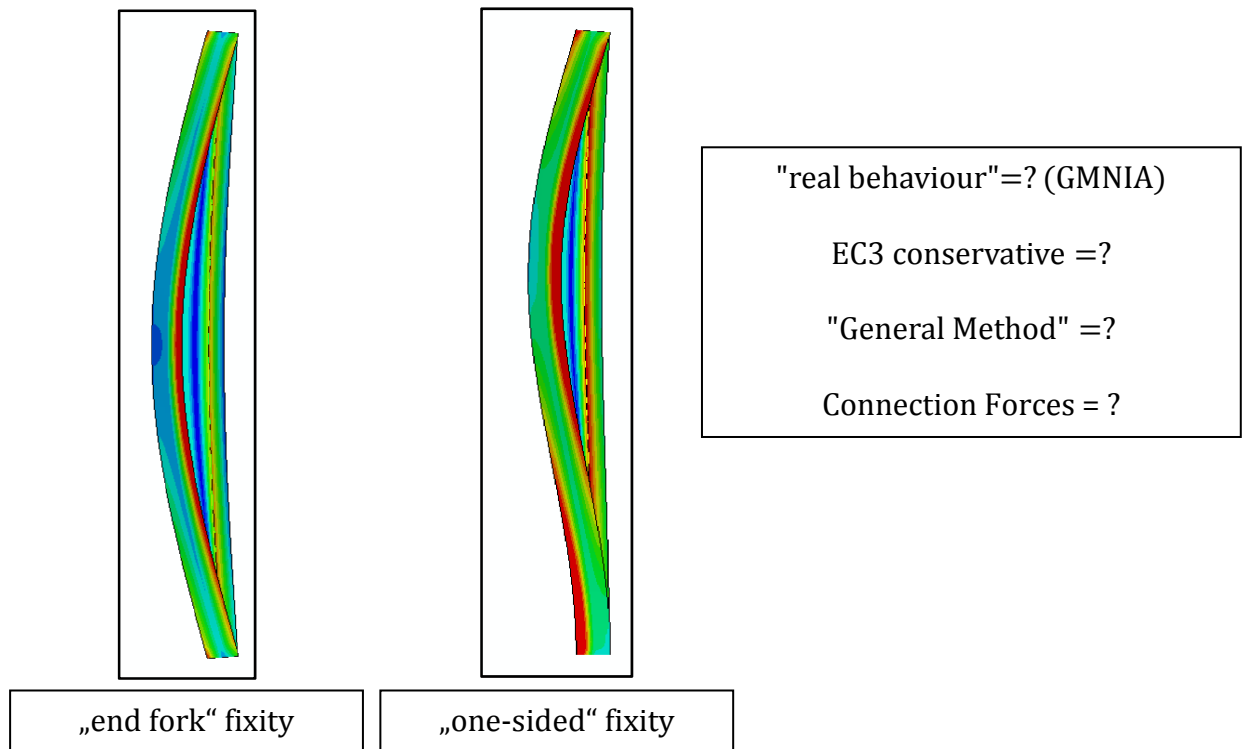


Fig. 1: Motivation of the thesis work

In the comparisons with the Eurocode rules, the main focus was put on the “interaction formulae” of section 6.3.3. of EN 1993-1-1. However, also the so-called “Overall” or “General Method”, which is included in one possible form of presentation in EN 1993-1-1, section 6.3.4, is taken into account.

Additionally, the topic of the determination of the critical bifurcation bending moment M_{cr} and the corresponding slenderness $\bar{\lambda}_{LT}$ by means of simple hand formulae (with the “ C_1 ” or “ k_c ” factors) is also treated extensively in this thesis.

For the identification of the studied case of end fixity, the following naming convention was used, in accordance with most literature on the topic [1][2]

- A **rotational fixity** about the z-z axis is denoted by the letter “**k**” and by a number that indicates the out-of-plane flexural buckling length for this case: e.g. $k=0.7$ indicates a rotational fixity about the z-axis at one end of the member, while $k=0.5$ would indicate a fixity at both member ends.
- A **warping impediment** is similarly represented by the letters “**k_w**”. Thus, $k_w=0.7$ would mean that warping is prevented at one end of the member.
- Note that the degree of fixation about the *strong* axis is practically irrelevant for the studied problem, as failure occurs about the weak axis in all studied cases.

Both factors vary from 0,5 for full fixity (restrained deformations) to 1,0 for no fixity (free deformations), and are equal to 0,7 in the case of one end fixed and one end free.

The following figure (Fig. 2) schematically shows three detail examples of a column which are used to visualize possible criteria for the selection of the factors k and k_w . The top end of the column is free (rotation as well as warping) in all cases.

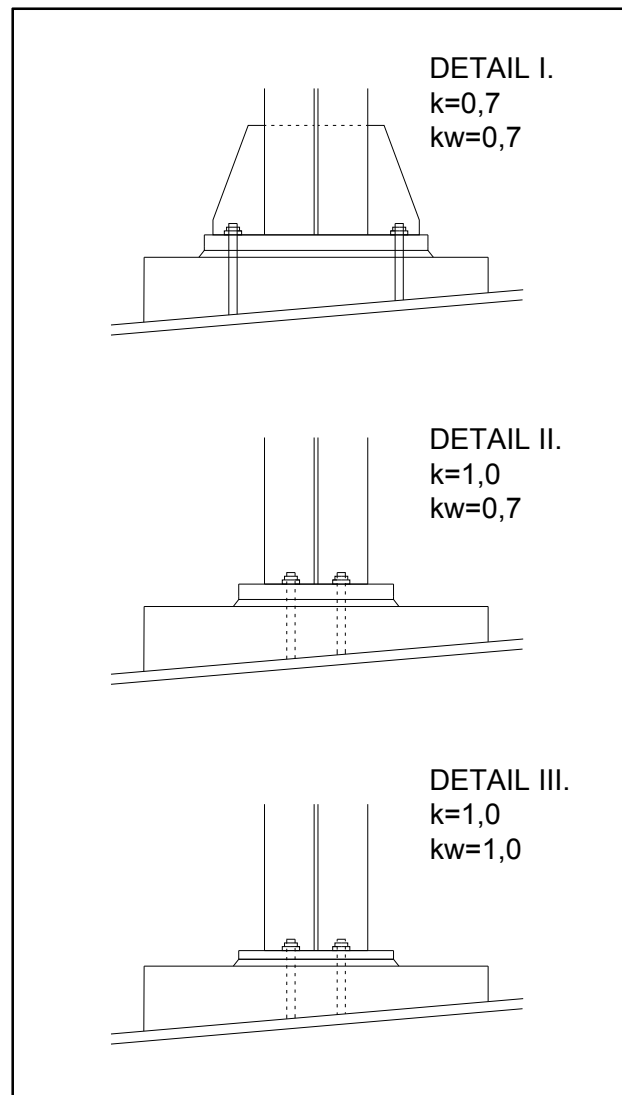


Fig. 2: Construction details of column bottoms under different support conditions

In detail I, the rotation about the weak (z-z) axis of the bottom section is restrained by the stiffeners and the anchor bolts, and the warping is also restrained by the relatively thick end plate. ($k=0,7$ and $k_w=0,7$)

In detail II, the rotation of the bottom section is only partially restrained due to the positioning of the anchor bolts and the deformability of the concrete layer underneath the end plate; conservatively, a factor of $k=1,0$ can be used for these conditions. However, warping of the end section is restrained by the thick end plate again. In this case the end section is able to rotate about the weak axis z, but it stays in plane. ($k=1,0$ and $k_w=0,7$)

In detail III, the rotation and the warping is also not restrained, because in addition to being able to rotate, the section will also feature some warping at the bottom section due to the the relatively thin end plate.

Finally, the consideration of end fixations in design against out-of-plane buckling, - while clearly advantageous for member design-, also raises the question of how to design the end connections/joints; due to the fixation, new stresses are caused in the joints (welds, bolts, etc.) which should then coherently be considered in design. The developing stresses are therefore also studied in this thesis.

Not all effects of member end fixations are explicitly omitted in the Eurocode design rules. Tab. 1 summarizes the main relationships of out-of-plane buckling design with the support conditions, stating whether or not out-of-plane fixations can be included or not in the determination of certain quantities. These points will be discussed more precisely in the following chapters.

Tab. 1: Influence of support conditions on the calculations

Taking into account the support conditions (rotation and warping) in...	
$N_{cr} \rightarrow \bar{\lambda}_z$	✓
$M_{cr} \rightarrow \bar{\lambda}_{LT}$	✓
$\bar{\lambda}_{LT} \rightarrow \chi_{LT}$?
N+M interaction	✗

In summary, providing some answers to the following questions and problems constituted the main **objective** of this thesis work (Fig. 3.):

- What kinds of influences do the boundary conditions have on the **elastic critical moment**? Is it possible to use classical “hand formulae” to calculate the critical LT buckling moment e.g. for end fixations $k=0,7$ $k_w=0,7$? If it is possible, how accurate is it?
- How does the **flexural buckling** strength change under support condition $k=0,7$ $k_w=0,7$? Are the “original” European flexural buckling curves compatible with other support conditions? Does the warping fixation have any effect on the flexural buckling behaviour?
- Is there any beneficial effect from the restraint of rotation and warping for cases of **lateral-torsional buckling** under bending alone? Is the use of the so-called “f-factor” in section 6.3.2.3 of EN 1993-1-1, which accounts for the effects of the bending moment diagram on the buckling reduction factor still accurate under different support conditions? Are the original LT-buckling curves compatible with other loading and support conditions?
- Are the **interaction formulae** for beam-columns ($N+M_y$) according to EC3 conservative for other boundary conditions of beam-columns ($k=0,7$ $k_w=0,7$ or

$k=1,0$ $k_w=0,7$)? Is the interaction factor k_{LT} correct for different boundary conditions?

- What are the main differences between the **overall concept** (“general method”, using an “overall” buckling reduction factor χ_{op} for out-of-plane failure) and the classical interaction concept? Do the values of buckling strength according to the overall concept fit better to the modelling results than in the case of the interaction concept?
- How high are the **strains/stresses in the end connections** of the members if end fixations are considered in design, and which support conditions generate them? Can the stresses be calculated “correctly” or safely approximated?

$M_{cr}/C_1 = ?$
$\chi_z = ?$
$\chi_{LT} = ?$
f – factor = ?
$k_{LT} = ?$
$\chi_{op} = ?$

Fig. 3: Objectives of the thesis work

1.2. Organization

The following paragraphs explain how this thesis was organized.

Following this introductory chapter, **Chapter 2** summarizes the basics of FEM, describes the types of the calculations and introduces the methodology of the modelling process.

The object of the first studies performed for this thesis was the calculation of the elastic critical moment M_{cr} according to several formulae in the literature under different loading and support conditions. The calculations using the formulae were compared to modelling results from the softwares ABAQUS and LTBeam, which are given in **Chapter 3**.

Chapter 4 focuses on the flexural buckling strength under different boundary conditions. In this part, the first GMNIA results are analysed and compared to the buckling curves of EC3.

One of the most important parts of this thesis is **Chapter 5**, which deals with lateral-torsional buckling under M alone. First of all, the main rules and factors according to EC3 are introduced. Afterwards, several parametric studies were carried out for two different sections, for three different support conditions and for five bending moment diagrams. In many comparison diagrams, the GMNIA results and buckling curves for LTB are discussed, and special attention is given to the influence of the support and loading conditions on the buckling strength.

Chapter 6 is concerned with the interaction concept, which is used for the design of beam-columns. After the summary of the EC3 formulation for beam-columns, the interaction curves obtained from numerical modelling results are discussed with regard to the topic of non-hinged support conditions. Two different sections were studied for three slendernesses, for three different support conditions and for three different loading conditions.

Chapter 7 focuses on the overall concept (“general method”), which is the other method given in Eurocode 3 for the out-of-plane buckling design of beam-columns. The chapter contains the main formulation and rules according to EC3, and some comparison were carried out with the GMNIA results of Chapter 6. Additionally, it discusses the differences between the results of the two design concept of beam-columns.

In **Chapter 8** a new design proposal for χ_{LT} , recently developed at Graz University of Technology, is introduced and compared to modelling results for some loading cases.

Chapter 9 contains a brief study about the additional stresses caused in the end connections by the rotation and warping fixations, in which a simple formula for the estimation of the additional “flange moments” $M_{z,fl}$ is compared to the moment obtained in the FEM calculations.

Finally, in **Chapter 10** the summary and conclusions of the thesis work are given.

2. Methodology

2.1. Basics of Finite Element Method

This part is a brief overview in the Finite Element Method (FEM) and in the most important terms.

In FEM, the structure is divided into small (finite) elements. For all of these elements there is a locally defined shape function, which determines the modes of deformation (and the degrees of freedom) in the element. The parameters that determines the correct combination of these shape functions are the node displacements of the elements. These (unknown) parameters (node displacements) are determined by the configuration of the sum of the system's internal and external potential energy, which is zero [3] [4] [5].

$$\Pi = \Pi_i + \Pi_e = 0 \quad (0.1)$$

After the calculation of the node displacements, the strains and stresses can be determined by the appropriate constitutive relationships between deformations and strains, and strains and stresses [4].

In every FEM model, the geometry of the structure is defined by **nodes**. After the node definition the following step is the selection of **elements**.

There are several types of elements [3]. The following types were used in the structural models created for this thesis:

- beam elements: elements in which one dimension, the length, is significantly larger than the other dimensions.
- shell elements: elements in which one dimension, the thickness is significantly smaller than the other dimensions and stresses exist only in plane (plane stress state).
- couplings (special elements): elements which constraint the deformations of specific nodes to a rigid body deformation of another reference node.

2.2. Types of calculations

The following types of analyses were employed in this thesis.

LBA: Linear Buckling Analysis (or Linear Bifurcation Analysis) is a linear elastic and geometrically linear eigenvalue analysis, in which the critical bifurcation loads (e.g. N_{cr} , M_{cr}) are determined. Theoretically there are infinite numbers of eigenvalues, but the main value of interest was always the first eigenvalue in this thesis work.

First of all the results of LBA analyses were used as basis for the non linear (GMNIA) analyses, in which the shape of the first buckling eigenmode represented the form of the geometrical imperfections. In addition, the correct value of the critical elastic bifurcation load was retrieved as well – especially for beams and beam-columns- in order to calculate the correct member slenderness with the use of LBA analyses.

MNA: Materially Non-linear Analysis is a type of analysis, in which the non-linear material behaviour of steel is considered (“plastic analysis”), but not the geometric non-linearities. In this thesis, the material was always considered to have an elastic-perfectly plastic bilinear stress-strain curve with a specific yield stress and -after reaching the yield stress- a perfectly plastic behaviour.

In MNA analyses, the member is geometrically perfect and no residual stresses are taken into account, therefore MNA can be used for the calculation of the plastic cross sectional resistance.

GMNIA: Geometrically and Materially Non-linear Analysis with Imperfections were used for modelling the elasto-plastic buckling behaviour. In geometrical non-linearity, the connection is not linear between applied loading and deformation, and equilibrium is determined for the deformed structure. In GMNIA models, the geometrical (shape deviations) and the structural (residual stresses) imperfections have to be represented as well. [6] [7]

Based on the results of GMNIA analyses, the ultimate buckling strength can be obtained, and the values represent the realistic behaviour of the member under the studied, specific boundary (support and loading) conditions.

2.3. Influences of structural parameters

Imperfections:

Depending on the fabrication technology, there are some imperfections (out-of-straightness) in all structural members, hence the **geometrical imperfections** of the structure have to be considered. The amplitude of these imperfections was assumed to be equal to $L/1000$ at the compression flange (Fig. 4). This value of imperfection was chosen following the recommendations of ECCS [8], note that the same values formed the basis for the development of the European buckling curves.

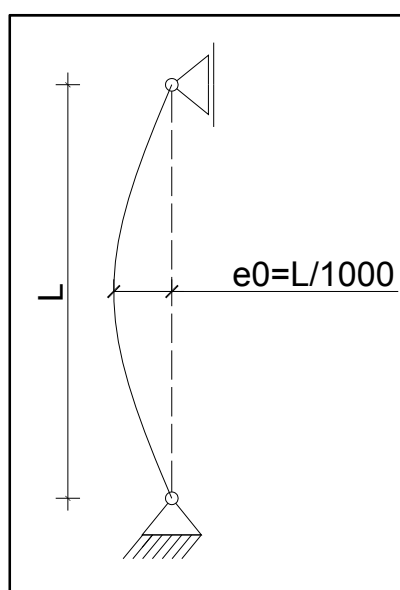


Fig. 4: Magnitude of geometrical imperfections in GMNIA models

Because of the influence of welding or hot-rolling procedures there are some **material imperfections, i.e. residual stresses**, in all structural members. The residual stresses cause an initial stress state in the sections, but the member is in equilibrium, of course.

The magnitude of the residual stresses is smaller for hot-rolled sections and higher for welded sections. In cases of I and H sections the residual stresses are positive (tension) in the connections of web and flanges and negative (compression) in the edges of the flanges and in the middle of the web.

The residual stresses were assumed to reach values of $0,3 \cdot f_y$ or $0,5 \cdot f_y$ depending on the depth to width ratio of the sections, following the provision given by ECCS (Fig. 5) [8].

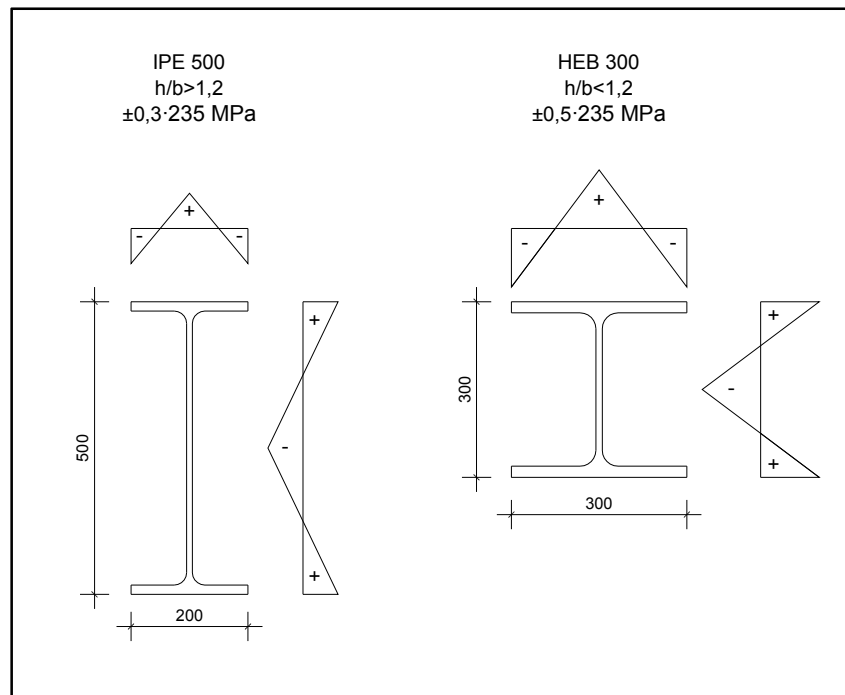


Fig. 5: Magnitude and distribution of residual stresses in GMNIA-models

Yield stress and strain hardening:

All calculations were carried out with the steel material S235, which has a **yield stress** of $f_y=235 \text{ N/mm}^2$.

Theoretically, the **strain hardening** (higher stresses than the yield stress) of the material could be used under large strains, see Fig. 6. Previous experience has shown that there would be no beneficial effect based on the assumption of strain hardening, because the deformation of the structure is not so high at the ultimate limit state in buckling problems that the strains could reach the limit for strain-hardening.

Based on this the strain hardening of the material were neglected in all calculations.

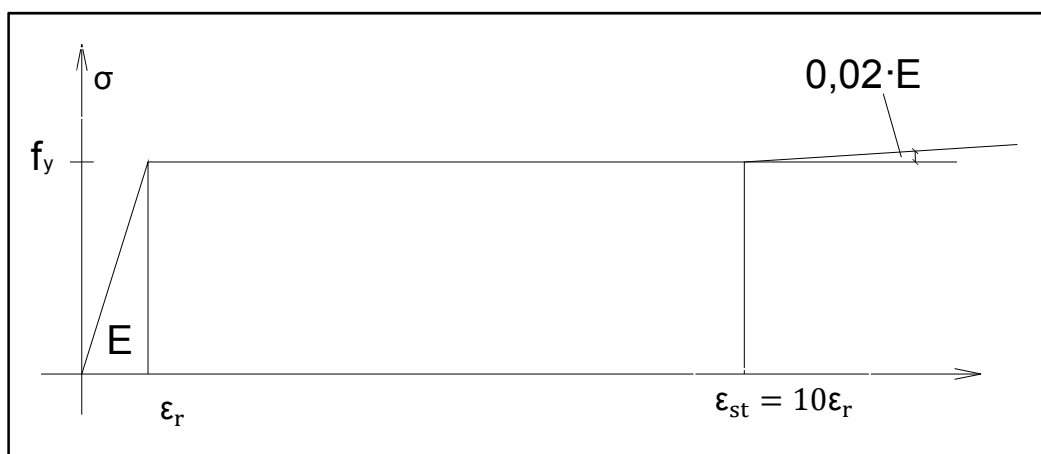


Fig. 6: Stress-strain curve of steel with strain-hardening effect

2.4. ABAQUS models

Sections:

The parametric studies in the thesis work were carried out for two different sections. The first section was the **European IPE 500 beam section** and the second was the **European wide flange HEB 300 beam section**, the shape and the dimensions of the sections are shown in Fig. 7.

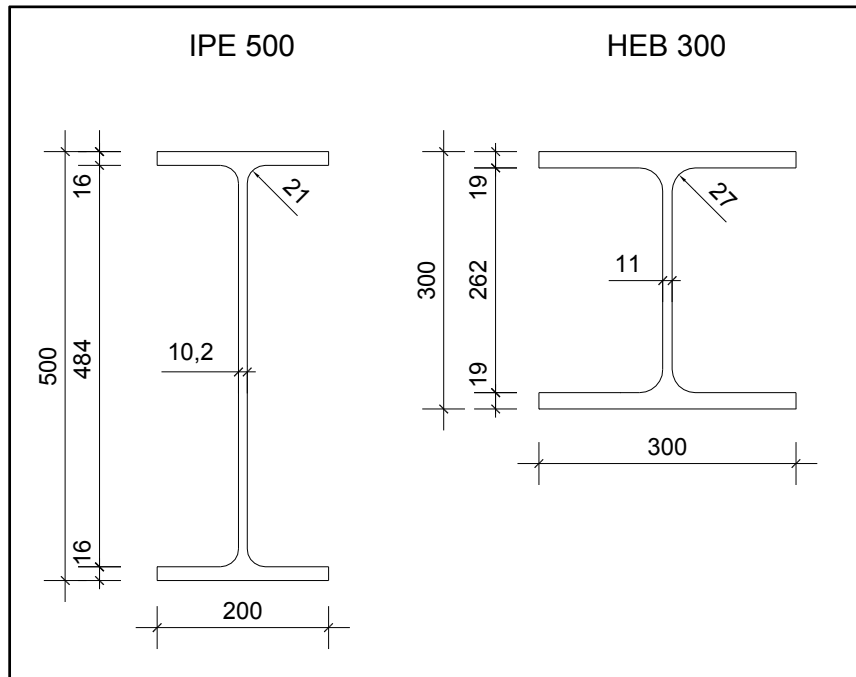


Fig. 7: Applied sections in ABAQUS-models

Elements:

In Fig. 8. the structure of the ABAQUS-model is illustrated. The two flanges and the web were defined as type **S4 shell elements**, which is a fully integrated, general-purpose, finite-membrane-strain shell element with 4 nodes [4].

The flange-web connection was modelled with rigid **tie couplings** along the whole member.

The fillet radius was substituted by a type **B31 beam element** with quadratic hollow section. Type B31 is a Timoshenko beam - which allows transverse shear deformation-in space with linear formulations [4]. The dimensions of the quadratic hollow section were so calculated that the area (A) and the torsional constant (I_t) of the section is equal to the area and torsional constant of two fillet radiuses of the detail (two beam sections per model).

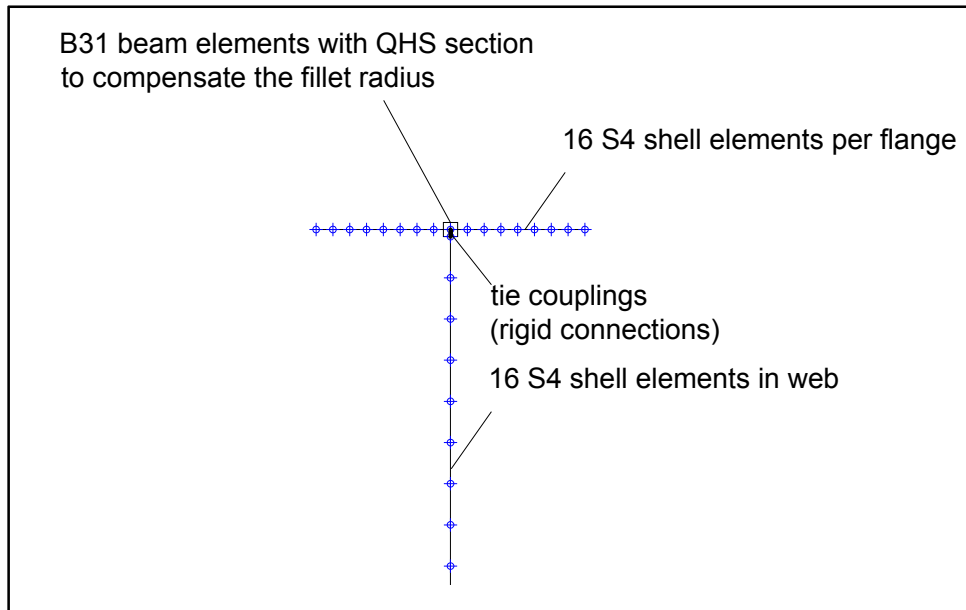


Fig. 8: Structure of the numeric model

One of the most important parts of the model was the definition of the support conditions at the two ends of the member.

The **rotation conditions** were defined directly in the **boundary conditions** (for example for the case $k=0,5$, the rotation about the weak axis was defined to be zero at both ends)

The **warping conditions** were defined with the use of **kinematic couplings**. For the case without warping all the elements of the section have to be coupled to the displacements and rotations of the middle point in the section. In order to have an end section with warping, the displacements of the flanges have not to be coupled to the rotations about the z-z- axis of the web. [4]

In Fig. 9 the kinematic couplings are represented in the end sections in case of $k_w=0,7$.

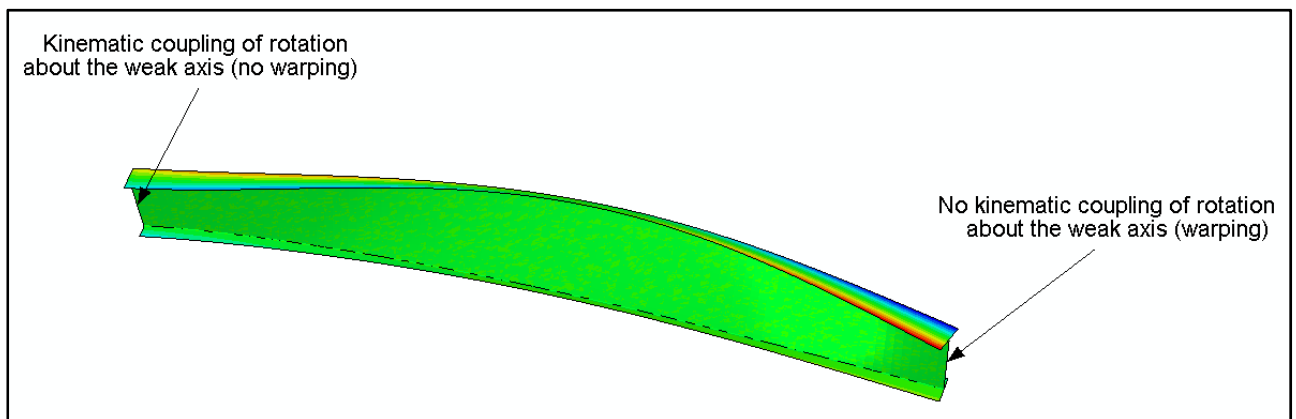


Fig. 9: Kinematic coupling in the end sections ($k=0,7$ $k_w=0,7$)

Input of geometrical imperfections:

The following procedure was used to include the geometrical imperfections in all calculations:

- Running of an LBA analysis in all cases in order to get the shape of the first eigenmode under specific boundary conditions
- Defining the imperfections by using the deformations of the member in the first eigenmode with a scaling factor of $e_0 = L/1000$ in the input file for the GMNIA analysis

Input of residual stresses:

In order to approach the linear distribution of residual stresses, an average value of initial stresses was define in every element. The stress distribution in 16 elements of the parts (flanges and web) can be considered as a good approximation (Fig. 10).

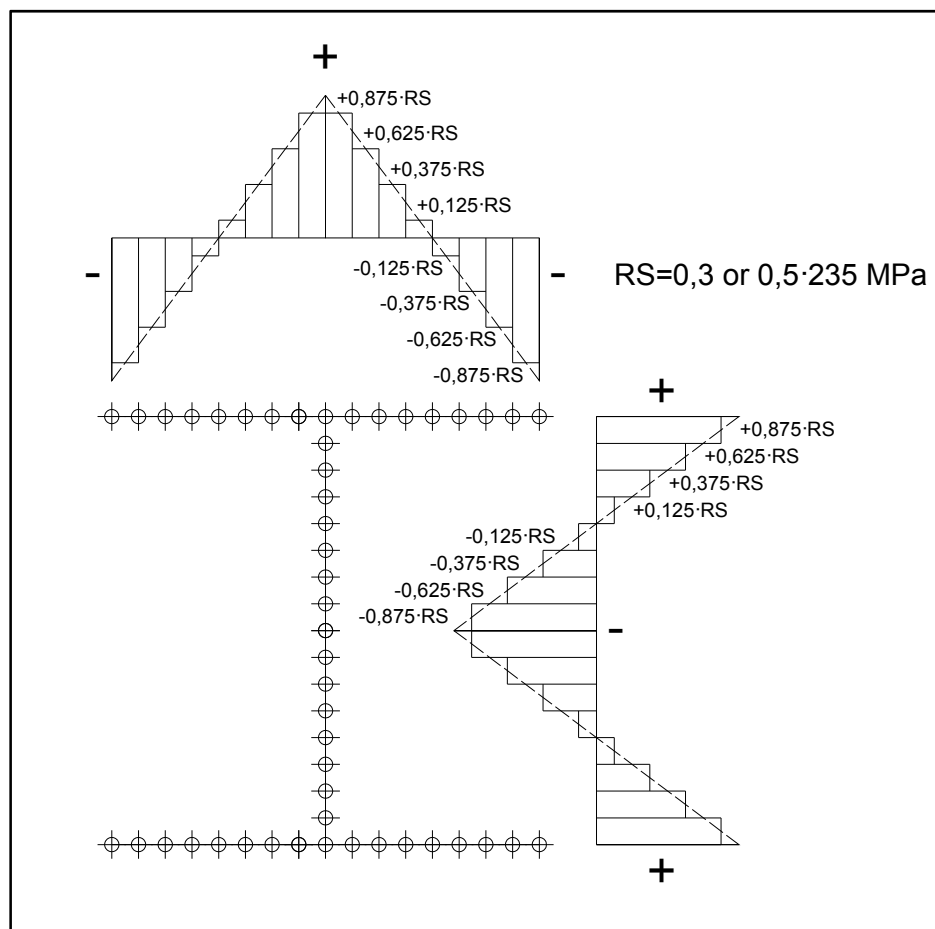


Fig. 10: Input of the residual stresses in ABAQUS-model

3. Elastic critical moment M_{cr} (LBA)

The linear elastic lateral torsional buckling (LTB) phenomenon appears under the critical moment M_{cr} about the strong axis. For beams with uniform doubly symmetric cross-section subjected to end moments or transversal loads applied in the centre of gravity of the section, the **elastic critical moment** can be estimated using the following expression [2]:

$$M_{cr} = C_1 \cdot \frac{\pi^2 \cdot EI_z}{(kL)^2} \cdot \left[\left(\frac{k}{k_w} \right)^2 \cdot \frac{I_w}{I_z} + \frac{(kL)^2 GI_t}{\pi^2 EI_z} \right]^{0,5} \quad (3.1)$$

where,

- C_1 is a coefficient depending on the loading and support conditions, the shape of the bending moment diagram and support conditions. [1]
- k and k_w are effective length factors for out-of-plane flexural buckling of the entire section and of the compression flange (“w” for “warping”).
- I_z is the second moment area about the weak axis z .
- I_w is the warping constant.
- I_t is the torsion constant.

The elementary variable that defines the susceptibility to instability of unrestrained beams is the **normalized slenderness for LTB**, which is defined as [1]:

$$\bar{\lambda}_{LT} = \sqrt{\frac{M_{pl}}{M_{Cr}}} \quad (3.2)$$

The slenderness for lateral-torsional buckling is governed by the plastic cross-sectional capacity M_{pl} and –more importantly here- the elastic critical moment M_{cr} . Thus, the calculation of the correct value of M_{cr} is crucial in LTB-problems.

3.1. Factors k and k_w

As in the Introduction was described more detailed, k and k_w factors are effective length factors that depend on the support conditions at the end sections.

The factor k refers to **end rotation** at the end sections about the weak axis z .

The factor k_w refers to **end warping** in the same cross sections.

3.2. Factor C_1

The **factor C_1** is a coefficient that depends on the shape of the bending moment diagram and support conditions (k and k_w). Different values of the factor C_1 reported in the literature are given in Tab. 2, which summarizes the values given in two codes [2][9] (ENV 1993-1-1:1992, ÖNORM B 1993-1-1) and the values given in the ECCS Design Manual [1], as well as one simple formulation that can be derived from the value of k_c given in the TU Graz lecture notes.[10]

The latter formulation comes from the equation:

$$\bar{\lambda}_{LT,non\ uniform} = k_c \cdot \bar{\lambda}_{LT,uniform} \quad (3.3)$$

where

$$k_c = \frac{1}{1,33 - 0,33\psi} \quad (3.4)$$

for end moments with ratio $\psi = M_2/M_1$, with M_1 the end moment with the largest absolute value. [10]


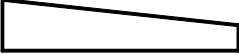
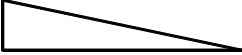
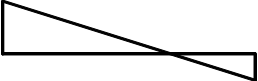
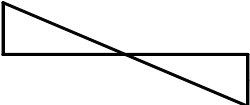
When the definition of λ in Eq. (3.2) is considered in combination with the definition of M_{cr} in Eq. (3.1), the following relationship becomes evident:

$$M_{Cr,non\ uniform} = C_1 \cdot M_{Cr,uniform} = \frac{1}{k_c^2} \cdot M_{Cr,uniform} \quad (3.5)$$

Thus, a formula for C_1 for end-moment diagrams can be expressed as

$$C_1 = \frac{1}{k_c^2} = \frac{1}{\left(\frac{1}{1,33 - 0,33\psi}\right)^2} \quad (3.6)$$

Tab. 2: Values of factor C_1 from the literature

Bending moment diagram	k	C_1			
		$1/k_c^2$	ENV	ÖNORM B (k=0.7 interpolated)	ECCS (k=0.7 interpolated)
$\psi=1.0$ 	1.0	1.000	1.000	1.000	1.000
	0.7	1.000	1.000	1.076	1.030
	0.5	1.000	1.000	1.127	1.050
$\psi=0.5$ 	1.0	1.357	1.32	1.320	1.310
	0.7	1.357	1.473	1.417	1.346
	0.5	1.357	1.514	1.482	1.370
$\psi=0$ 	1.0	1.769	1.879	1.847	1.770
	0.7	1.769	2.092	1.955	1.824
	0.5	1.769	2.150	2.027	1.860
$\psi=-0.5$ 	1.0	2.235	2.704	2.591	2.350
	0.7	2.235	3.009	2.584	2.392
	0.5	2.235	3.093	2.579	2.420
$\psi=-1.0$ 	1.0	2.756	2.752	2.733	2.600
	0.7	2.756	3.063	2.527	2.510
	0.5	2.756	3.149	2.390	2.450

Tab. 2 - as stated above - summarizes the values of C_1 found in the literature. It can be seen that the value of the factor C_1 can be different depending on the support condition, and that the difference is quite large (especially for $\Psi=-1,0$).

In this chapter, the results of several Linear Bifurcation Analyses (LBA) were carried out with the **program ABAQUS** are presented and compared with the values found in the literature. These were made in order to calculate the correct value of M_{cr} . As a result, one obtains buckling eigenvalues, which are the ratio between the critical moment M_{cr} and the load M_{Ed} .

In addition to a comparison with the values of the literature, the obtained C_1 values are compared to the results of calculations made with the **freeware software LTBeam**, developed by CTICM (Centre Technique Industriel de la Construction Métallique). LTBeam is a beam element modelling program based on the Finite Element Method, in which the user is able to define the degrees of freedom for the warping deformation and lateral flexural rotation [11]. The values of M_{cr} was obtained directly as a result.

From the “correct” values of M_{cr} (obtained from ABAQUS or LTBeam) the correct values of factor C_1 can be calculated using the formula:

$$C_{1,correct} = \frac{M_{cr,correct}}{\frac{\pi^2 \cdot EI_z}{(kL)^2} \cdot \left[\left(\frac{k}{k_w} \right)^2 \cdot \frac{I_w}{I_z} + \frac{(kL)^2 GI_t}{\pi^2 EI_z} \right]^{0,5}} \quad (3.7)$$

of course with the correct values of k and k_w (1,0 or 0,5 or 0,7) in all cases.

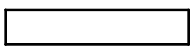
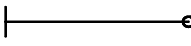
In the models for the calculation the variables were the following:

- member length
- member profile (IPE 500 or HEB 300)
- shape of the bending moment diagram ($\psi=1,0;0,5;0;-0,5;-1,0$)
- position of the bending moment (for example in case of $\psi=0$, $k=0,7$ $k_w=0,7$, there are two different cases: in the first case, the bending moment is 0 at the free end of the member and in the second it is 0 at the fix end)

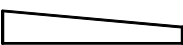
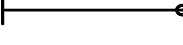
The summary of the results are shown in Tab. 3 to Tab. 14 for the IPE 500 section and in Tab. 15 to Tab. 26 for the HEB 300 section. In every table, the modelling results are compared with the literature values.

It has be noted that correct value of the elastic critical moment for different bending moment diagrams and support conditions was already discussed in the literature [12].

Tab. 3: Comparison of values of factor C_1 according to literature values and modelling results

		$\psi=1.0$		BOUNDARY CONDITIONS			
		IPE 500		$k=0.7 \quad kw=0.7$			
L (mm)	$\bar{\lambda}_z$ (k=1.0) S235	ABAQUS	LTBEAM	$1/k_c^2$	ENV	ÖNORM B (interpolated)	ECCS (interpolated)
2888	0.71	1.002	1.003	1.000	1.000	1.076	1.030
4324	1.07	0.987	1.005	1.000	1.000	1.076	1.030
5765	1.43	0.994	1.001	1.000	1.000	1.076	1.030
7221	1.79	1.001	1.003	1.000	1.000	1.076	1.030
8665	2.14	1.003	1.001	1.000	1.000	1.076	1.030
10089	2.50	1.003	1.001	1.000	1.000	1.076	1.030
11530	2.85	1.005	1.001	1.000	1.000	1.076	1.030

Tab. 4: Comparison of values of factor C_1 according to literature values and modelling results

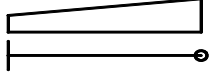
		$\psi=0.5$		BOUNDARY CONDITIONS			
		IPE 500		$k=0.7 \quad kw=0.7$			
L (mm)	$\bar{\lambda}_z$ (k=1.0) S235	ABAQUS	LTBEAM	$1/k_c^2$	ENV	ÖNORM B (interpolated)	ECCS (interpolated)
2888	0.71	1.393	1.479	1.357	1.473	1.417	1.346
4324	1.07	1.442	1.478	1.357	1.473	1.417	1.346
5765	1.43	1.457	1.472	1.357	1.473	1.417	1.346
7221	1.78	1.464	1.472	1.357	1.473	1.417	1.346
8665	2.14	1.468	1.471	1.357	1.473	1.417	1.346
10089	2.50	1.471	1.471	1.357	1.473	1.417	1.346
11530	2.85	1.474	1.470	1.357	1.473	1.417	1.346

Tab. 4 demonstrates the generally good agreement of the results of the models in the two programs (ABAQUS and LTBeam). For members of very small length in relation to the cross-sectional depth (i.e. members with lower slenderness), larger differences can be noted because of the different type of the elements in the two models. LTBeam treats the member as a beam element with rigid cross sections, while the model in ABAQUS was built up from three shell elements, so in ABAQUS the stability of small members is influenced by global and local - in this case: shear - buckling effects as well; for shorter

beams and non-uniform bending moment diagrams, shear becomes quite relevant for short beams loaded up to their bending capacity at one member end.

Similar results are represented in the following tables.

Tab. 5: Comparison of values of factor C_1 according to literature values and modelling results

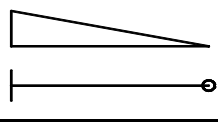
		$\psi=0.5$		BOUNDARY CONDITIONS			
		IPE 500		$k=0.7 \quad kw=0.7$			
L (mm)	$\bar{\lambda}_z$ (k=1.0) S235	ABAQUS	LTBEAM	$1/k_c^2$	ENV	ÖNORM B (interpolated)	ECCS (interpolated)
2888	0.71	1.140	1.208	1.357	1.473	1.417	1.346
4324	1.07	1.180	1.207	1.357	1.473	1.417	1.346
5765	1.43	1.191	1.203	1.357	1.473	1.417	1.346
7221	1.78	1.197	1.203	1.357	1.473	1.417	1.346
8665	2.14	1.201	1.202	1.357	1.473	1.417	1.346
10089	2.50	1.234	1.202	1.357	1.473	1.417	1.346
11530	2.85	1.206	1.202	1.357	1.473	1.417	1.346

In Tab. 6 to Tab. 8 it is clearly highlighted that the fixity of warping and end rotation about the weak axis has a considerable effect on the critical bending moment M_{cr} . If the warping fixation at one (or both) ends of the member is taken into account, the critical bending moment M_{cr} is higher. The higher the critical bending moment M_{cr} (and the factor of C_1), the lower the slenderness of the member (which is a beneficial effect).

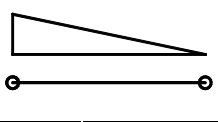
In the values of C_1 given in the literature, the warping effects are not taken into account.

The following Tab. 6 to Tab. 9 contain the results for a bending moment diagram with $\psi=0$.

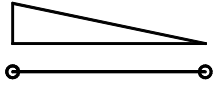
Tab. 6: Comparison of values of factor C_1 according to literature values and modelling results

		$\psi=0$		BOUNDARY CONDITIONS			
		IPE 500		$k=0.7$ $k_w=0.7$			
L (mm)	$\bar{\lambda}_z$ (k=1.0) S235	ABAQUS	LTBEAM	$1/k_c^2$	ENV	ÖNORM B (interpolated)	ECCS (interpolated)
2888	0.71	1.864	2.528	1.769	2.092	1.955	1.824
4324	1.07	2.302	2.519	1.769	2.092	1.955	1.824
5765	1.43	2.417	2.504	1.769	2.092	1.955	1.824
7221	1.79	2.454	2.496	1.769	2.092	1.955	1.824
8665	2.14	2.466	2.482	1.769	2.092	1.955	1.824
10089	2.50	2.468	2.472	1.769	2.092	1.955	1.824
11530	2.86	2.466	2.462	1.769	2.092	1.955	1.824
14442	3.57	2.458	2.440	1.769	2.092	1.955	1.824
17330	4.29	2.450	2.422	1.769	2.092	1.955	1.824

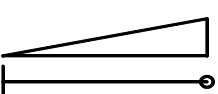
Tab. 7: Comparison of values of factor C_1 according to literature values and modelling results

		$\psi=0$		BOUNDARY CONDITIONS			
		IPE 500		$k=1.0$ $k_w=0.7$			
L (mm)	$\bar{\lambda}_z$ (k=1.0) S235	ABAQUS	LTBEAM	$1/k_c^2$	ENV	ÖNORM B	ECCS
2888	0.71	2.008	2.312	1.769	1.879	1.847	1.770
4324	1.07	2.199	2.294	1.769	1.879	1.847	1.770
5765	1.43	2.234	2.268	1.769	1.879	1.847	1.770
7221	1.79	2.232	2.253	1.769	1.879	1.847	1.770
8665	2.14	2.219	2.220	1.769	1.879	1.847	1.770
10089	2.50	2.201	2.197	1.769	1.879	1.847	1.770
11530	2.86	2.183	2.174	1.769	1.879	1.847	1.770
14442	3.57	2.146	2.129	1.769	1.879	1.847	1.770
17330	4.29	2.115	2.089	1.769	1.879	1.847	1.770

Tab. 8: Comparison of values of factor C_1 according to literature values and modelling results

		$\psi=0$		BOUNDARY CONDITIONS			
		IPE 500		$k=1.0 \quad kw=0.5$			
L (mm)	$\bar{\lambda}_z (k=1.0)$ S235	ABAQUS	LTBEAM	$1/k_c^2$	ENV	ÖNORM B	ECCS
2888	0.71	1.798	2.131	1.769	1.879	1.847	1.770
4324	1.07	2.024	2.125	1.769	1.879	1.847	1.770
5765	1.43	2.074	2.114	1.769	1.879	1.847	1.770
7221	1.79	2.089	2.109	1.769	1.879	1.847	1.770
8665	2.14	2.092	2.098	1.769	1.879	1.847	1.770
10089	2.50	2.090	2.090	1.769	1.879	1.847	1.770
11530	2.86	2.086	2.081	1.769	1.879	1.847	1.770
14442	3.57	2.076	2.061	1.769	1.879	1.847	1.770
17330	4.29	2.064	2.041	1.769	1.879	1.847	1.770

Tab. 9: Comparison of values of factor C_1 according to literature values and modelling results

		$\psi=0$		BOUNDARY CONDITIONS			
		IPE 500		$k=0.7 \quad kw=0.7$			
L (mm)	$\bar{\lambda}_z (k=1.0)$ S235	ABAQUS	LTBEAM	$1/k_c^2$	ENV	ÖNORM B (interpolated)	ECCS (interpolated)
2888	0.71	1.286	1.473	1.769	2.092	1.955	1.824
4324	1.07	1.411	1.476	1.769	2.092	1.955	1.824
5765	1.43	1.444	1.469	1.769	2.092	1.955	1.824
7221	1.78	1.456	1.468	1.769	2.092	1.955	1.824
8665	2.14	1.462	1.467	1.769	2.092	1.955	1.824
10089	2.50	1.466	1.465	1.769	2.092	1.955	1.824
11530	2.85	1.468	1.463	1.769	2.092	1.955	1.824

Particularly large differences are found between the results given in Tab. 6 (maximum bending moment at a fixed end about the weak axis) and Tab. 9 (maximum bending moment at the opposite end, where warping and rotation are free). In order to better explain the reasons for the obtained differences between the critical bending moments M_{cr} (and hence the values of C_1) between the numerical calculations and the literature values, it is useful to show the shape of the relevant buckling eigenmode.

In Fig. 11, the buckling form of the member with the length of $L=5765$ mm and the boundary conditions applicable to Tab. 6 is presented.

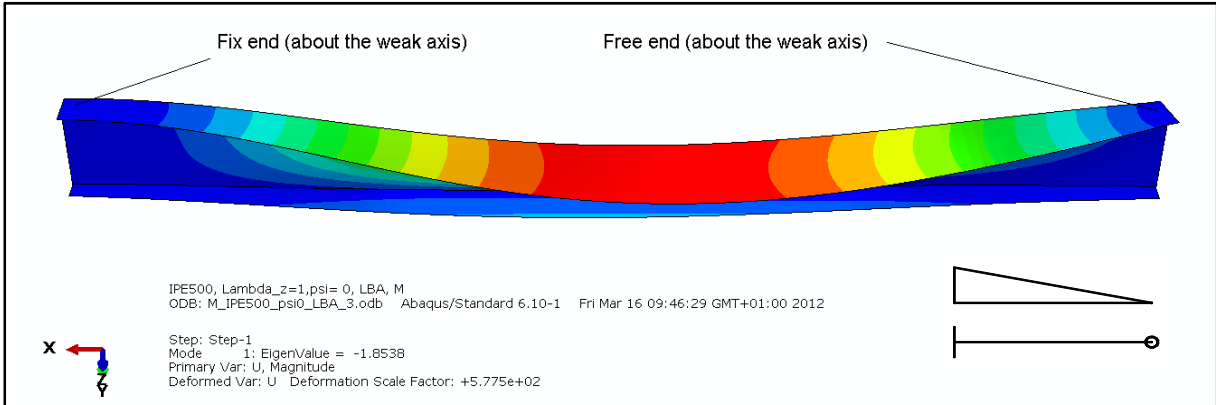


Fig. 11: Buckling form under boundary conditions $k=0,7$ $k_w=0,7$ $\psi=0$ (Eigenvalue=1,85)

In Fig. 12, again the buckling form of the member with the length of $L=5765$ mm is presented, however for the boundary conditions valid for Tab. 9. If we compare this form with the one in Fig. 11, we can see that the support conditions are the same, however the shape is different because of the inverse position of the moment diagram. In the second case, the location of maximum deformation of the eigenmode shape is much closer to the location of the maximum bending moment in the beam; this indicates that higher deviational forces are present in this case.

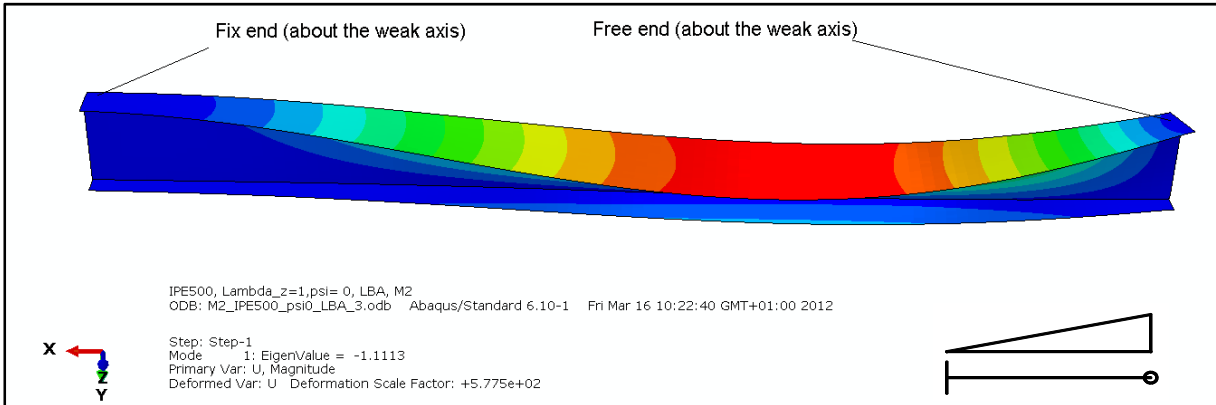
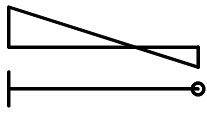


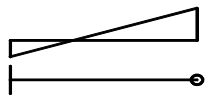
Fig. 12: Buckling form under boundary conditions $k=0,7$ $k_w=0,7$ $\psi=0$ with inverse position of the moment diagram (Eigenvalue=1,11)

More results, valid for bending moment diagrams with end moments of different sign, are shown in the following tables (Tab. 10 to Tab. 11)

Tab. 10: Comparison of values of factor C_1 according to literature values and modelling results

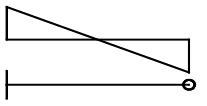
		$\psi=-0.5$		BOUNDARY CONDITIONS			
		IPE 500		k=0.7 kw=0.7			
L (mm)	$\bar{\lambda}_z$ (k=1.0) S235	ABAQUS	LTBEAM	$1/k_c^2$	ENV	ÖNORM B (interpolated)	ECCS (interpolated)
2888	0.71	1.689	3.675	2.235	3.009	2.584	2.392
4324	1.07	2.720	3.654	2.235	3.009	2.584	2.392
5765	1.43	3.190	3.616	2.235	3.009	2.584	2.392
7221	1.78	3.380	3.588	2.235	3.009	2.584	2.392
8665	2.14	3.450	3.557	2.235	3.009	2.584	2.392
10089	2.50	3.470	3.524	2.235	3.009	2.584	2.392
11530	2.85	3.467	3.492	2.235	3.009	2.584	2.392
14442	3.57	3.446	3.429	2.235	3.009	2.584	2.392
17330	4.29	3.409	3.373	2.235	3.009	2.584	2.392

Tab. 11: Comparison of values of factor C_1 according to literature values and modelling results

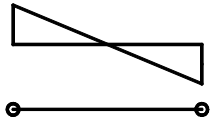
		$\psi=-0.5$		BOUNDARY CONDITIONS			
		IPE 500		$k=0.7$ $k_w=0.7$			
L (mm)	$\bar{\lambda}_z$ (k=1.0) S235	ABAQUS	LTBEAM	$1/k_c^2$	ENV	ÖNORM B (interpolated)	ECCS (interpolated)
2888	0.71	1.310	1.813	2.235	3.009	2.584	2.392
4324	1.07	1.637	1.809	2.235	3.009	2.584	2.392
5765	1.43	1.731	1.799	2.235	3.009	2.584	2.392
7221	1.78	1.764	1.795	2.235	3.009	2.584	2.392
8665	2.14	1.777	1.791	2.235	3.009	2.584	2.392
10089	2.50	1.782	1.786	2.235	3.009	2.584	2.392
11530	2.85	1.784	1.781	2.235	3.009	2.584	2.392

Tab. 12 shows an interesting result, because in this case the modelling results are lower than the values according to the literature, which means a lower value of M_{cr} and higher slenderness. It should be noted that both for ÖNORM B 1993-1-1 and the ECCS value, no values for $k / k_w=0.7$ are given; the results were thus interpolated for these cases.

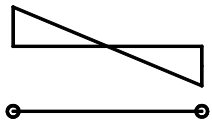
Tab. 12: Comparison of values of factor C_1 according to literature values and modelling results

		$\psi=-1.0$		BOUNDARY CONDITIONS			
		IPE 500		$k=0.7$ $k_w=0.7$			
L (mm)	$\bar{\lambda}_z$ (k=1.0) S235	ABAQUS	LTBEAM	$1/k_c^2$	ENV	ÖNORM B (interpolated)	ECCS (interpolated)
2888	0.71	1.202	2.123	2.756	3.036	2.527	2.510
4324	1.07	1.750	2.122	2.756	3.036	2.527	2.510
5765	1.43	1.955	2.110	2.756	3.036	2.527	2.510
7221	1.81	2.085	2.102	2.756	3.036	2.527	2.510
8665	2.14	2.058	2.094	2.756	3.036	2.527	2.510
10089	2.50	2.070	2.086	2.756	3.036	2.527	2.510
11553	2.86	2.079	2.077	2.756	3.036	2.527	2.510
12997	3.21	2.079	2.067	2.756	3.036	2.527	2.510
14442	3.57	2.076	2.058	2.756	3.036	2.527	2.510

Tab. 13: Comparison of values of factor C_1 according to literature values and modelling results

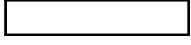
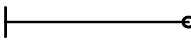
		$\psi=-1.0$		BOUNDARY CONDITIONS			
		IPE 500		$k=1.0$ $k_w=0.7$			
L (mm)	$\bar{\lambda}_z$ (k=1.0) S235	ABAQUS	LTBEAM	$1/k_c^2$	ENV	ÖNORM B	ECCS
2888	0.71	1.716	3.024	2.756	2.752	2.733	2.600
4324	1.07	2.496	3.022	2.756	2.752	2.733	2.600
5765	1.43	2.786	3.005	2.756	2.752	2.733	2.600
7221	1.81	2.901	2.992	2.756	2.752	2.733	2.600
8665	2.14	2.938	2.981	2.756	2.752	2.733	2.600
10089	2.50	2.954	2.968	2.756	2.752	2.733	2.600
11530	2.86	2.958	2.955	2.756	2.752	2.733	2.600
12997	3.21	2.955	2.938	2.756	2.752	2.733	2.600
14442	3.57	2.950	2.925	2.756	2.752	2.733	2.600

Tab. 14: Comparison of values of factor C_1 according to literature values and modelling results


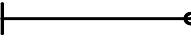
		$\psi=-1.0$		BOUNDARY CONDITIONS			
		IPE 500		$k=1.0$ $k_w=0.5$			
L (mm)	$\bar{\lambda}_z$ (k=1.0) S235	ABAQUS	LTBEAM	$1/k_c^2$	ENV	ÖNORM B	ECCS
2888	0.71	1.582	3.716	2.756	2.752	2.733	2.600
4324	1.07	2.762	3.706	2.756	2.752	2.733	2.600
5765	1.43	3.262	3.674	2.756	2.752	2.733	2.600
7221	1.81	3.463	3.644	2.756	2.752	2.733	2.600
8665	2.14	3.522	3.616	2.756	2.752	2.733	2.600
10089	2.50	3.538	3.581	2.756	2.752	2.733	2.600
11530	2.86	3.531	3.546	2.756	2.752	2.733	2.600
12997	3.21	3.512	3.506	2.756	2.752	2.733	2.600
14442	3.57	3.488	3.470	2.756	2.752	2.733	2.600

The following tables (Tab. 15 to Tab. 26) show the results of the ABAQUS and LTBeam LBA calculations for an HEB 300 section. Again, a comparison with the values reported in the literature is carried out.

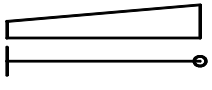
Tab. 15: Comparison of values of factor C_1 according to literature values and modelling results

		$\psi=1.0$		BOUNDARY CONDITIONS			
		HEB 300		$k=0.7 \quad kw=0.7$			
L (mm)	$\bar{\lambda}_z (k=1.0)$ S235	ABAQUS	LTBEAM	$1/k_c^2$	ENV	ÖNORM B (interpolated)	ECCS (interpolated)
5084	0.71	0.969	1.004	1.000	1.000	1.076	1.030
7626	1.07	0.991	1.002	1.000	1.000	1.076	1.030
10168	1.43	0.998	1.003	1.000	1.000	1.076	1.030
12710	1.79	1.001	1.003	1.000	1.000	1.076	1.030
15252	2.14	1.004	1.003	1.000	1.000	1.076	1.030
17793	2.50	1.006	1.004	1.000	1.000	1.076	1.030
20336	2.86	1.007	1.003	1.000	1.000	1.076	1.030

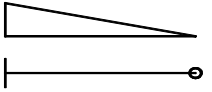
Tab. 16: Comparison of values of factor C_1 according to literature values and modelling results

		$\psi=0.5$		BOUNDARY CONDITIONS			
		HEB 300		$k=0.7 \quad kw=0.7$			
L (mm)	$\bar{\lambda}_z (k=1.0)$ S235	ABAQUS	LTBEAM	$1/k_c^2$	ENV	ÖNORM B (interpolated)	ECCS (interpolated)
5084	1.79	1.419	1.476	1.357	1.473	1.417	1.346
7626	2.14	1.452	1.472	1.357	1.473	1.417	1.346
10168	2.50	1.462	1.472	1.357	1.473	1.417	1.346
12710	2.86	1.467	1.471	1.357	1.473	1.417	1.346
15252	3.57	1.469	1.471	1.357	1.473	1.417	1.346
17793	4.29	1.471	1.470	1.357	1.473	1.417	1.346
20336	4.64	1.473	1.468	1.357	1.473	1.417	1.346

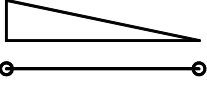
Tab. 17: Comparison of values of factor C_1 according to literature values and modelling results

		$\psi=0.5$		BOUNDARY CONDITIONS			
		HEB 300		$k=0.7 \quad kw=0.7$			
L (mm)	$\bar{\lambda}_z$ (k=1.0) S235	ABAQUS	LTBEAM	$1/k_c^2$	ENV	ÖNORM B (interpolated)	ECCS (interpolated)
5084	0.71	1.164	1.206	1.357	1.473	1.417	1.346
7626	1.07	1.190	1.203	1.357	1.473	1.417	1.346
10168	1.43	1.198	1.203	1.357	1.473	1.417	1.346
12710	1.79	1.202	1.203	1.357	1.473	1.417	1.346
15252	2.14	1.204	1.203	1.357	1.473	1.417	1.346
17793	2.50	1.206	1.203	1.357	1.473	1.417	1.346
20336	2.86	1.207	1.202	1.357	1.473	1.417	1.346

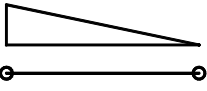
Tab. 18: Comparison of values of factor C_1 according to literature values and modelling results

		$\psi=0$		BOUNDARY CONDITIONS			
		HEB 300		$k=0.7 \quad kw=0.7$			
L (mm)	$\bar{\lambda}_z$ (k=1.0) S235	ABAQUS	LTBEAM	$1/k_c^2$	ENV	ÖNORM B (interpolated)	ECCS (interpolated)
5084	0.71	1.818	2.507	1.769	2.092	1.955	1.824
7626	1.07	2.422	2.479	1.769	2.092	1.955	1.824
10168	1.43	2.427	2.457	1.769	2.092	1.955	1.824
12710	1.79	2.419	2.437	1.769	2.092	1.955	1.824
15252	2.14	2.410	2.420	1.769	2.092	1.955	1.824
17793	2.50	2.401	2.406	1.769	2.092	1.955	1.824
20336	2.86	2.394	2.393	1.769	2.092	1.955	1.824

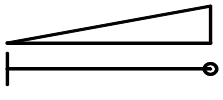
Tab. 19; Comparison of values of factor C_1 according to literature values and modelling results

		$\psi=0$		BOUNDARY CONDITIONS			
		HEB 300		$k=1.0 \quad kw=0.7$			
L (mm)	$\bar{\lambda}_z$ (k=1.0) S235	ABAQUS	LTBEAM	$1/k_c^2$	ENV	ÖNORM B (interpolated)	ECCS (interpolated)
5084	0.71	2.180	2.266	1.769	1.879	1.847	1.770
7626	1.07	2.176	2.210	1.769	1.879	1.847	1.770
10168	1.43	2.139	2.159	1.769	1.879	1.847	1.770
12710	1.79	2.102	2.115	1.769	1.879	1.847	1.770
15252	2.14	2.068	2.076	1.769	1.879	1.847	1.770
17793	2.50	2.040	2.044	1.769	1.879	1.847	1.770
20336	2.86	2.017	2.016	1.769	1.879	1.847	1.770

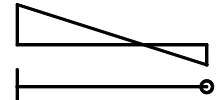
Tab. 20; Comparison of values of factor C_1 according to literature values and modelling results

		$\psi=0$		BOUNDARY CONDITIONS			
		HEB 300		$k=1.0 \quad kw=0.5$			
L (mm)	$\bar{\lambda}_z$ (k=1.0) S235	ABAQUS	LTBEAM	$1/k_c^2$	ENV	ÖNORM B (interpolated)	ECCS (interpolated)
5084	0.71	2.005	2.116	1.769	1.879	1.847	1.770
7626	1.07	2.049	2.094	1.769	1.879	1.847	1.770
10168	1.43	2.047	2.075	1.769	1.879	1.847	1.770
12710	1.79	2.036	2.055	1.769	1.879	1.847	1.770
15252	2.14	2.022	2.035	1.769	1.879	1.847	1.770
17793	2.50	2.008	2.017	1.769	1.879	1.847	1.770
20336	2.86	1.996	1.999	1.769	1.879	1.847	1.770

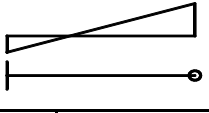
Tab. 21: Comparison of values of factor C_1 according to literature values and modelling results

		$\psi=0$		BOUNDARY CONDITIONS			
		HEB 300		$k=0.7$ $k_w=0.7$			
L (mm)	$\bar{\lambda}_z$ (k=1.0) S235	ABAQUS	LTBEAM	$1/k_c^2$	ENV	ÖNORM B (interpolated)	ECCS (interpolated)
5084	0.71	1.416	1.473	1.769	2.092	1.955	1.824
7626	1.07	1.450	1.467	1.769	2.092	1.955	1.824
10168	1.43	1.458	1.465	1.769	2.092	1.955	1.824
12710	1.79	1.461	1.462	1.769	2.092	1.955	1.824
15252	2.14	1.462	1.459	1.769	2.092	1.955	1.824
17793	2.50	1.462	1.457	1.769	2.092	1.955	1.824
20336	2.86	1.462	1.454	1.769	2.092	1.955	1.824

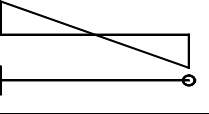
Tab. 22: Comparison of values of factor C_1 according to literature values and modelling results

		$\psi=-0.5$		BOUNDARY CONDITIONS			
		HEB 300		$k=0.7$ $k_w=0.7$			
L (mm)	$\bar{\lambda}_z$ (k=1.0) S235	ABAQUS	LTBEAM	$1/k_c^2$	ENV	ÖNORM B (interpolated)	ECCS (interpolated)
5084	0.71	1.922	3.617	2.235	3.009	2.584	2.392
7626	1.07	3.406	3.542	2.235	3.009	2.584	2.392
10168	1.43	3.411	3.473	2.235	3.009	2.584	2.392
12710	1.79	3.375	3.410	2.235	3.009	2.584	2.392
15252	2.14	3.335	3.355	2.235	3.009	2.584	2.392
17793	2.50	3.299	3.309	2.235	3.009	2.584	2.392
20336	2.86	3.269	3.268	2.235	3.009	2.584	2.392

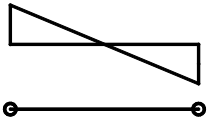
Tab. 23: Comparison of values of factor C_1 according to literature values and modelling results

		$\psi=-0.5$		BOUNDARY CONDITIONS			
		HEB 300		$k=0.7$ $kw=0.7$			
L (mm)	$\bar{\lambda}_z$ (k=1.0) S235	ABAQUS	LTBEAM	$1/k_c^2$	ENV	ÖNORM B (interpolated)	ECCS (interpolated)
5084	0.71	1.712	1.803	2.235	3.009	2.584	2.392
7626	1.07	1.763	1.790	2.235	3.009	2.584	2.392
10168	1.43	1.771	1.781	2.235	3.009	2.584	2.392
12710	1.79	1.770	1.771	2.235	3.009	2.584	2.392
15252	2.14	1.766	1.763	2.235	3.009	2.584	2.392
17793	2.50	1.762	1.755	2.235	3.009	2.584	2.392
20336	2.86	1.759	1.748	2.235	3.009	2.584	2.392

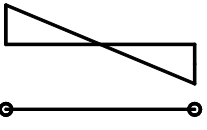
Tab. 24: Comparison of values of factor C_1 according to literature values and modelling results

		$\psi=-1.0$		BOUNDARY CONDITIONS			
		HEB 300		$k=0.7$ $kw=0.7$			
L (mm)	$\bar{\lambda}_z$ (k=1.0) S235	ABAQUS	LTBEAM	$1/k_c^2$	ENV	ÖNORM B (interpolated)	ECCS (interpolated)
5084	0.71	1.945	2.113	2.756	3.036	2.527	2.510
7626	1.07	2.049	2.091	2.756	3.036	2.527	2.510
10168	1.43	2.057	2.073	2.756	3.036	2.527	2.510
12710	1.79	2.051	2.055	2.756	3.036	2.527	2.510
15252	2.14	2.041	2.038	2.756	3.036	2.527	2.510
17793	2.50	2.031	2.023	2.756	3.036	2.527	2.510
20336	2.86	2.022	2.009	2.756	3.036	2.527	2.510

Tab. 25: Comparison of values of factor C_1 according to literature values and modelling results

		$\psi=-1.0$		BOUNDARY CONDITIONS			
		HEB 300		$k=1.0 \quad kw=0.7$			
L (mm)	$\bar{\lambda}_z$ (k=1.0) S235	ABAQUS	LTBEAM	$1/k_c^2$	ENV	ÖNORM B (interpolated)	ECCS (interpolated)
5084	0.71	2.773	3.009	2.756	2.752	2.733	2.600
7626	1.07	2.915	2.976	2.756	2.752	2.733	2.600
10168	1.43	2.924	2.948	2.756	2.752	2.733	2.600
12710	1.79	2.912	2.918	2.756	2.752	2.733	2.600
15252	2.14	2.893	2.890	2.756	2.752	2.733	2.600
17793	2.50	2.874	2.865	2.756	2.752	2.733	2.600
20336	2.86	2.856	2.840	2.756	2.752	2.733	2.600

Tab. 26: Comparison of values of factor C_1 according to literature values and modelling results

		$\psi=-1.0$		BOUNDARY CONDITIONS			
		HEB 300		$k=1.0 \quad kw=0.5$			
L (mm)	$\bar{\lambda}_z$ (k=1.0) S235	ABAQUS	LTBEAM	$1/k_c^2$	ENV	ÖNORM B (interpolated)	ECCS (interpolated)
5084	0.71	2.264	3.672	2.756	2.752	2.733	2.600
7626	1.07	3.447	3.596	2.756	2.752	2.733	2.600
10168	1.43	3.441	3.520	2.756	2.752	2.733	2.600
12710	1.79	3.392	3.440	2.756	2.752	2.733	2.600
15252	2.14	3.333	3.364	2.756	2.752	2.733	2.600
17793	2.50	3.276	3.295	2.756	2.752	2.733	2.600
20336	2.86	3.223	3.231	2.756	2.752	2.733	2.600

3.3. Conclusions

The following conclusions can be drawn from the Linear Bifurcation Analyses (LBA) described in this section of the thesis:

- The elastic critical moment M_{cr} of the member with the same length and section depends on the support conditions (rotation and warping fixities) and the load conditions (shape and position of the bending moment diagram)
- There is a wide range of different values of the factor C_1 in cases under the same support and load conditions according to the literature and the numerical modelling results.
- The use of simple, dedicated numerical programs –such as LTBeam– is highly recommended because the warping fixation can be taken into account which gives – in most cases – a beneficial result contrary to the calculation with the factor of C_1 according to the literature.
- The values for C_1 found in the literature only cover certain boundary conditions (both ends equal). Furthermore, while the literature values of C_1 are mostly lower (i.e. conservative) in comparison with numerical calculations, this is not always the case for all boundary conditions; this could lead to unsafe results in some cases.

4. Flexural Buckling (pure compression, GMNIA)

In this chapter the most important facts about the basic stability phenomenon of compressed members, i.e. flexural buckling, are summarized.

4.1. Elastic Bifurcation and Eurocode 3 Design Rules

The **elastic critical load** (Euler's critical load) of a pinned member under ideal conditions (no imperfections, member perfectly straight, no plasticity) corresponds to the point of bifurcation of equilibrium (elastic buckling), which –for weak-axis buckling– is calculated as follows [1]:

$$N_{Cr,z} = \frac{\pi^2 \cdot EI_z}{L_{cr}^2} \quad (4.1)$$

where L_{cr} is the **critical length** depending on the support conditions (rotation fixity) of the member:

$$L_{cr} = k \cdot L \quad (4.2)$$

The **normalized slenderness** coefficient for the flexural buckling case is defined as follows [1]:

$$\bar{\lambda} = \frac{\sqrt{N_{pl}}}{\sqrt{N_{cr}}} = \frac{\sqrt{A \cdot f_y}}{\sqrt{N_{cr}}} \quad (4.3)$$

Based on the previous expressions, the member slenderness (and the critical load) for the same length and material depends on:

- the support conditions (only rotation fixity matters)
- I_z , i.e. the second moment of area about the weak axis z

The **buckling resistance** of the member according to EC3 (class 1, 2 or 3 cross sections) is defined by the following term [13]:

$$N_{b,Rd} = \chi \cdot N_{pl} \quad (4.4)$$

where χ is the **reducing factor accounting for the risk of flexural buckling** (perfect elastic-plastic behaviour). The EC3 formula for the buckling reduction factor was derived in [14] on the basis of elastic second-order theory and calibrated to match the experimental/numerical ECCS column buckling curves, presented in [15]. The formulation found in the Eurocode is as follows [13]:

$$\chi = \frac{1}{\phi + \sqrt{\phi^2 - \bar{\lambda}^2}} \quad (4.5)$$

with

$$\phi = 0,5 \cdot [1 + \alpha(\bar{\lambda} - 0,2) + \bar{\lambda}^2] \quad (4.6)$$

where α is the imperfection factor.

According to the equations of EC3, the material behaviour of steel is perfect elastic-plastic and the geometric (lack of linearity and verticality, eccentricity of load) and material imperfections (residual stresses) are taken into account. [1]

4.2. GMNIA Buckling Curves

In this thesis, the focus is put on the effect of boundary conditions on the out-of-plane stability of beam-columns. For this reason, the following considerations are concerned with boundary conditions that differ from the “classic” pinned-pinned conditions, by adding fixity to at least one of the column ends.

In Fig. 13, the buckling curve valid for an IPE 500 section according to EC3 is compared with GMNIA analyses for a case with a one-sided rotational fixity about the weak-axis ($k=0.7$). Thereby, the obtained GMNIA results for $k=0.7$ are plotted over two different values of slenderness in order to illustrate the large benefit obtained from the consideration of end fixities:

- When the GMNIA results are plotted over the “correct” value of slenderness, i.e. the slenderness calculated by considering the fixity at one column end, the difference between the GMNIA results and the code are quite small. This confirms that the EC3 flexural buckling curves are quite accurate even for columns that show some degree of out-of-plane fixity.
- In a second form of presentation, the same GMNIA results (calculated for $k=0.7$) are plotted over an “incorrect” slenderness, often used in design by “cautious” engineers: in this case, the slenderness is calculated for $k=1.0$, ignoring any fixity. The large difference between the GMNIA and code results for this type of representation illustrate the large benefit of the fixation

One example is discussed in more detail: if the “correct” slenderness is $\bar{\lambda} = 0,7$ ($k=0,7$), χ according to EC3 is 0,78; however, the same member designed for $k=1,0$ would have a slenderness of $\bar{\lambda} = 1,0$ and a buckling reduction factor χ of just 0,6. This would mean that a conservatism of 30% was added to the weak-axis buckling design by omitting the effects of the end fixity.

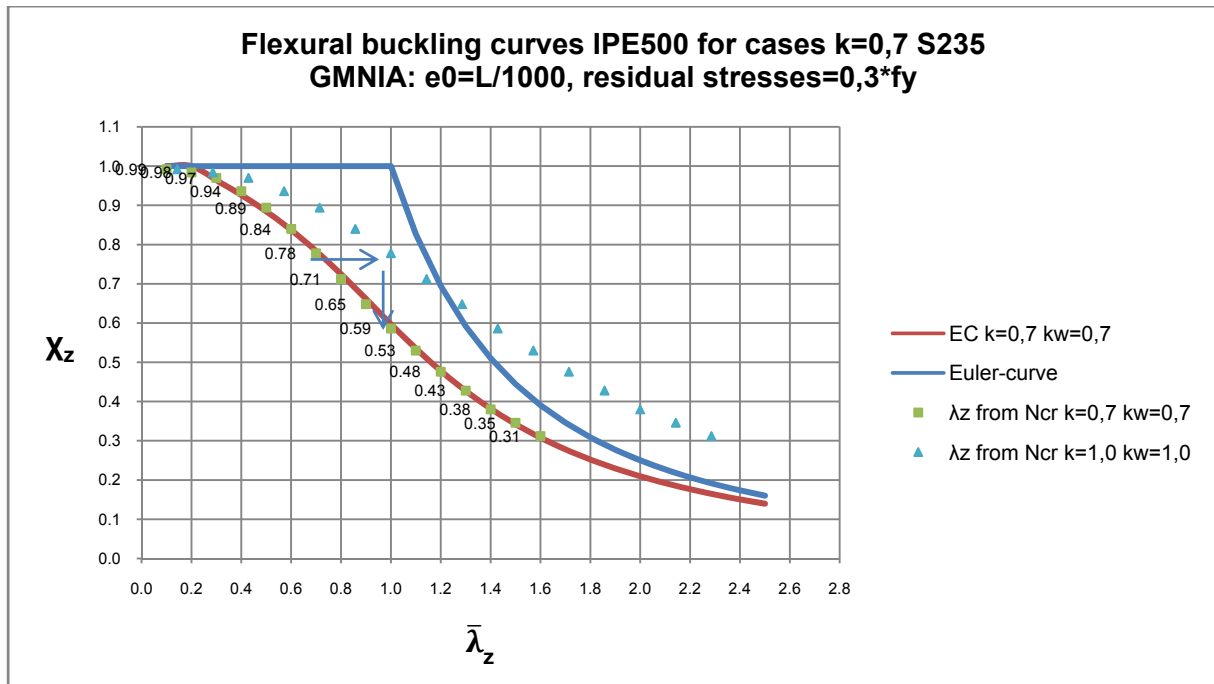


Fig. 13

Fig. 14 can be used to explain the reason why the European buckling curves manage to describe the different out-of-plane boundary conditions so well: it can be seen that the initial geometric imperfection amplitude of the model in relation to the critical length L_{cr} ($0,7L$) is equal to the imperfection assumption according to the development of the EC3 buckling curves, which is:

$$\frac{\bar{e}_0}{L} = \frac{0,7 \cdot L / 1000}{0,7 \cdot L} = \frac{1}{1000}$$

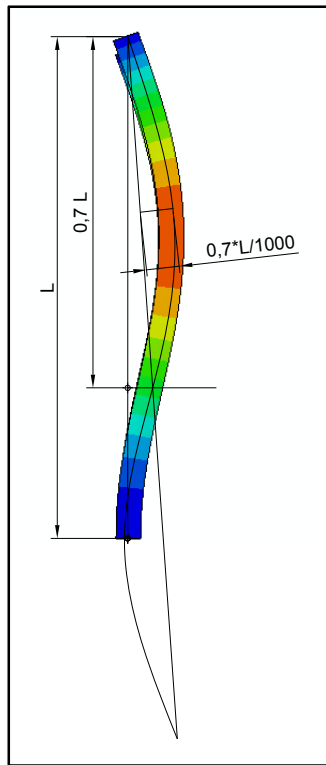


Fig. 14: Magnitude of geometric imperfections under support condition $k=0,7$

In Fig. 15 the GMNIA results for case with a one-sided rotational fixity about the weak axis and with HEB 300 section are shown. In this diagram the results are plotted in the same way as Fig. 13, so the same GMNIA results are in relation to the “correct” and the “incorrect” flexural slenderness. In addition the buckling curve according to the EC3 valid for HEB 300 section and the Euler-curve are compared to the modelling results.

It can again be seen that if the “correct” slenderness is $\bar{\lambda} = 0,6$ ($k=0,7$), χ according to EC3 is 0,79; however, the same member designed for $k=1,0$ would have a slenderness of $\bar{\lambda} = 0,86$ and a buckling reduction factor χ of just 0,63. This would mean that a conservatism of 37% was added to the weak-axis buckling design by omitting the effects of the end fixity.

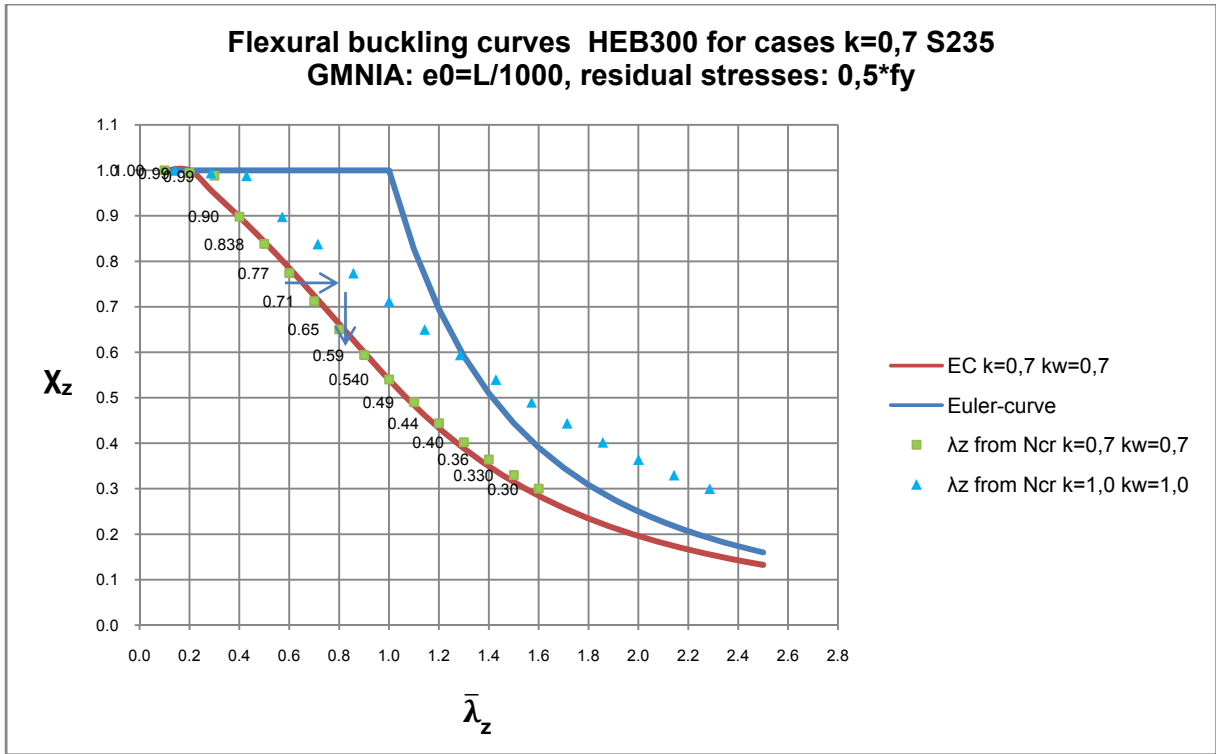


Fig. 15

4.3. Conclusions

The content of this chapter can be summarized and commented upon as follows:

- The first parametric studies in this thesis were carried out for the cases of flexural buckling of sections IPE 500 and HEB 300. In the GMNIA models the support condition were $k=0,7$ $k_w=0,7$, and these conditions will be treated as the “basic case” also in the following chapters.
- The results of the two studies have indicated that the modelling results fit very accurately to the EC3 buckling curves, thus the EC3 buckling curves are confirmed to be compatible and valid for these support conditions as well. This could be explained by the fact that the geometrical imperfection amplitude of $L/1000$ is proportionally still present -in a calculation that uses the first buckling eigenmode as imperfection shape- for the “equivalent column- length of $0,7L$, see Fig. 14. The same would also be true for a buckling length factor of $k=0,5$. It is less clear -and could be a topic of more studies- that this would also apply for cases where the buckling length is larger than 1.0
- If the rotation restraint is taken into account ($k=0,7$), the buckling strength of members with intermediate slenderness is about 30% higher for section IPE 500 and about 35% higher for section HEB 300 than in the cases of “pin-ended” members ($k=1,0$).
- Finally, it can be established that the warping restraint has no influence on the flexural buckling behaviour, as expected.

5. Lateral-Torsional Buckling (pure bending, GMNIA)

In standard, open cross sectional shapes, such as I or H profiles, bent about the major axis y, the typical instability phenomenon is lateral-torsional buckling.

For perfect beams with uniform doubly symmetric cross-sections and linear elastic material behaviour the elastic critical moment is determined as follows, see also Chapter 3:

$$M_{cr} = C_1 \cdot \frac{\pi^2 \cdot EI_z}{(kL)^2} \cdot \left[\left(\frac{k}{k_w} \right)^2 \cdot \frac{I_w}{I_z} + \frac{(kL)^2 GI_t}{\pi^2 EI_z} \right]^{0,5} \quad (3.1)$$

And the **slenderness for lateral-torsional buckling** is:

$$\bar{\lambda}_{LT} = \sqrt{\frac{M_{pl}}{M_{Cr}}} \quad (3.2)$$

Based on the previous expressions, the member slenderness (and the critical moment) for a certain member length and material depends on the:

- shape and position of the bending moment diagram
- support conditions (rotation and warping fixity)
- (plastic) cross-sectional bending capacity.
- bending stiffness (I_z)
- torsion stiffness (I_t)
- warping stiffness (I_w)

The **lateral-torsional buckling resistance** of a prismatic member according to EC3 (class 1 or 2 cross sections) is calculated as follows [13]:

$$M_{b,Rd} = \chi_{LT} \cdot M_{pl} \quad (5.1)$$

According to EC3, two different sets of formulae can be used, the first called “**general case**” and the second called “**specific case**”. The specific case can be used for double-symmetric hot-rolled or equivalent welded sections.

Tab. 27 represent the formulations for the two cases. [1]

Tab. 27: Comparison of “general” and “specific” cases for LT-buckling formulation

		“General case”	“Specific case”
Reduction factor χ_{LT}		$\frac{1}{\phi_{LT} + \sqrt{\phi_{LT}^2 - \bar{\lambda}_{LT}^2}}$	$\frac{1}{\phi_{LT} + \sqrt{\phi_{LT}^2 - 0,75 \cdot \bar{\lambda}_{LT}^2}}$
Factor ϕ_{LT}		$0,5 \cdot [1 + \alpha(\bar{\lambda}_{LT} - 0,2) + \bar{\lambda}_{LT}^2]$	$0,5 \cdot [1 + \alpha(\bar{\lambda}_{LT} - 0,4) + 0,75 \cdot \bar{\lambda}_{LT}^2]$
Buckling curve for I or H rolled sections	h/b < 2 (HEB 300)	a ($\alpha=0,21$)	b ($\alpha=0,34$)
	h/b > 2 (IPE 500)	b ($\alpha=0,34$)	c ($\alpha=0,49$)

Under non uniform bending moment loading, the member resistance to lateral-torsional buckling is higher compared to uniform bending moment loading, and this beneficial effect can be considered.

According to EC3 the **shape of the bending moment diagram** can be taken into account by using the **modified reduction factor** $\chi_{LT,mod}$ [13]:

$$\chi_{LT,mod} = \frac{\chi_{LT}}{f} \quad (5.2)$$

where f is a increasing factor:

$$f = 1 - 0,5(1 - k_c) [1 - 2,0(\bar{\lambda}_{LT} - 0,8)^2] \text{ but } f \leq 1,0 \quad (5.3)$$

It shall be noted that this expression is only given in section 6.3.2.3 of the code, which describes the “specific case” LT-buckling curves. However, in this thesis this formula is applied to both methods (“general” and “specific case”) in order to see the benefits of the formula when applied also to the general case.

In summary, in the EC3 formulation of the resistance to lateral-torsional buckling the following parameters are thus considered:

- shape of bending moment diagram – explicitly by the factor f
- geometrical imperfections (initial lateral displacements, initial torsional rotations, eccentricity of load) – implicitly in the buckling reduction factor
- structural imperfections (residual stresses) – again implicitly in

The formulation does not explicitly take into account the rotation and warping fixity conditions on the resistance side; it only can account for it by the calculation of the slenderness to lateral-torsional buckling with the “correct” value of M_{cr} .

5.1. GMNIA analyses for different cases of support conditions

In this chapter, GMNIA results for different fixation and warping conditions -but the same length and load conditions- are compared. The analyses were carried out for both studied sections (IPE 500 and HEB 300), for three different shape of linear bending moment diagram ($\Psi=1,0$; 0 ; -1) and for three different member lengths ($L/h=5$; 15 ; 25).

Only the result of analyses which indicated a pure type of failure stemming from LTB have been shown, the other types of failure were local (shear or flange) buckling appeared to be relevant (this only happened for very short beams) were omitted.

In Fig. 16 to Fig. 18. the failures of a stocky member under uniform bending moment are illustrated where the red parts (plastic zones) indicate that the behaviour is very near to a completely plastic failure. It can be seen as well that the member resistance to LTB is increased by the fixation of the rotation and warping.

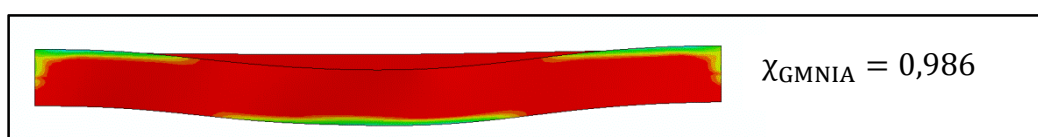


Fig. 16: LTB in case of $k=0,5$ $k_w=0,5$ $\Psi=1,0$ for IPE 500 section $L=2,5$ m

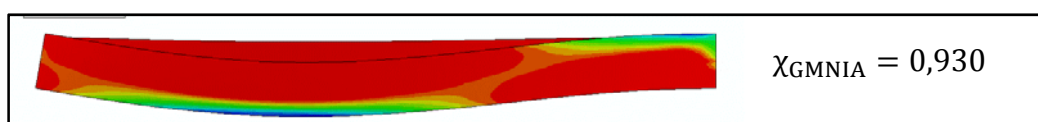


Fig. 17: LTB in case of $k=0,7$ $k_w=0,7$ $\Psi=1,0$ for IPE 500 section $L=2,5$ m

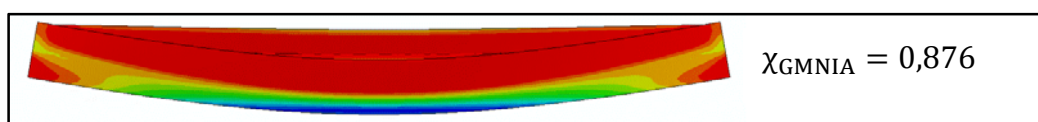


Fig. 18: LTB in case of $k=1,0$ $k_w=1,0$ $\Psi=1,0$ for IPE 500 section $L=2,5$ m

Fig. 19 to Fig. 21 represent a member with “intermediate” slenderness. The GMNIA results show that the resistant to LTB of these members are lower than in case of stocky members. In these members, there are less plastic zones at the failure load, and the

plastic zones are in the near of the fixations and generally in the inner side - according to the direction of the lateral displacement – of the upper flange.

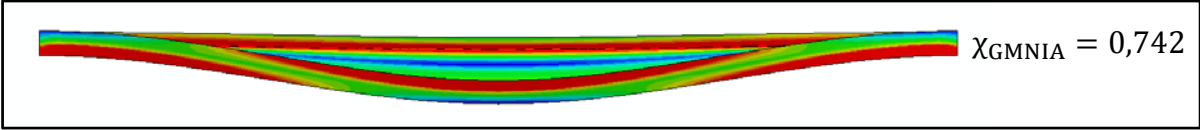


Fig. 19: LTB in case of $k=0,5$ $k_w=0,5$ $\Psi=1,0$ for IPE 500 section $L=7,5$ m

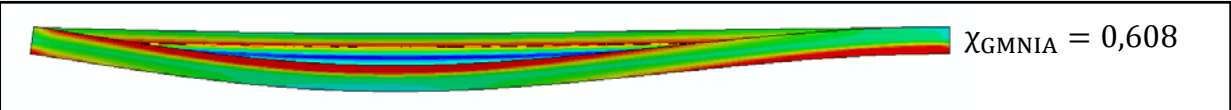


Fig. 20: LTB in case of $k=0,7$ $k_w=0,7$ $\Psi=1,0$ for IPE 500 section $L=7,5$ m

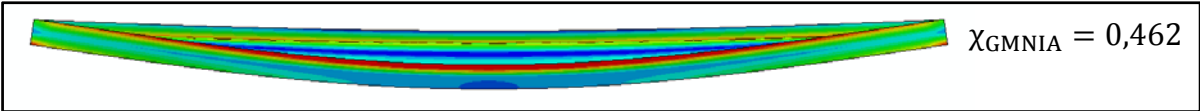


Fig. 21: LTB in case of $k=1,0$ $k_w=1,0$ $\Psi=1,0$ for IPE 500 section $L=7,5$ m

The next figures (Fig. 22 to Fig. 24) a member with large slenderness are shown. In case of these members the resistance is much more less than in case of the stocky and “intermediate” members. It can be seen that there are very few plastic zones, and the behaviour is almost completely elastic.

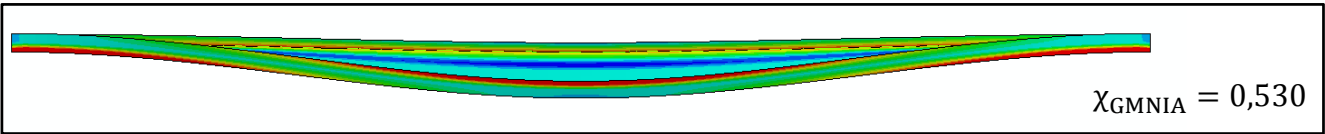


Fig. 22: LTB in case of $k=0,5$ $k_w=0,5$ $\Psi=1,0$ for IPE 500 section $L=12,5$ m

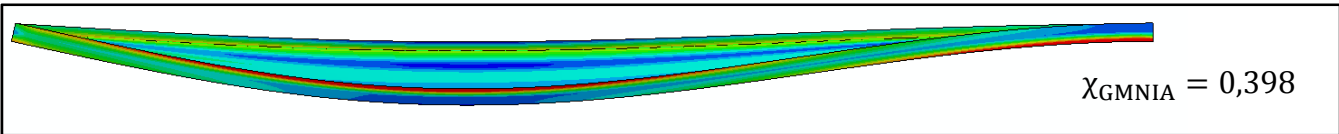


Fig. 23: LTB in case of $k=0,7$ $k_w=0,7$ $\Psi=1,0$ for IPE 500 section $L=12,5$ m

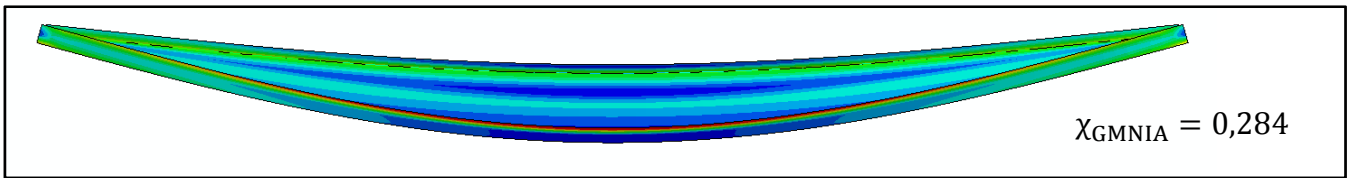


Fig. 24: LTB in case of $k=1,0$ $k_w=1,0$ $\Psi=1,0$ for IPE 500 section $L=12,5$ m

Fig. 25 to Fig. 30 shows the results for the case of $\psi=1,0$. The beneficial effect of the non-uniform bending moment can be followed in the values of χ_{GMNIA} , which are higher than in the case of $\psi=1,0$ (for example: 0,742 ;0,608 ;0,462 respectively for $L=7,5$ m and $\psi=1,0$).

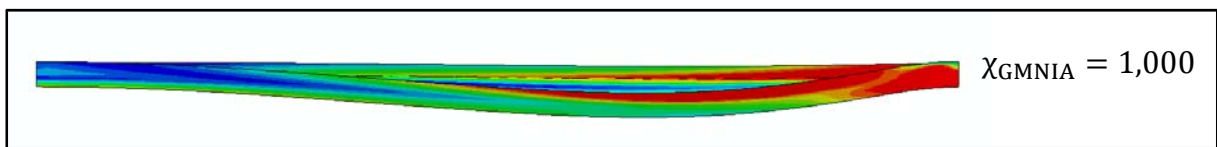


Fig. 25: LTB in case of $k=0,5$ $k_w=0,5$ $\Psi=0$ for IPE 500 section $L=7,5$ m

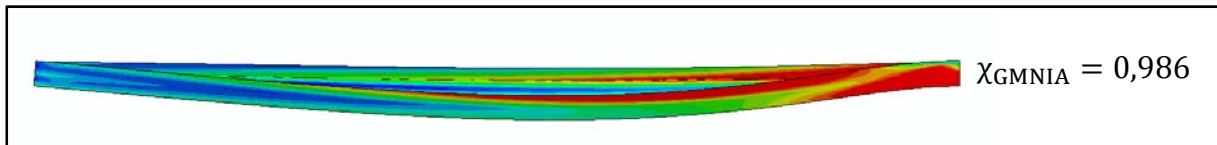


Fig. 26: LTB in case of $k=0,7$ $k_w=0,7$ $\Psi=0$ for IPE 500 section $L=7,5$ m

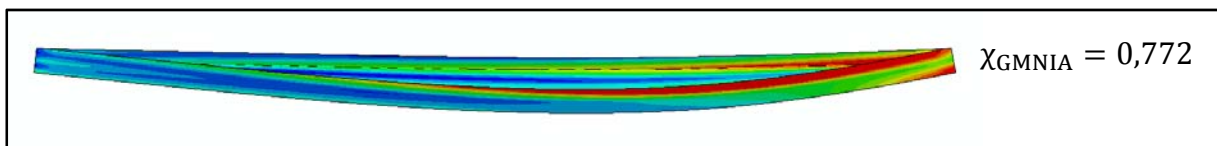


Fig. 27: LTB in case of $k=1,0$ $k_w=1,0$ $\Psi=0$ for IPE 500 section $L=7,5$ m

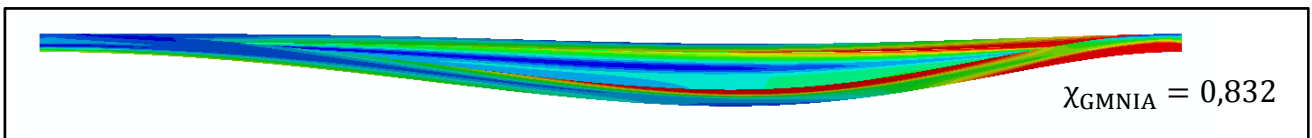


Fig. 28: LTB in case of $k=0,5$ $k_w=0,5$ $\Psi=0$ for IPE 500 section $L=12,5$ m

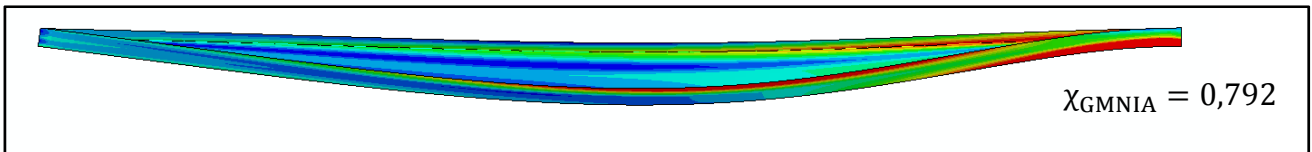


Fig. 29: LTB in case of $k=0,7$ $k_w=0,7$ $\Psi=0$ for IPE 500 section $L=12,5$ m

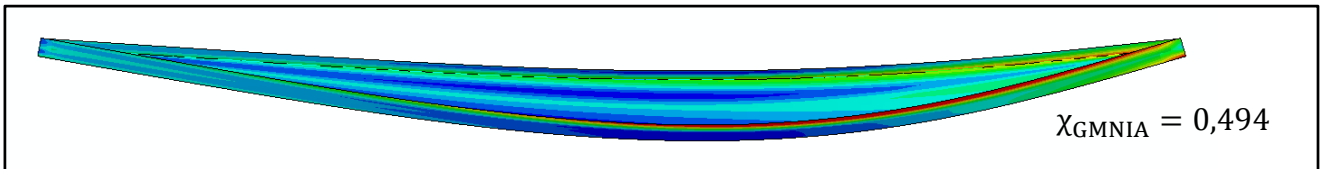


Fig. 30: LTB in case of $k=1,0$ $k_w=1,0$ $\Psi=0$ for IPE 500 section $L=12,5$ m

In Fig. 31 to Fig. 36 are the result the cases for $\Psi=-1$. In cases of “intermediate” members ($L=7,5$ m) the failure behaviour is almost plastic ($\chi_{GMNIA}>0,9$), because of the beneficial effect of the shape of the moment diagram. The symmetric load condition combined with a symmetric support condition ($k=0,5/k_w=0,5$ or $k=1,0/k_w=1,0$) result to a completely symmetric failure shape (Fig. 31; Fig. 33; Fig. 34; Fig. 36).

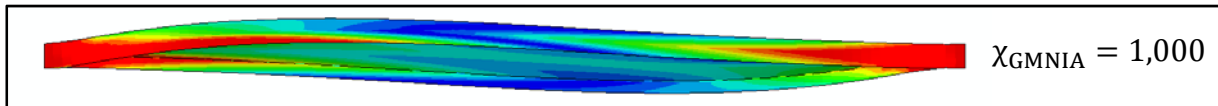


Fig. 31: LTB in case of $k=0,5$ $k_w=0,5$ $\Psi=-1$ for IPE 500 section $L=7,5$ m

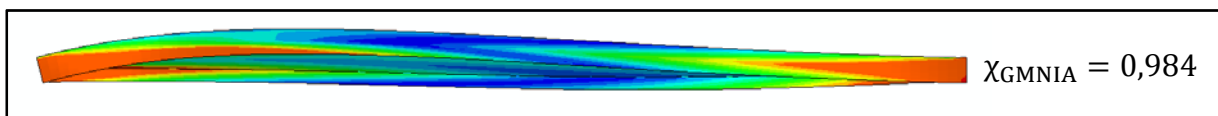


Fig. 32: LTB in case of $k=0,7$ $k_w=0,7$ $\Psi=-1$ for IPE 500 section $L=7,5$ m

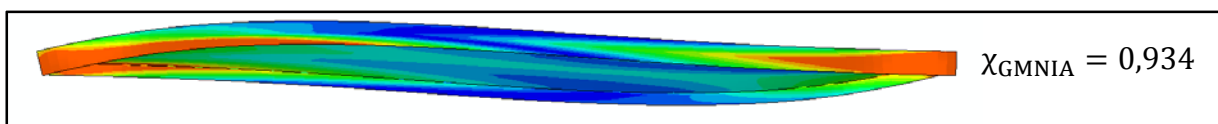


Fig. 33: LTB in case of $k=1,0$ $k_w=1,0$ $\Psi=-1$ for IPE 500 section $L=7,5$ m

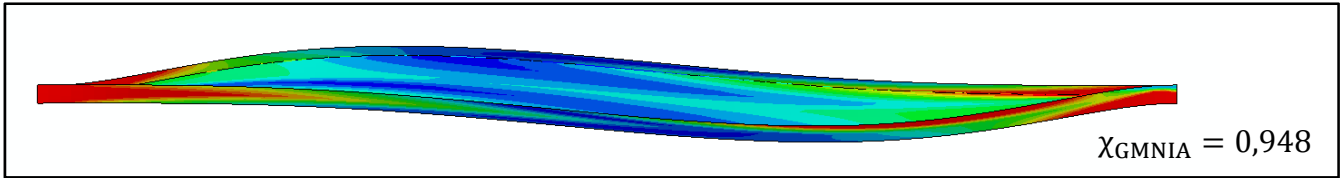


Fig. 34: LTB in case of $k=0,5$ $k_w=0,5$ $\Psi=-1$ for IPE 500 section $L=12,5$ m

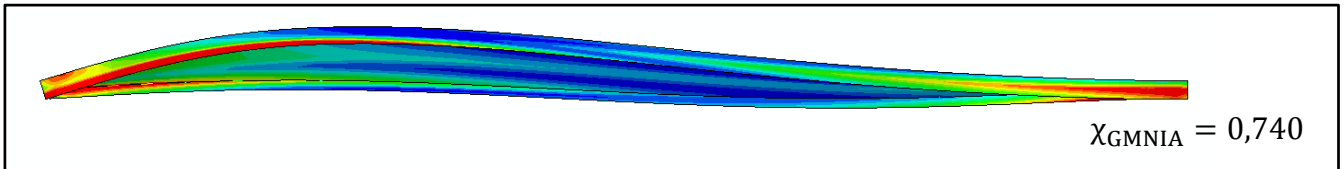


Fig. 35: LTB in case of $k=0,7$ $k_w=0,7$ $\Psi=-1$ for IPE 500 section $L=12,5$ m

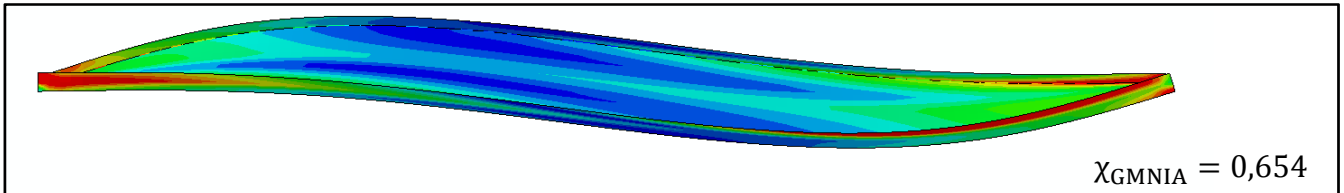


Fig. 36: LTB in case of $k=1,0$ $k_w=1,0$ $\Psi=-1$ for IPE 500 section $L=12,5$ m

The following figures (Fig. 37 to Fig. 42) represent the result of the analyses for section HEB 300, which are similar tendency to the results for section IPE 500. Based on these results one can see that the section HEB 300 is less sensitive to LTB, because the wider and thicker flange makes the section more resistant against to LTB. Based on this fact there are less results with the type of LTB, and the plastic cross section failure is more likely.



Fig. 37: LTB in case of $k=0,5$ $k_w=0,5$ $\Psi=1$ for HEB 300 section $L=4,5$ m

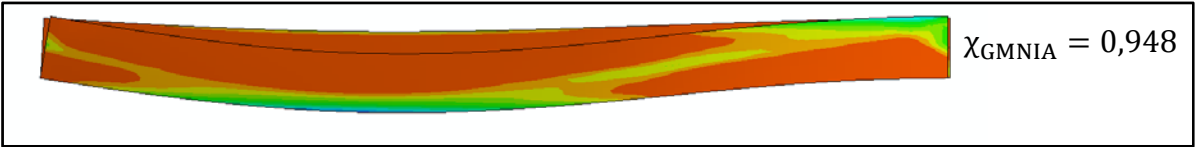


Fig. 38: LTB in case of $k=0,7$ $k_w=0,7$ $\Psi=1$ for HEB 300 section $L=4,5$ m

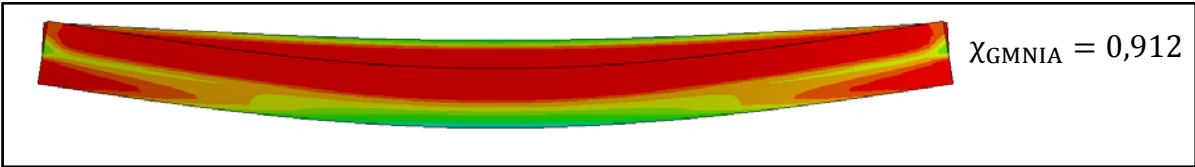


Fig. 39: LTB in case of $k=1,0$ $k_w=1,0$ $\Psi=1$ for HEB 300 section $L=4,5$ m

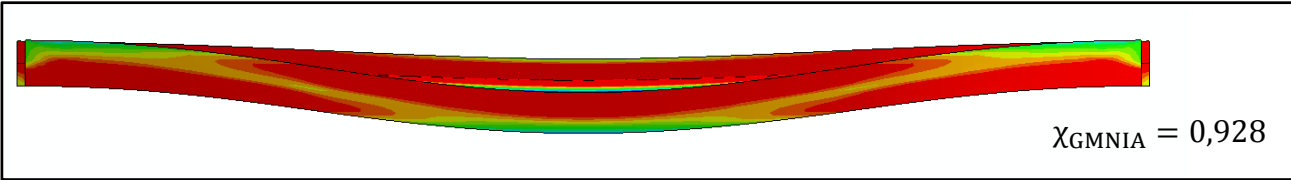


Fig. 40: LTB in case of $k=0,5$ $k_w=0,5$ $\Psi=1$ for HEB 300 section $L=7,5$ m

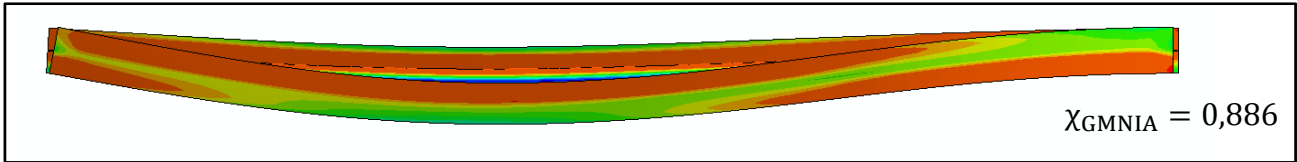


Fig. 41: LTB in case of $k=0,7$ $k_w=0,7$ $\Psi=1$ for HEB 300 section $L=7,5$ m

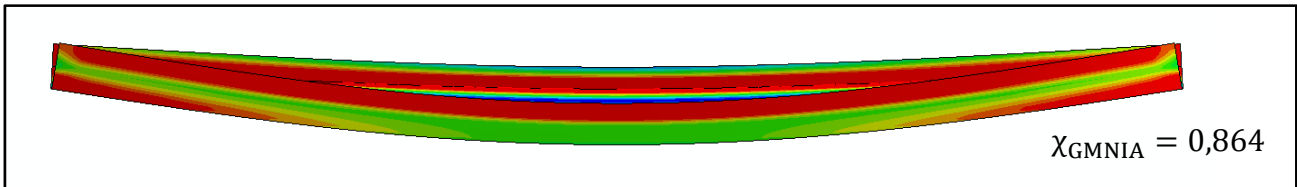


Fig. 42: LTB in case of $k=1,0$ $k_w=1,0$ $\Psi=1$ for HEB 300 section $L=7,5$ m

5.2. GMNIA buckling curves for the support condition $k=0,7$ $k_w=0,7$

Having now shown the general behaviour in LT-buckling for different beams of different slenderness, the following section is dedicated to the shape of the (GMNIA) buckling curves obtained for a boundary condition with one end of the beam fixed against rotation and warping ($k=0,7$, $k_w=0,7$). In all the following figures, the numerical results are compared to both the “general” and the “specific case” buckling curves in EC3; thereby, the f-factor, which accounts for the influence of the bending moment diagram on the reduction factor χ_{LT} , is always applied to both methods.

In Fig. 43 to Fig. 47 the results of GMNIA analyses for the IPE 500 section are compared to the EC3 LTB curves under several boundary conditions. The shape of the bending moment is different in all the cases/diagrams.

Fig. 43 indicates that the GMNIA results fit very accurately with the buckling curve of the “general case” in the case of uniform moment diagram. This means that this buckling curve correctly reflects the member capacity, provided that the member slenderness for LTB is “correctly” determined. On the other hand, the “specific case” LT-buckling curve is up to 15% “unconservative” for this load case and section, indicating that this buckling curve is not able to accurately describe the behaviour and strength of the slender IPE 500 section under constant bending moment.

It shall be noted that the inaccuracy of the “specific case” curves for slender sections and certain load cases was already noted in the literature [16][17][18].

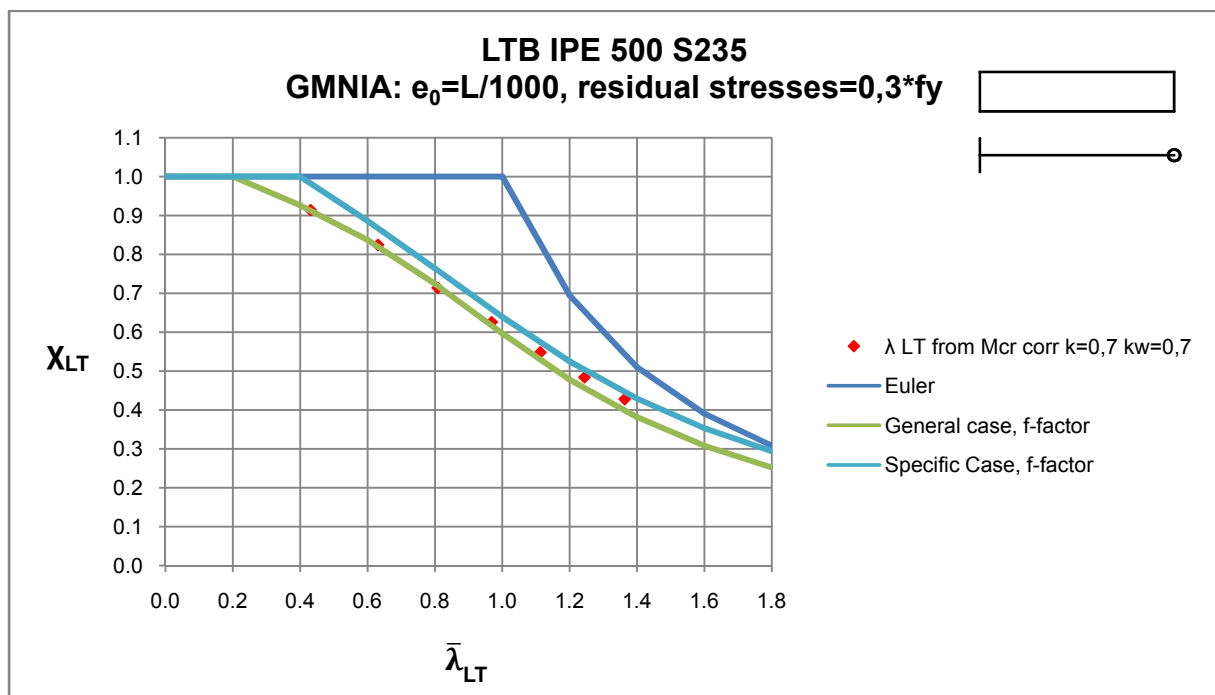


Fig. 43

Fig. 44 illustrates the numerical results for the load case $\psi=0,5$, and the comparison with the European buckling curves shows that the results fit to the “specific case”, in which the “f-factor” was also applied.

In Fig. 44 the GMNIA results of load case $\psi=0,5$ are plotted over two different values of slenderness for LTB. In the first case, the slenderness is “correctly” calculated (by using LTBeam) and in the other case the slenderness is calculated by using the formula (2.6) and by neglecting the benefit obtained from the consideration of end fixities ($k=1,0$ $k_w=1,0$).

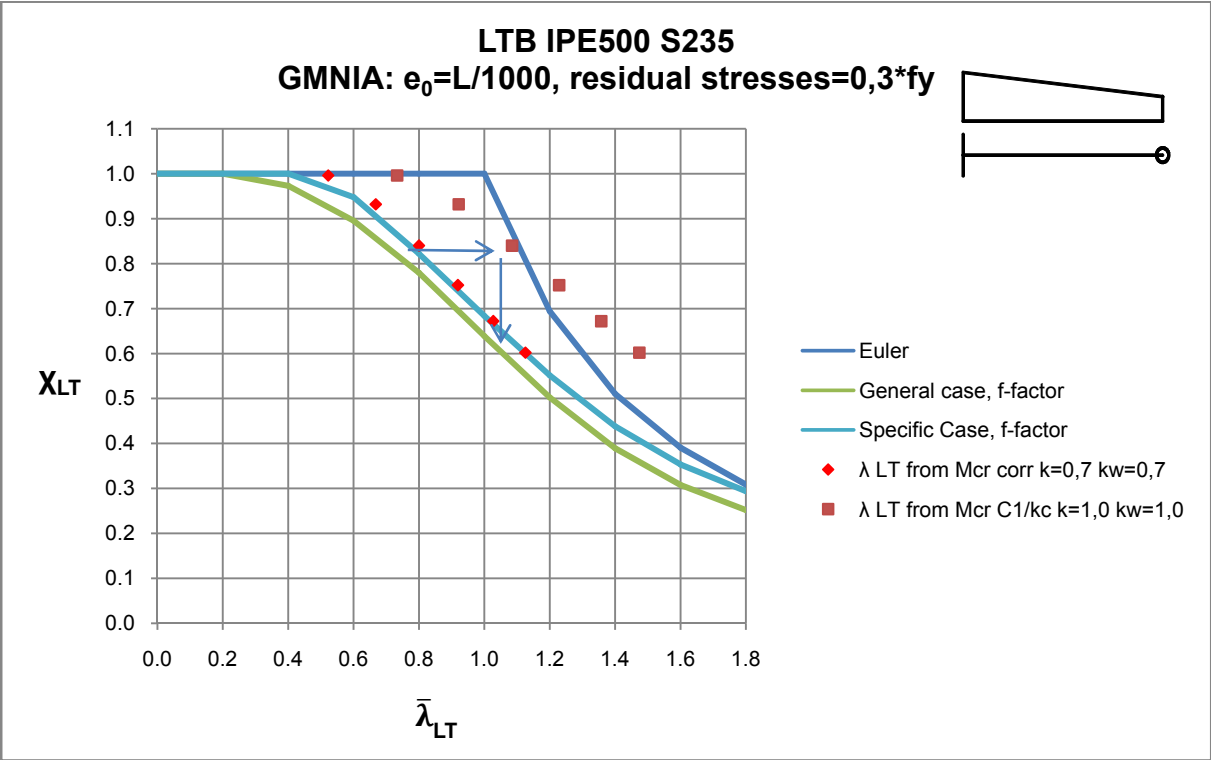


Fig. 44

Fig. 45 shows that the buckling curve of the “specific” case with f-factor again approaches the values of buckling resistance in GMNIA analyses very accurately for loading condition $\psi=0$.

The large advantages obtained in terms of the resistance for LTB of a member due to the presence of end fixations can be discussed by carrying out a comparison of the GMNIA results obtained for the boundary condition $k=0,7, k_w=0,7$ with the EC3 rules and by plotting the GMNIA results over different values of slenderness evaluated for three different support conditions. (Fig. 45)

The three different boundary conditions are:

- $k=0,7, k_w=0,7$ – the “correct” slenderness
- $k=1,0, k_w=0,7$ – an “intermediate” slenderness
- $k=1,0, k_w=1,0$ – the “conservative” slenderness most often used in design

It’s important to note that the same GMNIA results ($k=0,7, k_w=0,7$) were plotted over these three different slendernesses.

It can be noticed that, if any fixity are ignored by the support conditions ($k=1,0, k_w=1,0$), the member slendernesses are much higher than with the calculation of the “real” support conditions, thus the design value of the buckling resistance according to EC3 would be thought to be about 50% lower than it actually is.

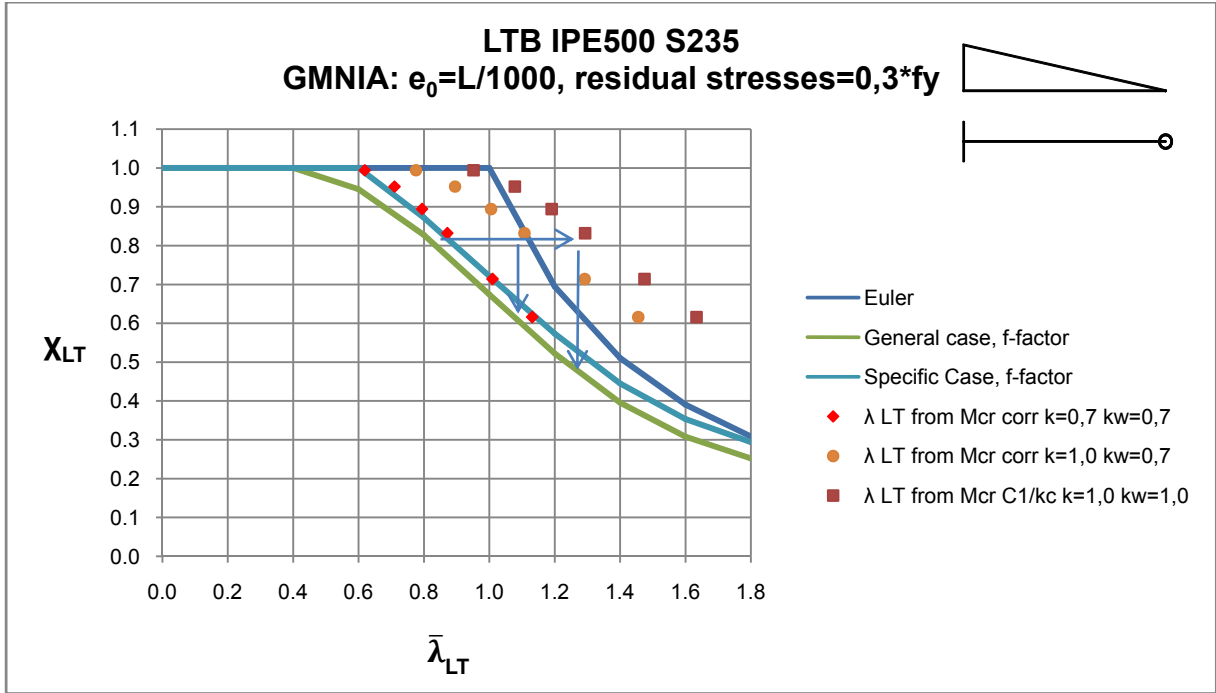


Fig. 45

Fig. 46 represents the GMNIA results for loading case $\psi=-0,5$, for which the buckling curve of the “specific” case is again inaccurate (and unconservative) for slendernesses $0,8 < \bar{\lambda}_{LT}$ if the member slenderness for LTB is calculated “correctly”.

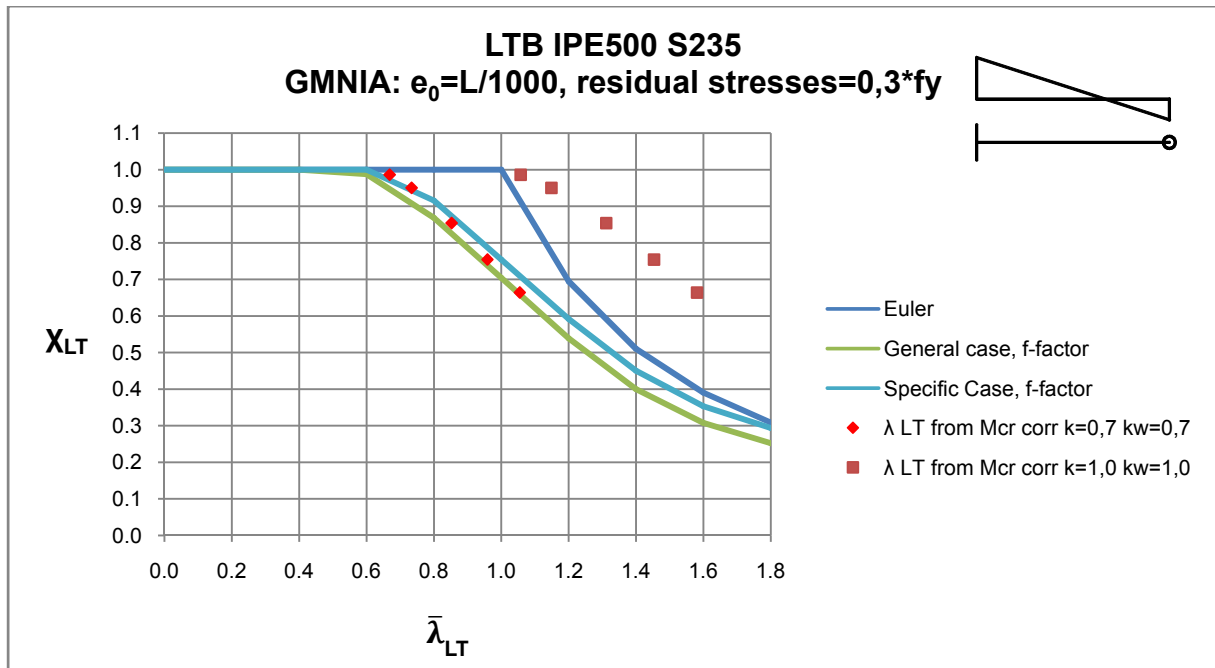


Fig. 46

In Fig. 47 the modelling result are presented for the load case $\psi=-1,0$. For this boundary condition the “specific” case with the f-factor is unconservative compared to every GMNIA results.

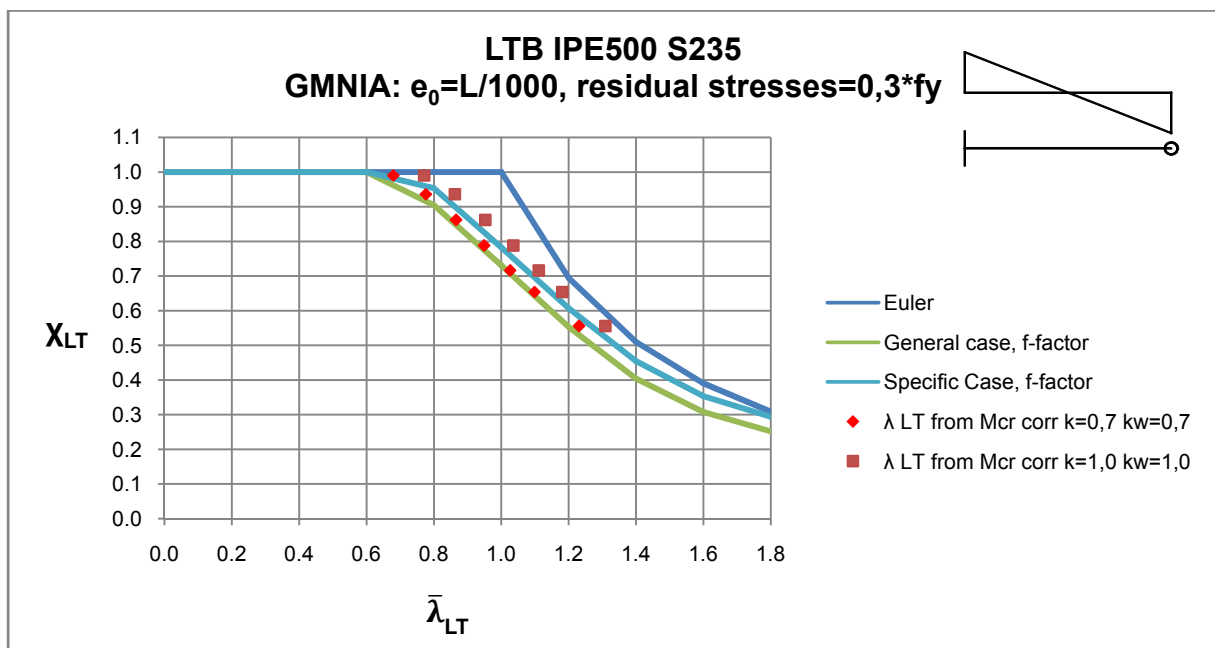


Fig. 47

In Fig. 48 to Fig. 52. the GMNIA results for section HEB 300 are plotted, and these results are compared to the EC3 buckling curves for LTB. In the case of these analyses the relation between the curves and the GMNIA values are relatively similar to the cases for section IPE 500.

Again, the “specific case” is shown to be unconservative for the load case with constant bending moment diagram, see the following Fig. 48. The “general case” is far more accurate for this section.

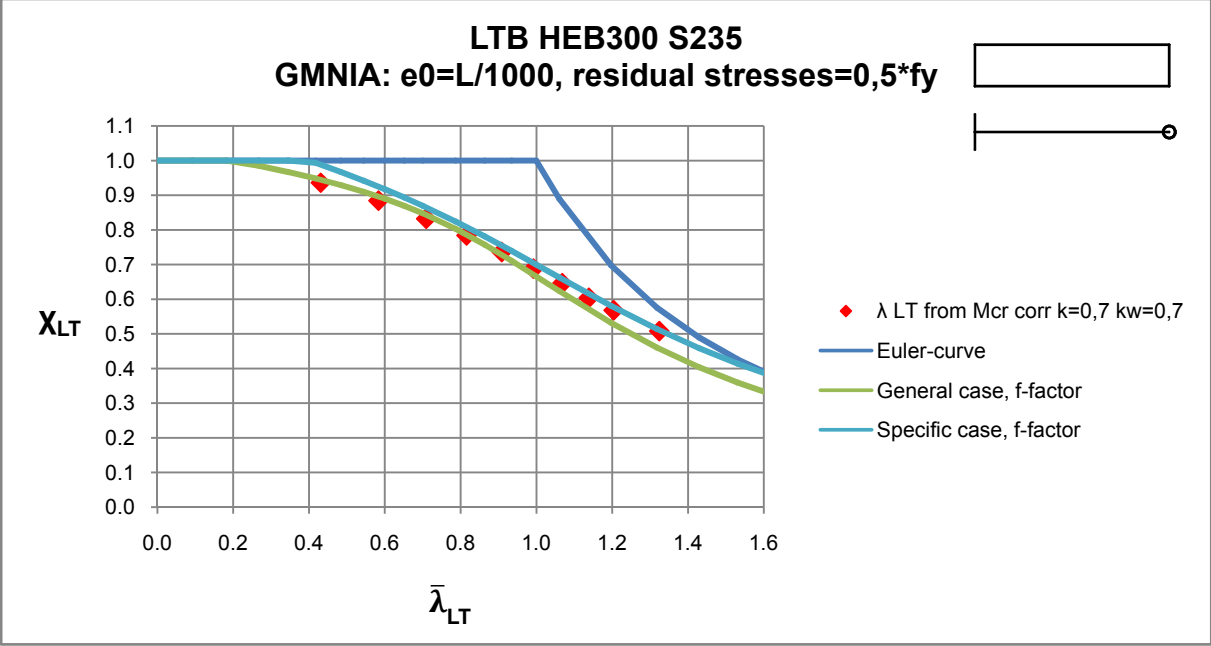


Fig. 48

As is indicated in Fig. 49, both of the buckling curves are on the safe side for load condition $\psi=0,5$ and for section HEB 300, and the “specific” case is more accurate, than the “general” case. The same phenomena have been noticed previously for section IPE 500 (Fig. 44).

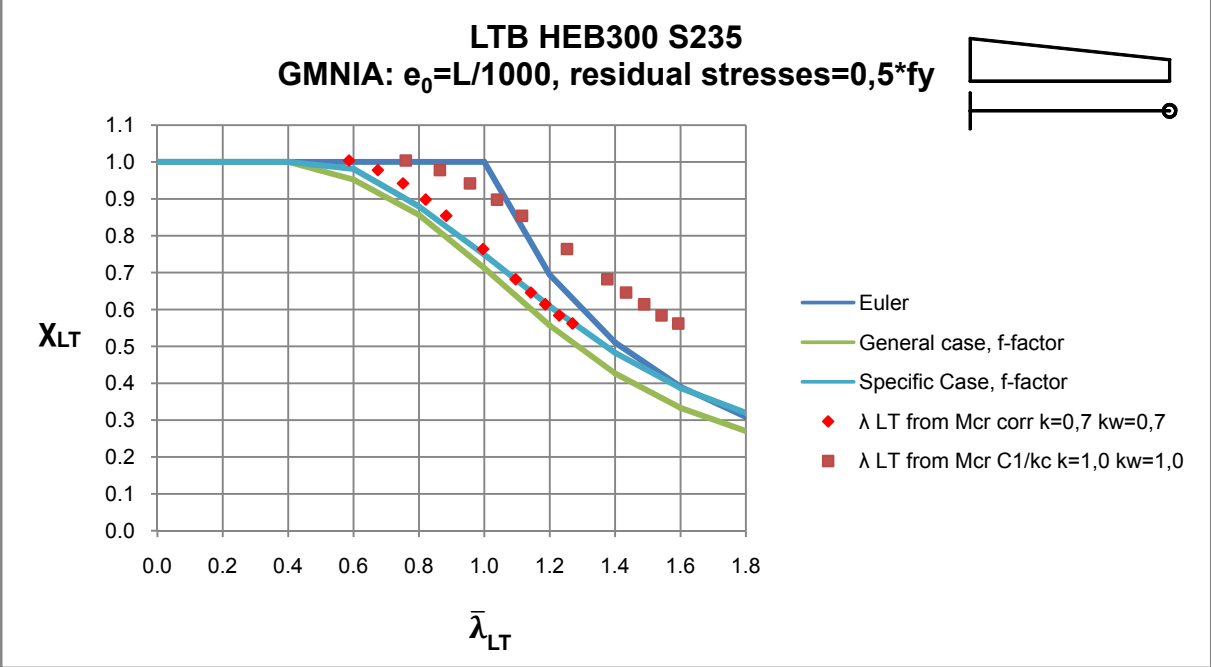


Fig. 49

The buckling curve of the “specific” case is on the “unconservative” side for higher slendernesses ($0,8 < \bar{\lambda}_{LT}$), as it is indicated in Fig. 50.

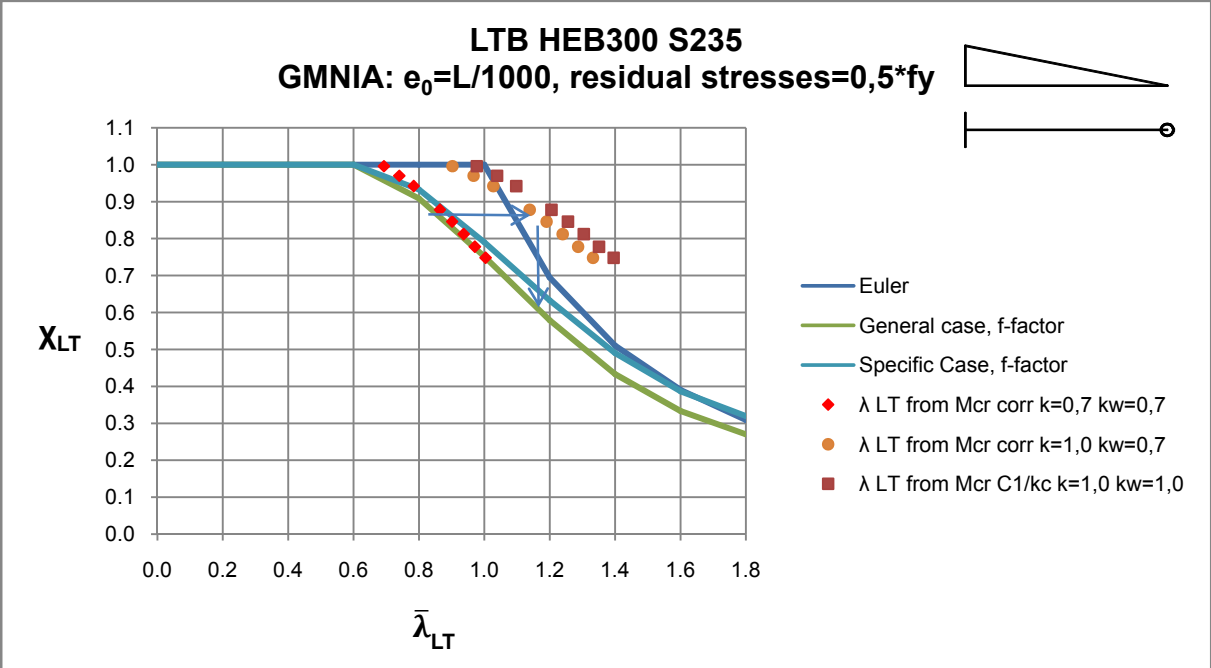


Fig. 50

The first case, in which the GMNIA results were lower, than the values of the buckling curves of the “general” case according to EC3 are plotted in Fig. 51. Theoretically these result show that the EC3 curves are not on the safe side, but these slendernesses for LTB refer to extremely long ($L > 20$ m) members, so practically there is no significant risk.

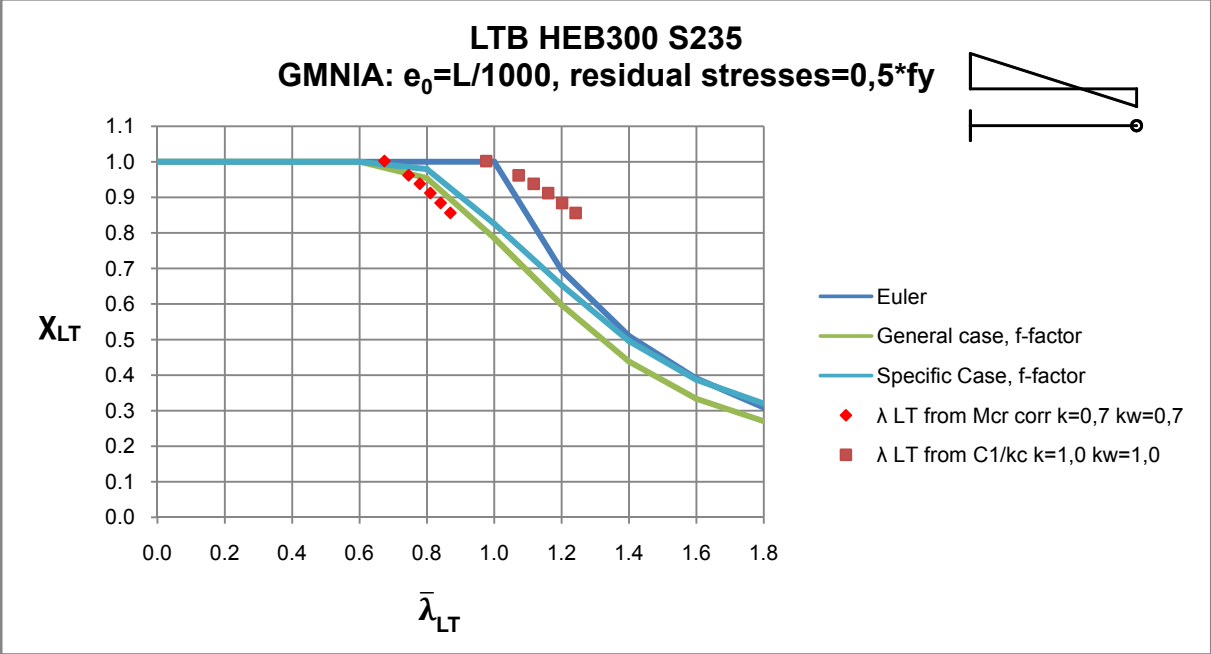


Fig. 51

In Fig. 52 the buckling curve of the “general” case is “unconservative” for slendernesses $0,8 < \bar{\lambda}_{LT} < 0,9$. Notice, however, that the slendernesses where LT-buckling becomes relevant at all refer to very long ($L > 20$ m, $L/b > 65$) members.

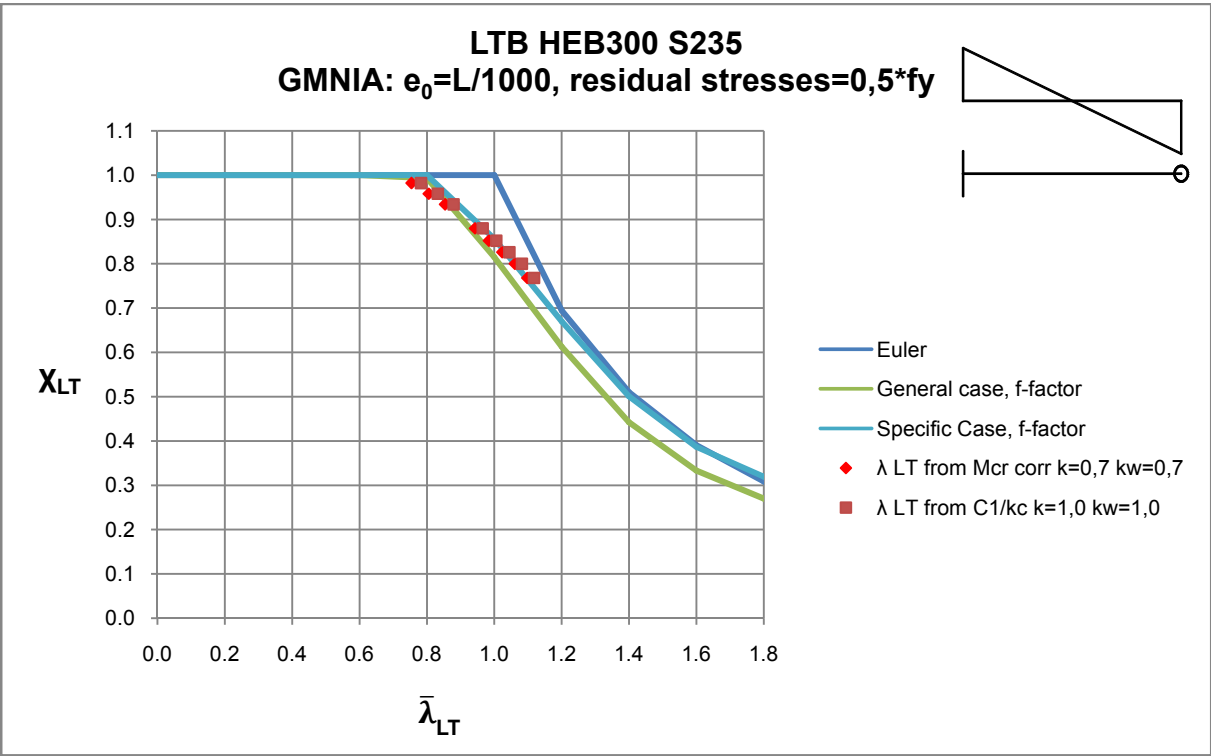


Fig. 52

5.3. GMNIA analyses for cases with equal slenderness for LTB

In Tab. 28 two different GMNIA analyses are compared where the member length and the boundary conditions were different. In Case 2 the member length was “chosen” (by iteration in LTBeam) so that the value of the critical bending moment became the same in both cases. In this way the slenderness of the two members is the same under completely different boundary conditions, which means the same resistance to LTB according to EC3. The load case in both cases was a constant bending moment with $\psi=1,0$.

Based on the GMNIA results it can be noticed that the resistance values of χ_{GMNIA} in both cases are unsignificantly different. However this is only one specific comparison, but it can be noted that the resistance is influenced by the boundary conditions and not only governed by the slenderness for LTB.

Although this analysis showed a slight difference between the two cases, it can be stated that the (correct) slenderness can be confirmed to be an excellent parameter to describe the LT buckling strength of a member, at least for cases with the same load case, but with different boundary conditions.

Tab. 28: Comparison of two cases with the same slendernesses, but different boundary conditions

IPE 500 section	Case 1	Case 2
L (mm)	5000	7150
k	1.0	0.7
k_w	1.0	0.7
Ψ	1.0	1.0
M_{cr,FEM} (kNm)	558.81	558.81
$\bar{\lambda}_{LT,corr}$	0.96	0.96
χ_{GMNIA}	0.632	0.628

5.4. Conclusions

The following conclusions can be drawn from the Geometrically and Materially Nonlinear Analyses with Imperfections (GMNIA) described in this section of the thesis:

- In most of the cases the numerical results are on the conservative (safe) side of the buckling curves according to EC3. Based on this result, the buckling curves for members with double symmetric I cross-sections – which are valid under “fork conditions” ($k=1,0$ $k_w=1,0$) – can be used in practical design even if the member slenderness for LTB is calculated “correctly” for the case of support condition $k=0,7$ $k_w=0,7$. This is particularly true for the “general case” buckling curves, while for the “specific case” some more “unconservative” cases were noted.
- Under non-uniform bending moment loading the resistance to LTB is higher compared to the case of uniform bending moment loading for the same member.
- The restraint of rotation and warping at the end of the member increases the resistance to LTB. The higher the “level” of restraint (k/k_w from 1,0 to 0,5 is more restrained) the higher is the resistance to LTB.
- In practical design, the loading and support conditions can be taken into account only at the calculation of slenderness $\bar{\lambda}_{LT}$, which result in a less slender member with a higher resistance and higher value of χ_{LT} . According to EC3 there is no factor which takes into account the different boundary conditions at the correlation between $\bar{\lambda}_{LT}$ and χ_{LT} , which means members with the same slenderness for LTB have the same resistance even if they are under completely different boundary conditions. Additional benefits could be achieved if e.g. the factor f (which accounts for the bending moment diagram on the resistance term
- Under the same boundary conditions and length members with wide-flanged H sections are less sensitive to LTB than narrow-flange I sections because of the wider and thicker flanges.

6. Interaction concept for beam columns **(compression and bending, GMNIA)**

Beam-columns are defined as members subjected to combined compression and bending. In practical design, the members of frame structures are treated as beam-columns, because the columns are subjected to the combination of both type of these loads (primary load: compression, secondary load: bending) and the beams (primary load: bending, secondary load: compression) as well. [1]

The behaviour of beam-columns is similar to the behaviour of columns or beams depending on the slenderness:

- stocky members: plastic cross sectional failure
- members with intermediate slenderness: elasto-plastic stability failure governed by the geometrical and material imperfections
- members with high slenderness: elastic behaviour stability failure

For the treatment of the beam-column behaviour the main issue is the consideration and formulation of the **interaction of compression and bending**, because these effects cannot be linearly superposed in most cases. The accurate formulation of the interaction is crucial because the two effects can reduce or increase the influence of each other. [16]

According to EC3 there are two different concepts in order to calculate the interaction behaviour of beam-columns:

- The **interaction concept**, and
- The **overall concept** (“overall slenderness”, “general method”)

In this chapter, the main topic is the interaction concept, while the overall concept is the focus of Chapter 7.

In the interaction concept, the utilizations for compression (flexural buckling) and bending (LT-buckling) are added together with the use of interaction **multiplier k** by the bending term [19]:

$$\frac{N_{Ed}}{N_{pl}\cdot\chi/\gamma_{M1}} + k \cdot \frac{M_{Ed}}{M_{Rk}\cdot\chi_{LT}/\gamma_{M1}} \leq 1,0 \quad (6.1)$$

In EC3, two methods are given for the calculation of the interaction factors k [1]:

- Method 1 developed by a group of French and Belgian researchers
- Method 2 developed by a group of Austrian and German researchers

In the following parts of the chapter only the Method 2 will be introduced.

In EC3 there are four different interaction formulae depending on the buckling mode and the torsional restraints.

From the aspect of **torsional restraints** there are [19]:

- torsionally stiff members (for example: circular hollow sections; failure: flexural buckling)
- torsionally flexible members (for example I and H sections without intermediate torsional restraints; failure: LTB)

From the aspect of buckling mode there are [19]:

- buckling about the strong axis (y-y)
- buckling about the weak axis (z-z)

In this work the IPE 500 and HEB 300 sections were investigated in the case of LTB without intermediate restraints, which are therefore buckling about the weak axis.

In this case, the verification of the member **buckling resistance** according to the EC3 ("Eq. 4") is always given by the following expression [19]:

$$\frac{N_{Ed}}{\chi_z \cdot N_{pl,Rd}} + k_{LT} \cdot \frac{M_{y,Ed}}{\chi_{LT} \cdot M_{pl,y,Rd}} \leq 1,0 \quad (6.2)$$

6.1. Interaction factor k_{LT}

The **interaction factor** in the buckling case of LTB and buckling about the weak axis is [19]:

$$k_{LT} = 1 - \frac{0,1 \cdot \bar{\lambda}_z \cdot n_z}{C_{mLT} - 0,25} \geq 1 - \frac{0,1 \cdot n_z}{C_{mLT} - 0,25} \quad (6.3)$$

$$\text{and for } \bar{\lambda}_{LT} \leq 0,4: k_{LT} = 0,6 + \bar{\lambda}_{LT} \quad (6.4)$$

with n_z , which is the utilization factor for the weak-axis flexural buckling term:

$$n_z = \frac{N_{Ed}}{\chi_z \cdot N_{pl,Rd}} \quad (6.5)$$

The effect of the **shape of the bending moment diagram** is implicit in the factor k_{LT} and considered by the **factor C_{mLT}** , which in the case of constant moment diagram can be calculated as follows [19]:

$$C_{mLT} = 0,6 + 0,4\Psi \geq 0,4 \quad (6.6)$$

6.2. Plotting the n-m interaction curves according to EC3

The basic type of plot used to illustrate the interaction behaviour of a beam-column under N+M is a representation in the **n-m coordinate system**, where the vertical axis is n and the horizontal axis is m; these variables are described below. One point of the n-m coordinate system means a specific combination of compression and bending moment according to the plastic resistance.

The interaction curve plots the points for the maximum obtainable values for n and m:

$$n = \frac{N_{Ed}}{N_{pl,Rd}} \quad (6.7)$$

$$m = \frac{M_{y,Ed}}{M_{pl,y,Rd}} \quad (6.8)$$

Accordingly, the maximum obtainable value of bending moment can be calculated if the value of compression is fixed (and vice versa).

In order to plot the interaction curve according to EC3 the unequation (6.2) has to be set equal to 1.0 (definition of failure) and rewritten as follows:

$$\frac{N_{Ed}}{\chi_z \cdot N_{pl,Rd}} + k_{LT} \cdot \frac{M_{y,Ed}}{\chi_{LT} \cdot M_{pl,y,Rd}} = n \cdot \frac{1}{\chi_z} + m \cdot k_{LT} \cdot \frac{1}{\chi_{LT}} = 1,0 \quad (6.9)$$

In Eq. (6.9) there are two variables, which are n and m. If the variable n is chosen arbitrarily (several values from 0 to χ_z), the variable m can be calculated using the following formula:

$$m = \left(1 - \frac{n}{\chi_z}\right) \cdot \frac{\chi_{LT}}{k_{LT}} \quad (6.10)$$

In this way the interaction curves according to EC3 can be plotted in all cases.

6.3. Input and output of GMNIA for beam-columns

When defining load parameters for GMNIA analyses to be plotted in the n-m interaction diagram, it is important that the results describe the behaviour in the n-m coordinate system with the same “density” for different ratios of n/m. The unit quarter circle (radius=1,0) was divided into eight parts in order to have an equal distribution of load cases. In this way the result was nine different load cases, i.e. combinations of n and m.

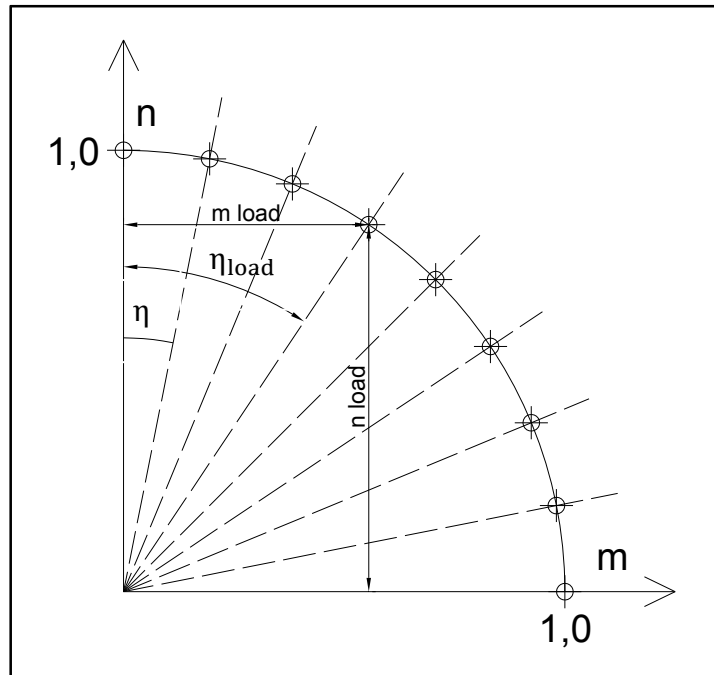


Fig. 53: Distribution of load inputs in parametric studies of interaction curves

In Fig. 53 the defined reference load cases are illustrated, where all points have n_{load} and m_{load} coordinates, which describe the value of compression and bending moment applied in the GMNIA calculations:

$$n_{load} = \frac{N_{Ed}}{N_{pl}} \quad (6.11)$$

$$m_{load} = \frac{M_{Ed}}{M_{pl}} \quad (6.12)$$

Accordingly, every load case is “fully” described by the “direction angle” of the line, which is:

$$\eta_{load} = \frac{m_{load}}{n_{load}} \quad (6.13)$$

In this explanation if $\eta_{load}=0$, that means $n=1$ and $m=0$ (pure compression) and if $\eta_{load}=\infty$, that means $n=0$ and $m=1$ (pure bending). The angle η can thus be interpreted

as a load eccentricity (M_{Ed}/N_{Ed}), normalized by the plastic core dimension (M_{pl}/N_{pl}) of the section.

From the definition in Eq. (6.13) comes the value of bending moment, which is:

$$m_{load} = \eta_{load} \cdot n_{load} \quad (6.14)$$

$$n_{load}^2 + m_{load}^2 = 1 \quad (6.15)$$

Eq (6.15) can be modified into:

$$n_{load}^2 + (\eta_{load} \cdot n_{load})^2 = 1 \quad (6.16)$$

and

$$n_{load}^2 \cdot (1 + \eta_{load}^2) = 1 \quad (6.17)$$

From the expression in Eq. (6.17) comes the value of compression, which is:

$$n_{load} = \left(\frac{1}{(1 + \eta_{load}^2)} \right)^{\frac{1}{2}} \quad (6.18)$$

As a result of the GMNIA analyses, the **load proportionality factor (LPF)** is obtained for every case. The LPF is the ratio between the aimed load and the reached level of input load (the resistance):

$$LFP = \frac{n}{n_{load}} = \frac{m}{m_{load}} \quad (6.19)$$

Fig. 54 illustrates the definition of the LPF.

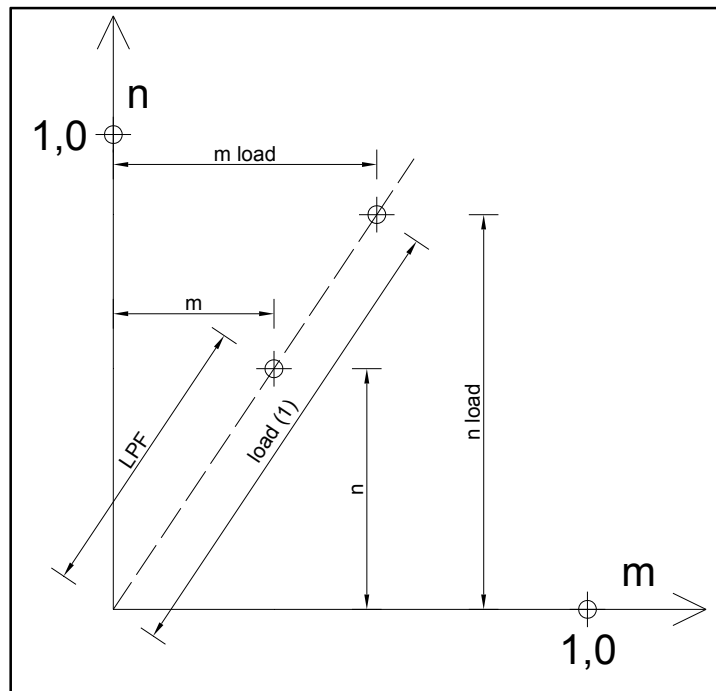


Fig. 54: Definition of Load Proportionality Factor

Based on the LPF the maximum obtainable values of compression and bending are:

$$m = n_{\text{load}} \cdot \text{LPF} \quad (6.20)$$

$$m = m_{\text{load}} \cdot \text{LPF} \quad (6.21)$$

In this way the results of GMNIA analyses can be plotted in the n-m coordinate system.

6.4. GMNIA analyses for beam-columns

In this subsection the results of GMNIA analyses of beam-columns for several different cases are introduced. The results are plotted in the n-m coordinate system and are compared to the curves according to EC3.

The “variables” in the parametric studies were the following:

- cross section: IPE 500 or HEB 300
- slenderness: $\bar{\lambda}_z = 0,5$; $\bar{\lambda}_z = 1,0$ or $\bar{\lambda}_z = 1,5$ (calculated for $k=0,7$)
- load conditions: $\Psi=1,0$; $\Psi=0$ or $\Psi=-1,0$
- support conditions:
 1. $k=0,7$ $k_w=0,7$
 2. $k=0,7$ $k_w=0,7$
 3. $k=1,0$ $k_w=1,0$

The following points were treated in the same manner in all plots:

- the reduction factor χ_{LT} for LT-buckling was always calculated with the “specific case” curves.
- The GMNIA calculations were carried out for a clearly defined boundary condition and load case. The Eurocode curves (i.e. the evaluation of the interaction formulae) were plotted for either exactly the boundary condition considered in the GMNIA calculation, or for “more conservative” boundary conditions; the latter was done to illustrate the gains that are obtained from applying the Eurocode “as it is”, but by considering the “true” boundary conditions.

In Fig 55. the results for the basic studied case ($k=0,7$ $k_w=0,7$) are compared to the Eurocode curves for cases $k=0,7$ $k_w=0,7$ and $k=1,0$ $k_w=0,7$ under the same member length.

In the case of $k=0,7$ $k_w=0,7$ the member slenderness for LTB was calculated correctly by using the first eigenvalue in the LBA analyses. Based on Fig. 55, the results fit fairly accurately to the curve according to EC3, with the exception of the point where $n=0$

(pure bending), for which it was already discussed that the “specific case” LT buckling curves may not be conservative in all cases.

If the Eurocode formula is evaluated of $k=1,0$ $k_w=1,0$ the beneficial effect gained from the support conditions (rotational and warping fixation) are neglected, thus the calculated member resistance is also lower.

The slenderness for LTB was calculated by using Eq. (3.6), and χ_{LT} was calculated by using the “specific case” formulation combined with Eq. (5.2) (f -factor) in all cases.

In Fig. 55 the difference between the resistance in two case is indicated, which is approximately 10 to 15% .

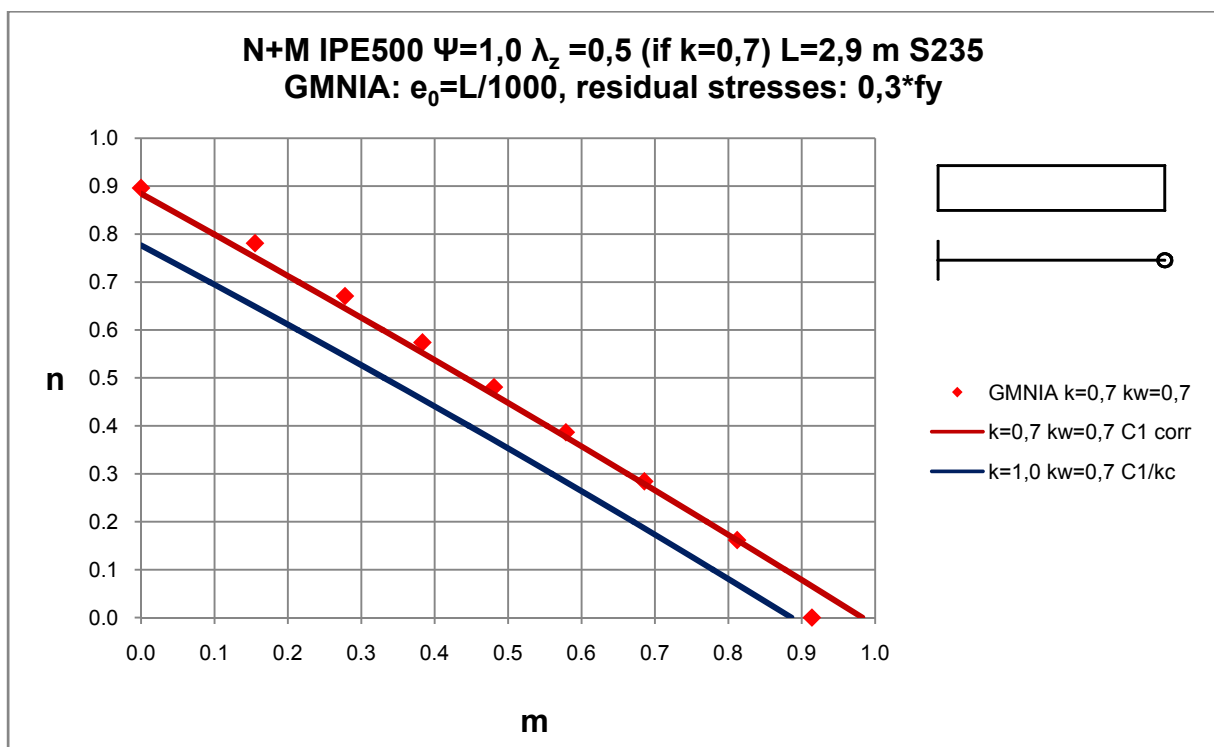


Fig. 55

In Fig. 56 and Fig. 57 the GMNIA-results for the case of constant bending moment diagram are represented for more slender members. In the vertical (n-) axis the curves - and the GMNIA-results as well - are reaching the values of resistance for flexural buckling (pure compression), in addition in the horizontal (m-) axis the values of resistance for LTB (pure bending).

Between these two intersections the curves are almost linear, but the distributions of GMNIA-results are slightly curved from above.

In addition to cases $k=0,7$ $k_w=0,7$ and $k=1,0$ $k_w=1,0$ one more case is shown, this is $k=1,0$ $k_w=0,7$. Under this support condition the rotation is not restrained on both sides, and the warping is one-sidedly restrained. This “intermediate” case was investigated in order to illustrate the different influence of the rotational and warping fixation on the resistance.

Fig. 56 and Fig. 57 indicate that the rotational fixation has more influence on the resistance than the warping fixation. In addition, the warping fixation affects the resistance only when bending/LT-buckling is clearly dominant (by pure compression not at all).

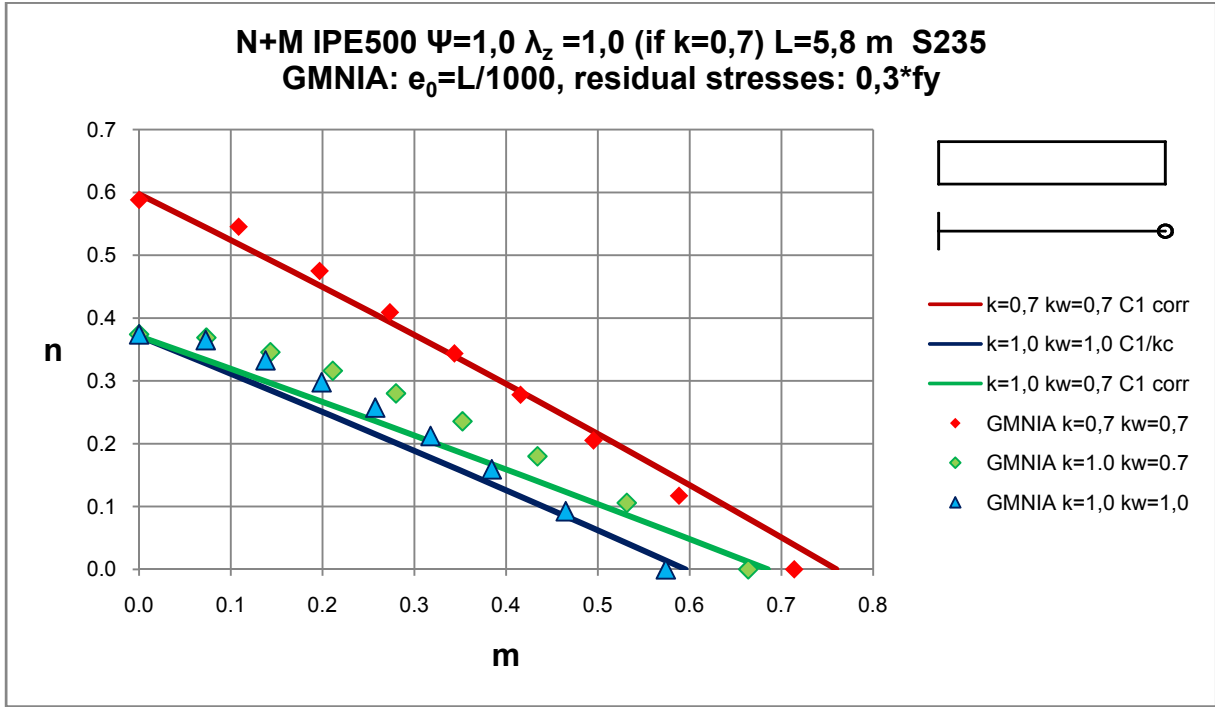


Fig. 56

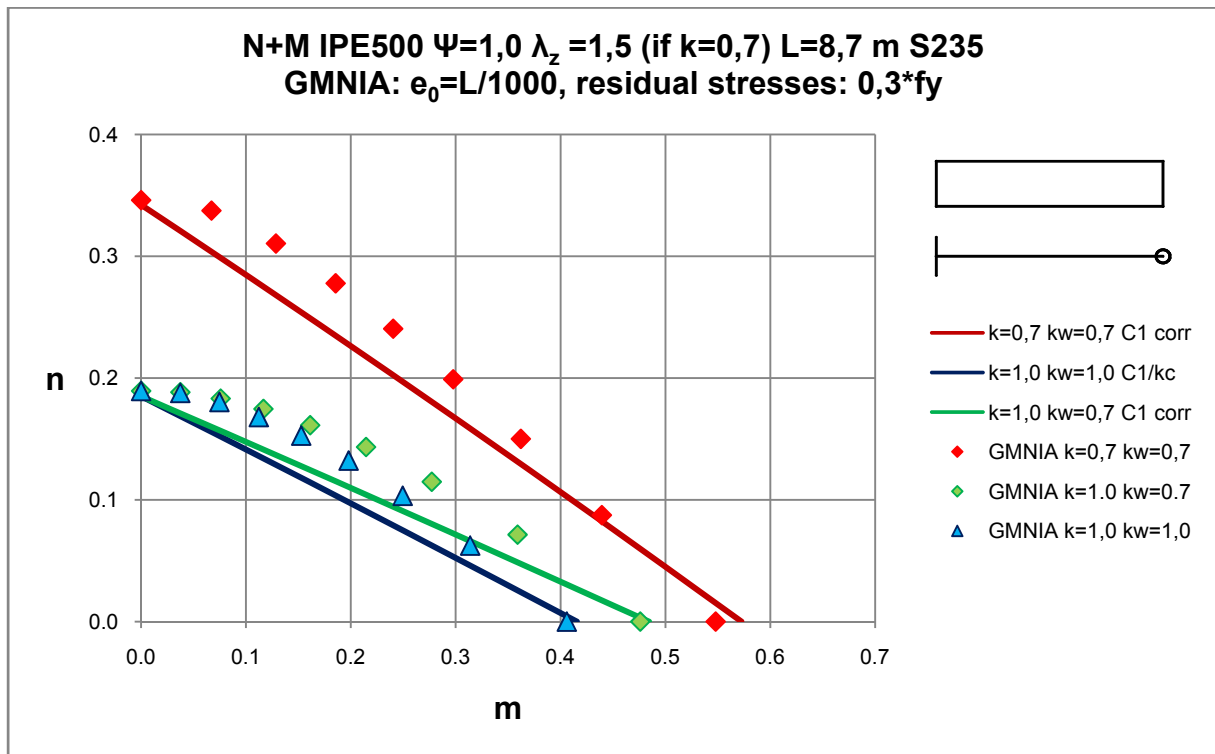


Fig. 57

In Fig. 58 the case of a stocky member loaded by a triangular bending moment diagram ($\psi=0$) is illustrated, where the support conditions have less influence on the resistance when bending is dominant (in pure bending there is no influence at all), because the type of the failure is plastic cross section failure (and not elastic-plastic stability failure). This is due to the fact that the buckling reduction factor $\chi_{LT}=1.0$ regardless of the considered boundary condition. Nevertheless, the Eurocode curves would approximate the realistic GMNIA calculation results (obtained for $k=0.7$ and $k_w=0.7$) far better if the boundary condition for flexural buckling were considered correctly.

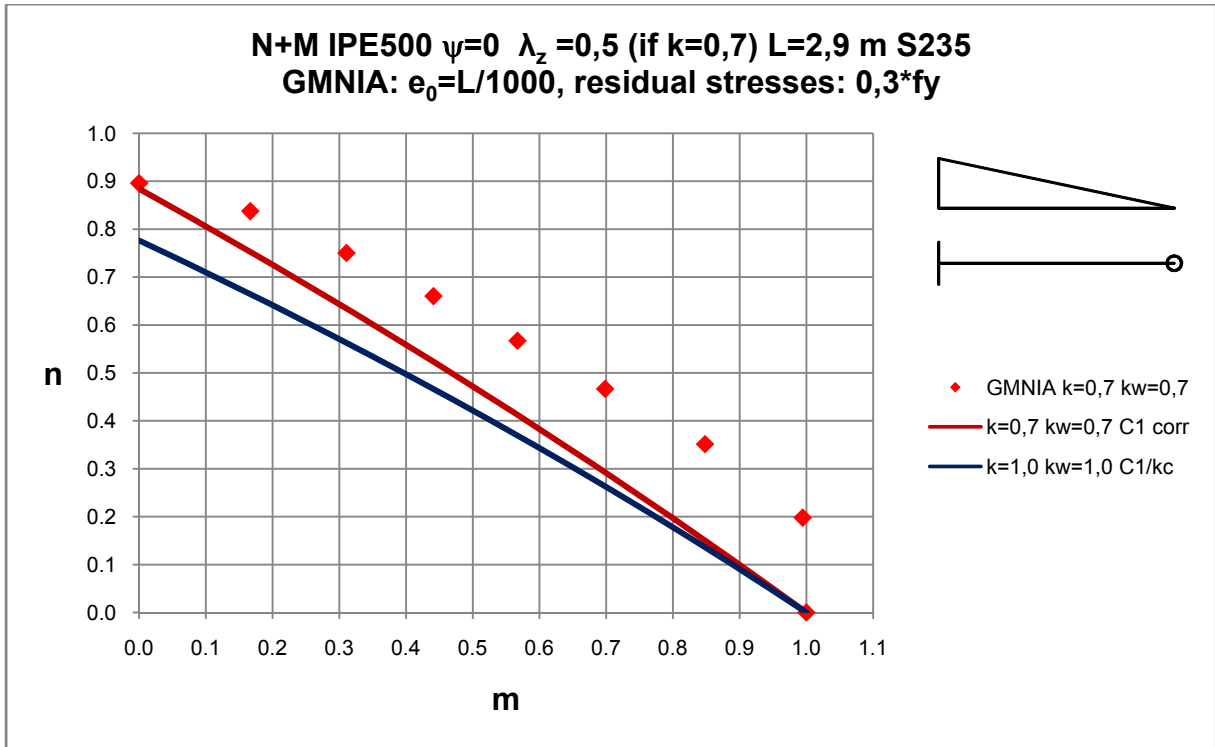


Fig. 58

In Fig. 59 and Fig. 60 the difference between the three cases are similar to the results in Fig. 56 and Fig. 57, even though the buckling reduction factor χ_{LT} is much higher due to the far more beneficial bending moment diagram.

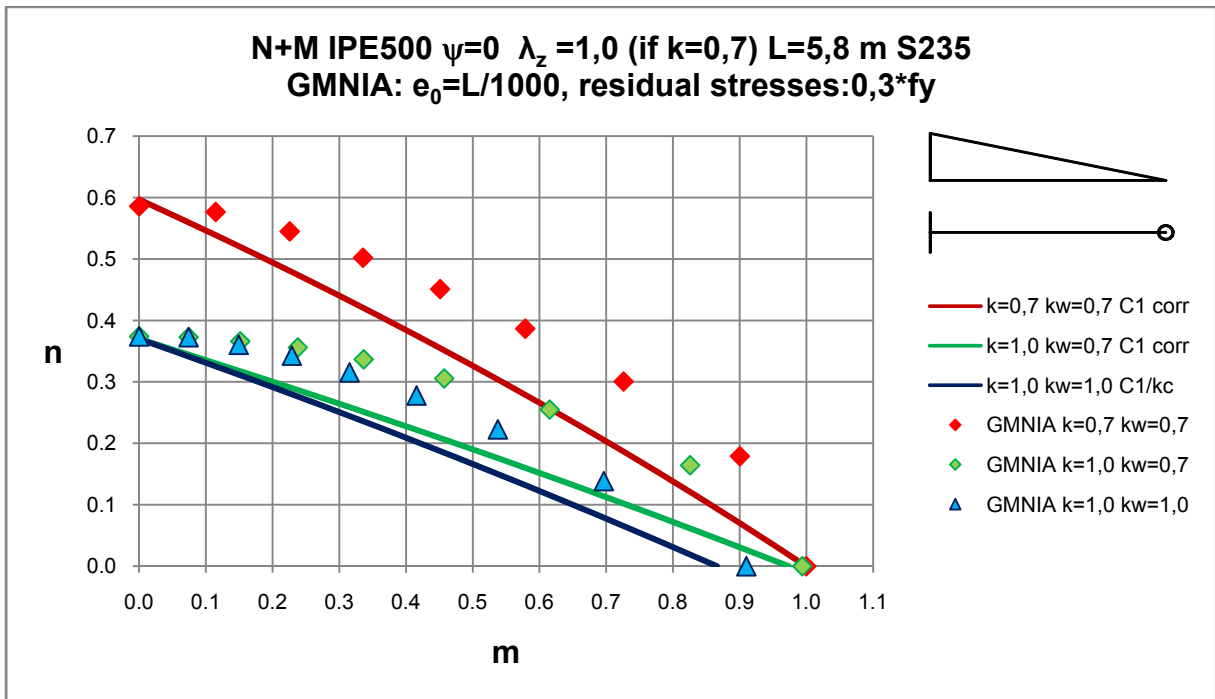


Fig. 59

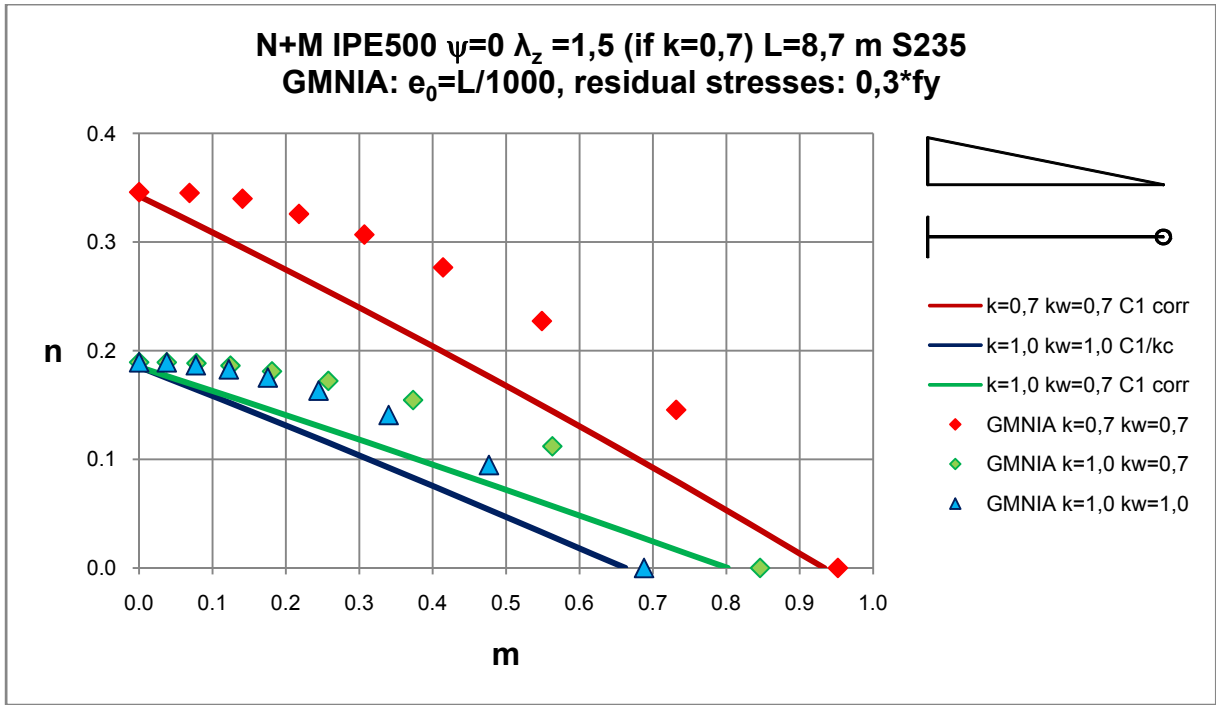


Fig. 60

In Fig. 61 It can be seen that the GMNIA analyses indicate a different behaviour of a very stocky member loaded by a sign-changing bending moment diagram and no axial force; the failure mode here is a plastic cross sectional shear failure under dominant bending. The cause of the failure is that the member is relatively short, so the shear forces are very high and local shear failure occurs under pure bending.

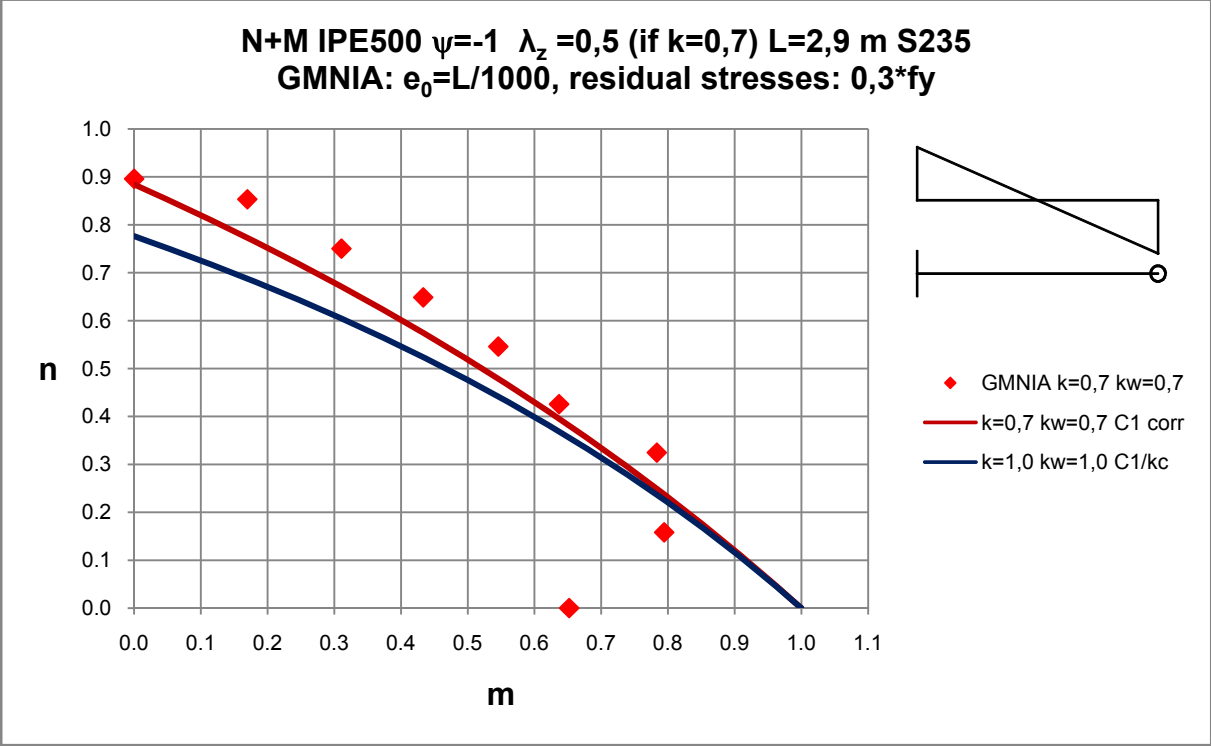


Fig. 61

The GMNIA result and the failure mode is shown in Fig. 62 for the case $n=0$ $m=1,0$ ($\chi_{GMNIA}=0,65$).

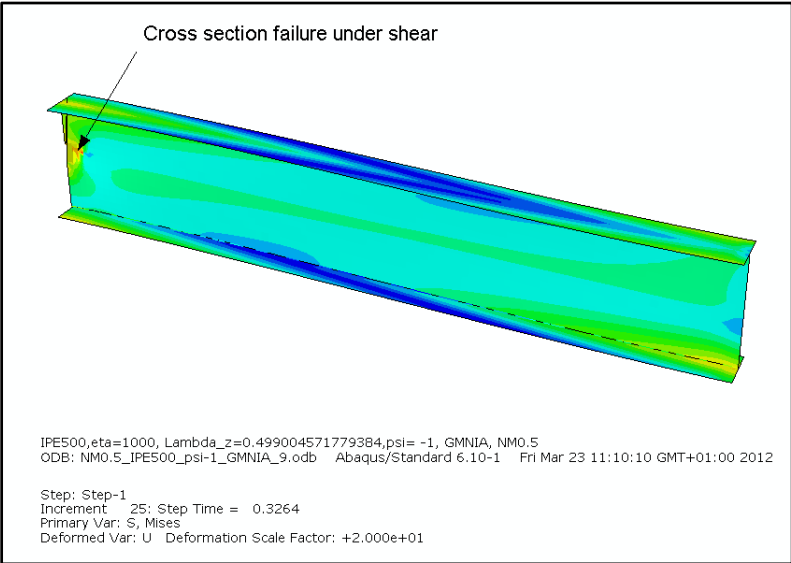


Fig. 62: Cross section failure of a stocky member under shear

In Fig. 63 and Fig. 64 one can see that the warping fixation has very little influence on the resistance of members of realistic length, loaded by sign-changing bending moment diagrams, and when bending is dominant also the rotation does not affect the ultimate strength, because the failure is fully (or near to) plastic and it is not a stability failure.

More interestingly, one can see that for slender members, particularly when no end fixations are considered, the sign-changing bending moment diagram is rather poorly described by the Eurocode interaction curves. These curves, which are dominated by the factor k_{LT} , always have the tendency to (near-) linearly fall from the value χ_z to the value χ_{LT} , with only a very slight upward bend of the curve even in extreme bending moment cases such as a linear case with $\psi=-1.0$.

The GMNIA calculations, however, showed that there is hardly any interaction between N and M for this load case, slender columns and lower values of M; this is represented by the near horizontal distribution of the GMNIA results for the cases with $k=1,0$. This can be explained by the fact that the failure location for these boundary conditions and low bending moment is at mid-span, where the moment is zero. With higher m, the failure location moves farther toward the member ends.

In the case where $k=0,7$, the failure location for weak-axis flexural buckling is also not at mid-span, so there is immediately a (small) interaction with even small values of m.

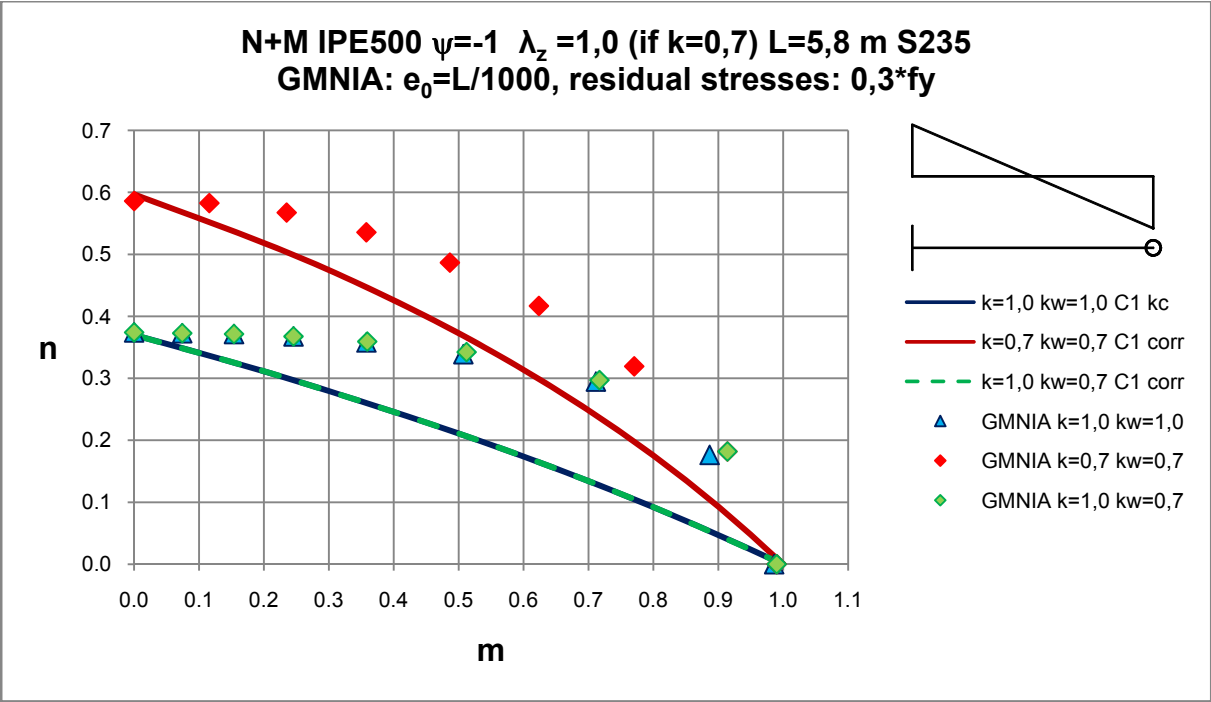


Fig. 63

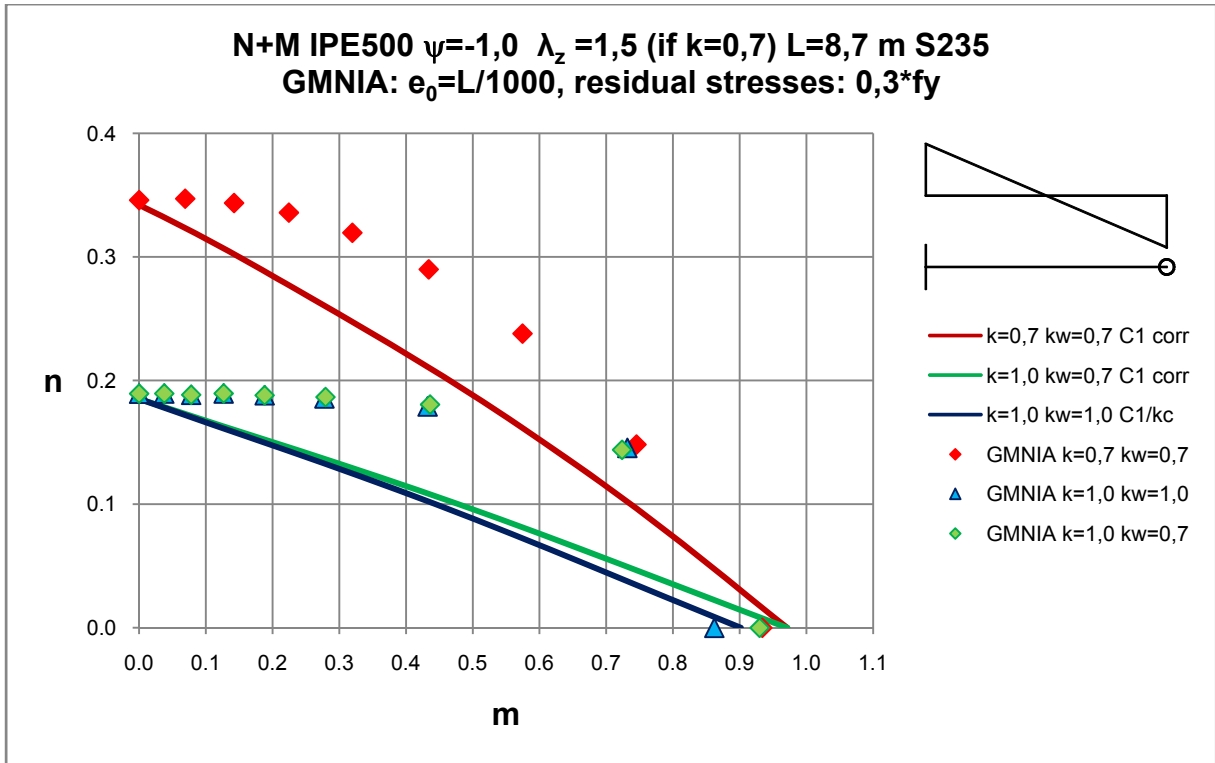


Fig. 64

In Fig. 65 to Fig. 73 similar GMNIA-results are shown for the studied cases where the section was an HEB 300. The tendencies are exactly the same as shown for the IPE 500 section.

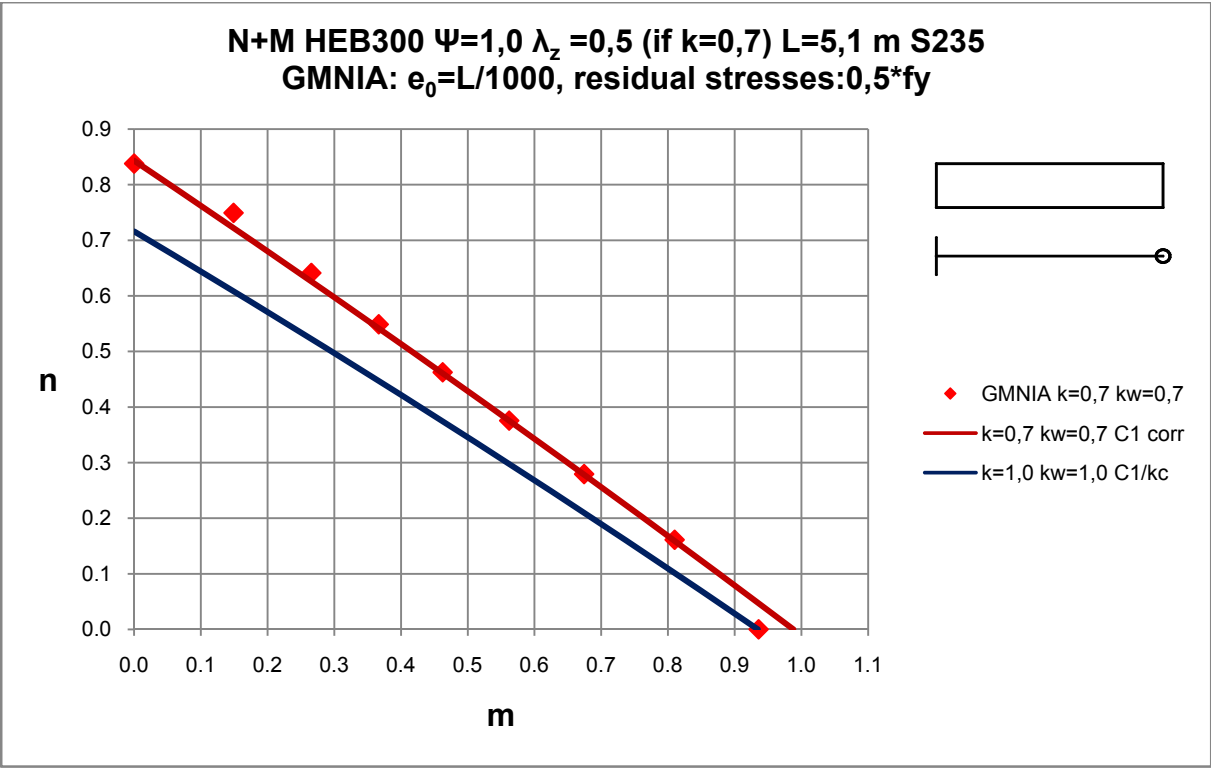


Fig. 65

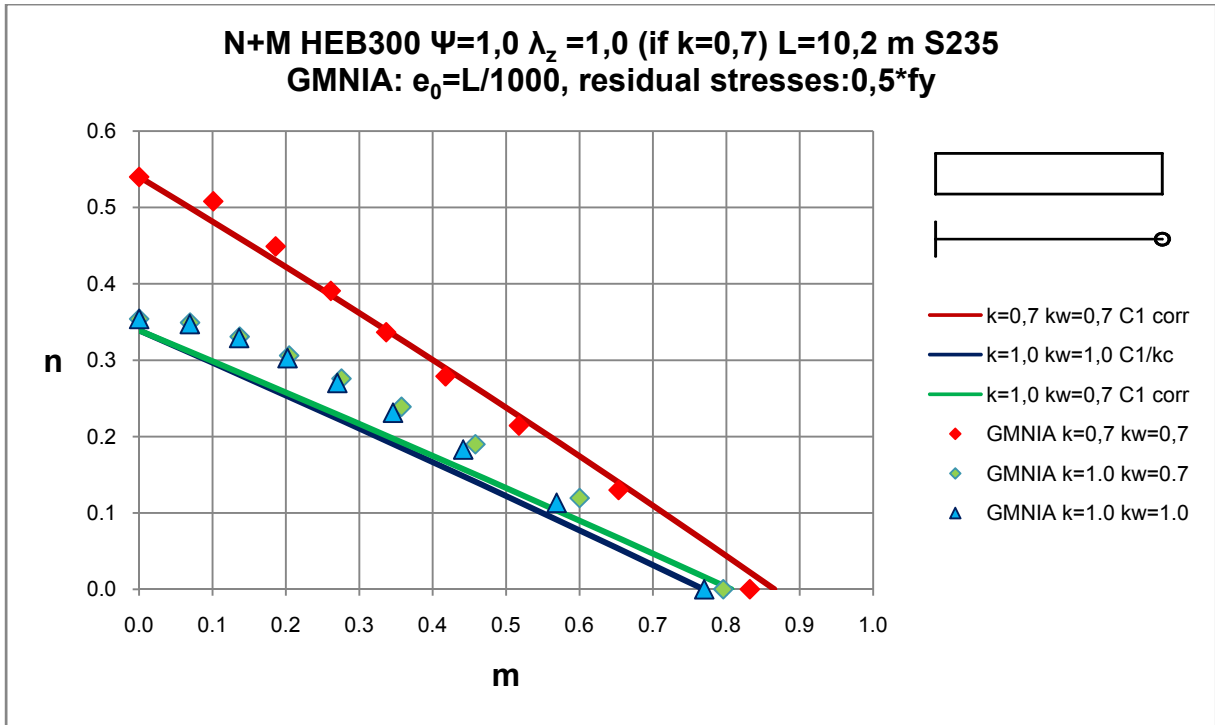


Fig. 66

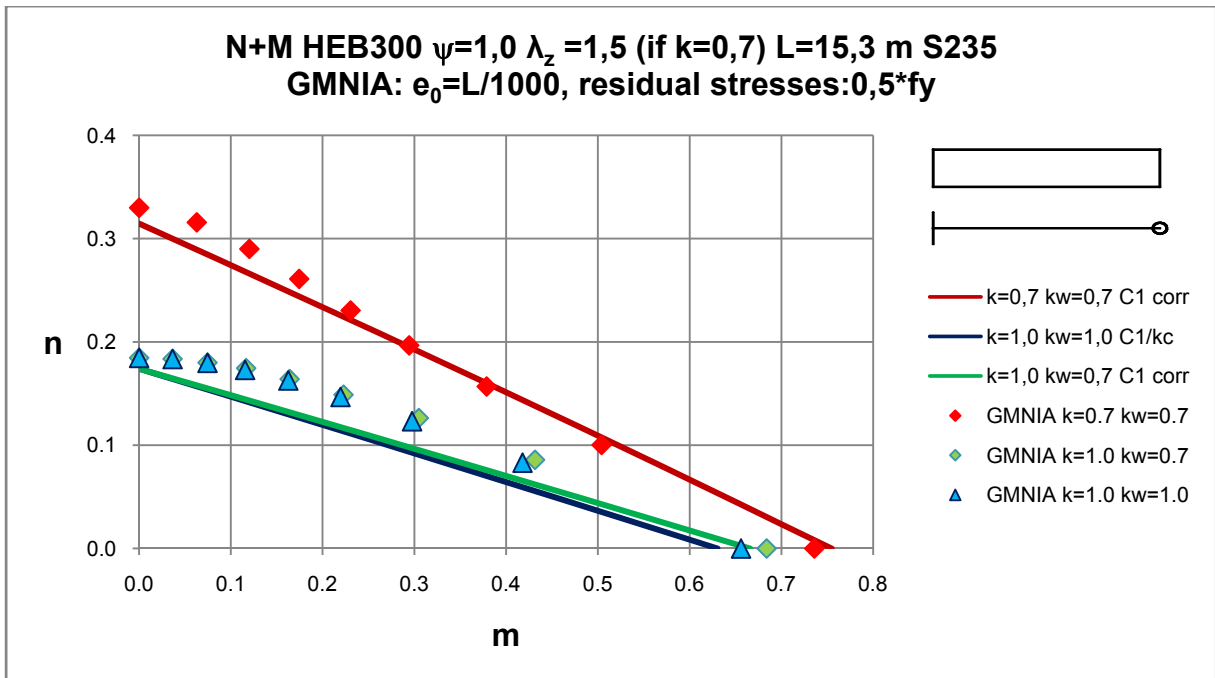


Fig. 67

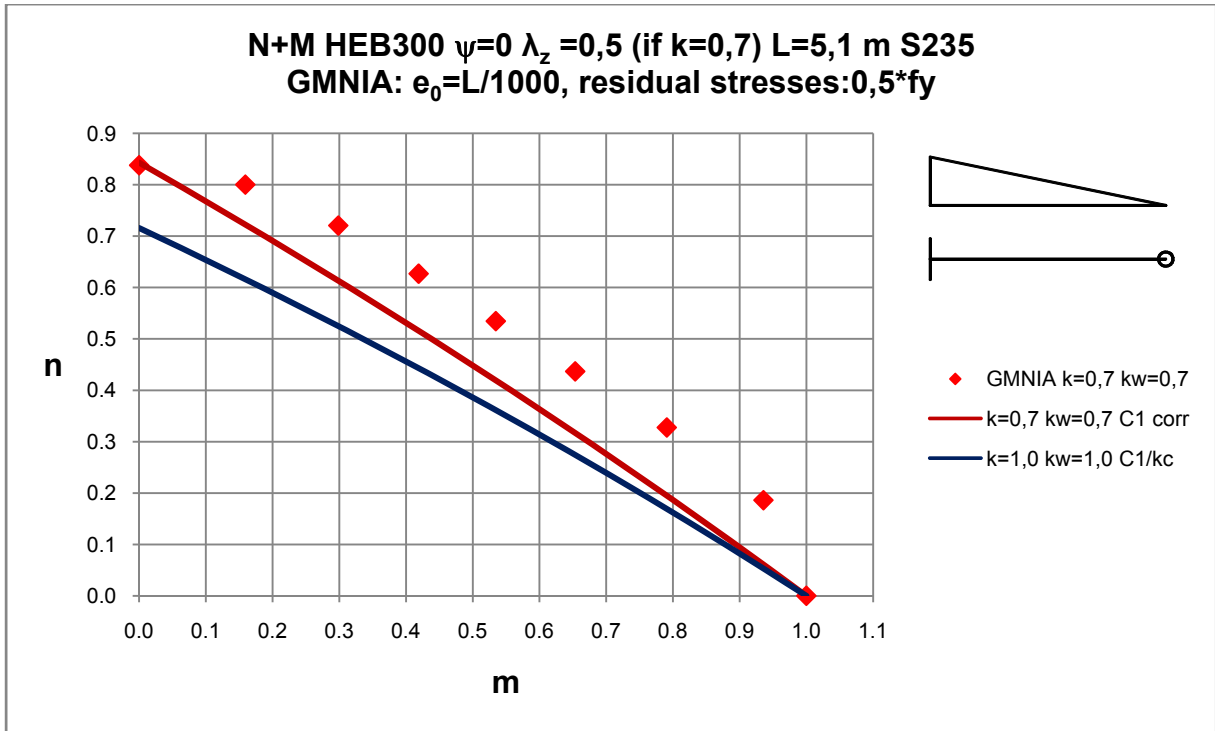


Fig. 68

It can be seen in Fig. 69 and Fig. 70 that the warping fixation effect much less the resistance of the section HEB 300 than in the cases of section IPE 500, and larger differences can be noted between the GMNIA-results and the EC3 interaction curves under the same conditions. This is due to the strongly reduced tendency of this section to fail in LT buckling, which is not well reflected by the interaction formulae: they always predict a near-linear interaction between χ_Z and χ_{LT} , whereby the latter is often near or at 1,0 for this section and an actually curved interaction curve (similar in shape to the cross-sectional capacity curve) would need to be approximated instead.

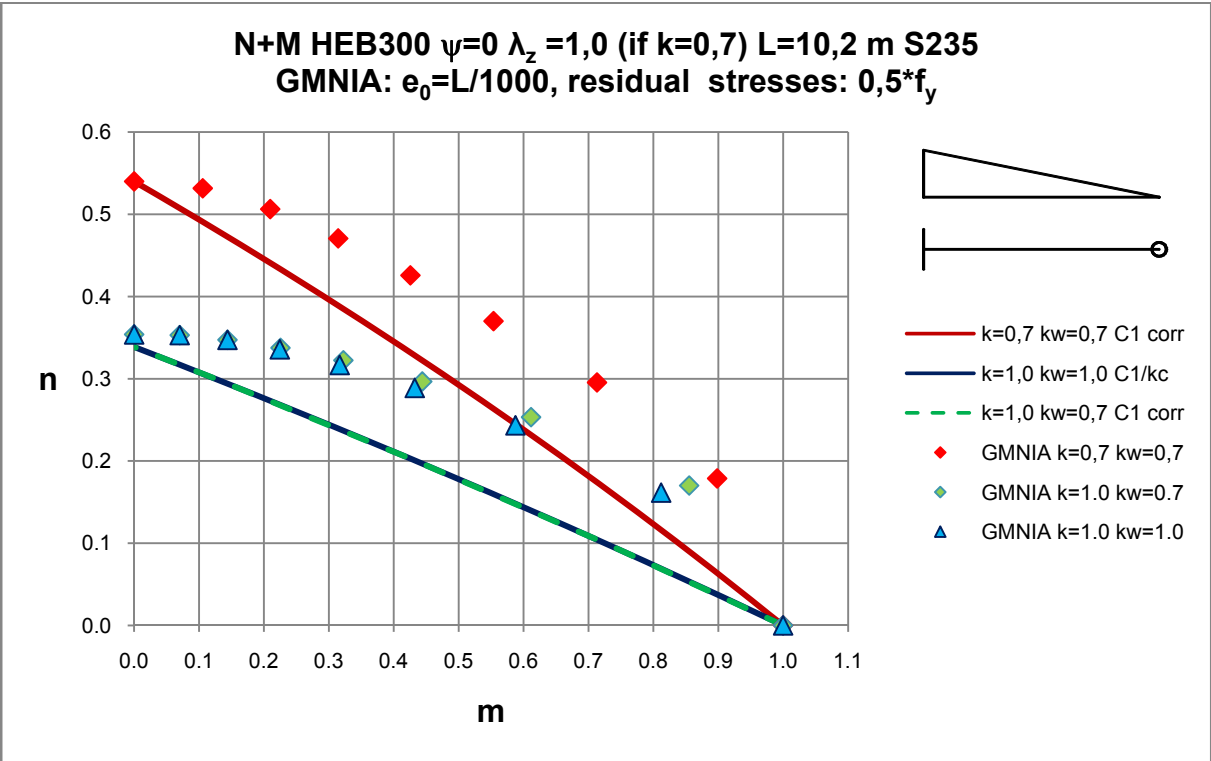


Fig. 69

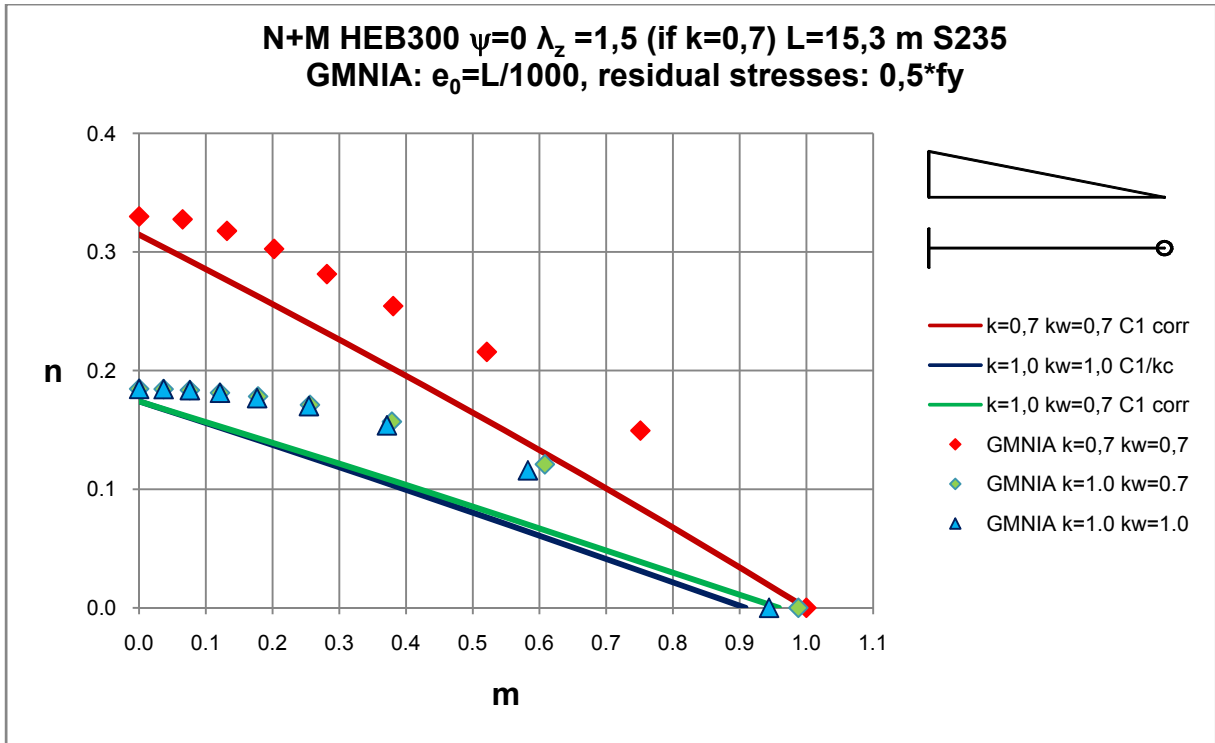


Fig. 70

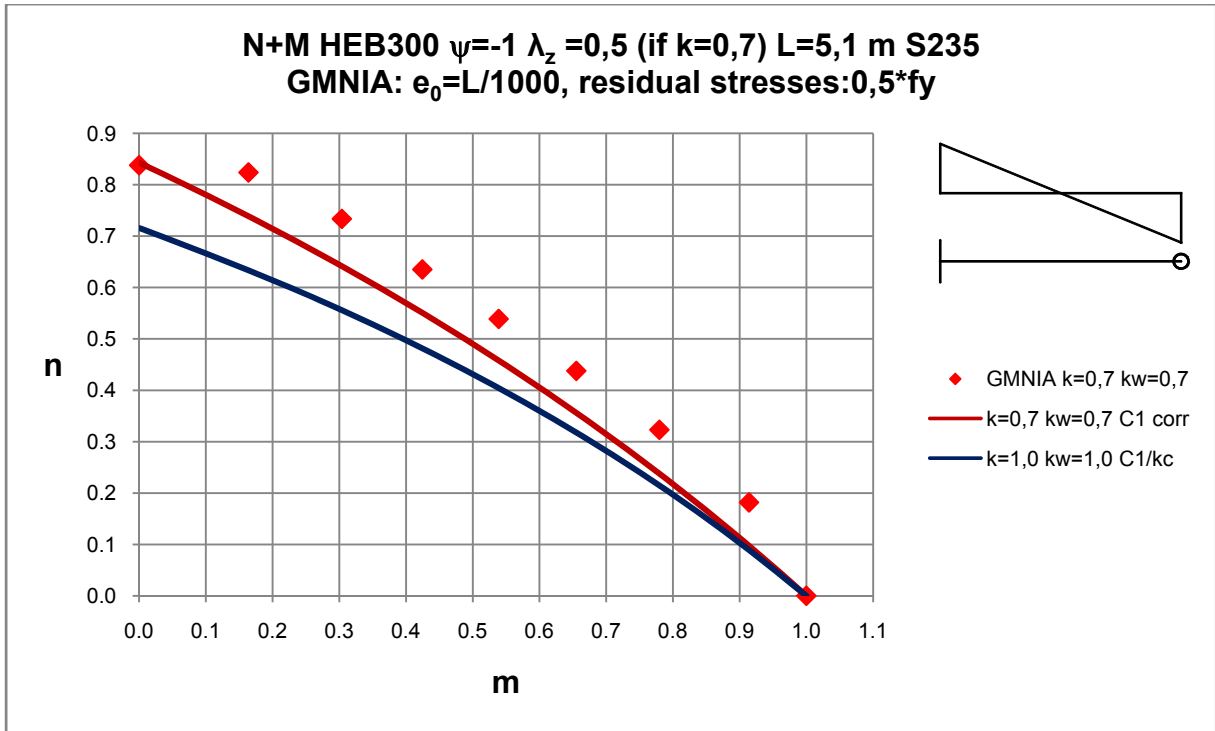


Fig. 71

Based on the Fig. 72 to Fig. 73 the beneficial effect of the warping fixation disappear if $\psi=-1$.

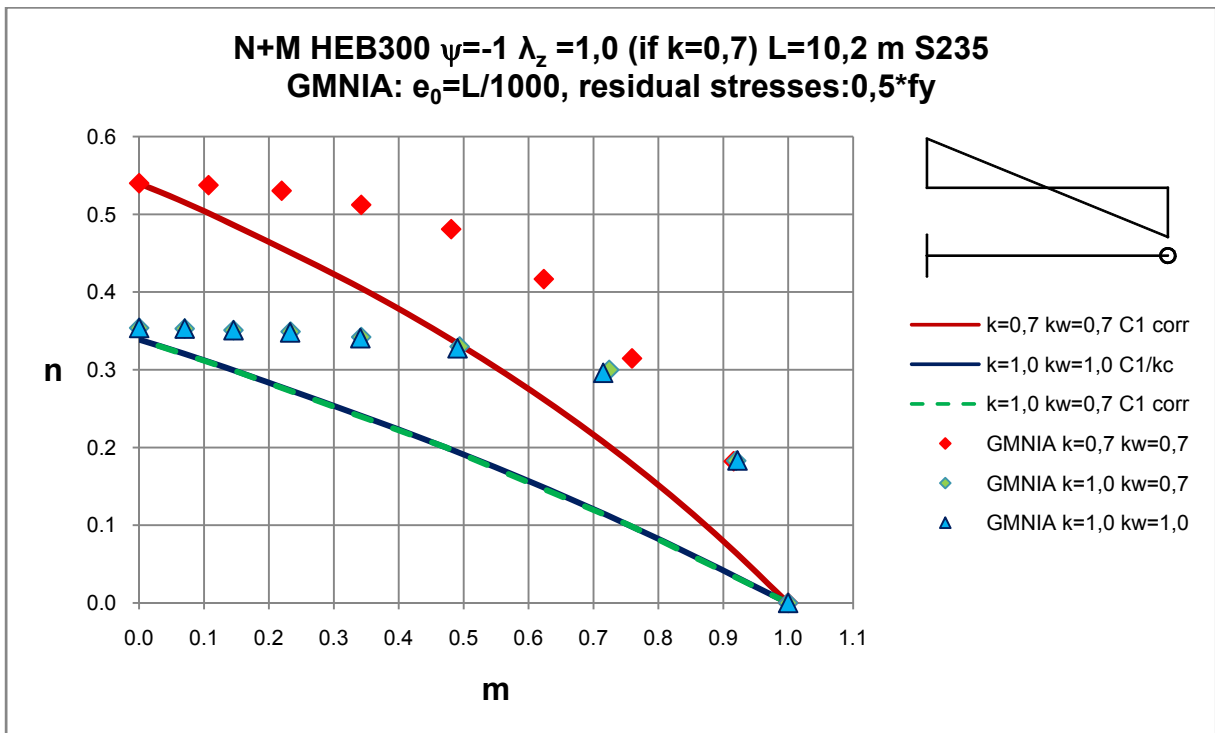


Fig. 72

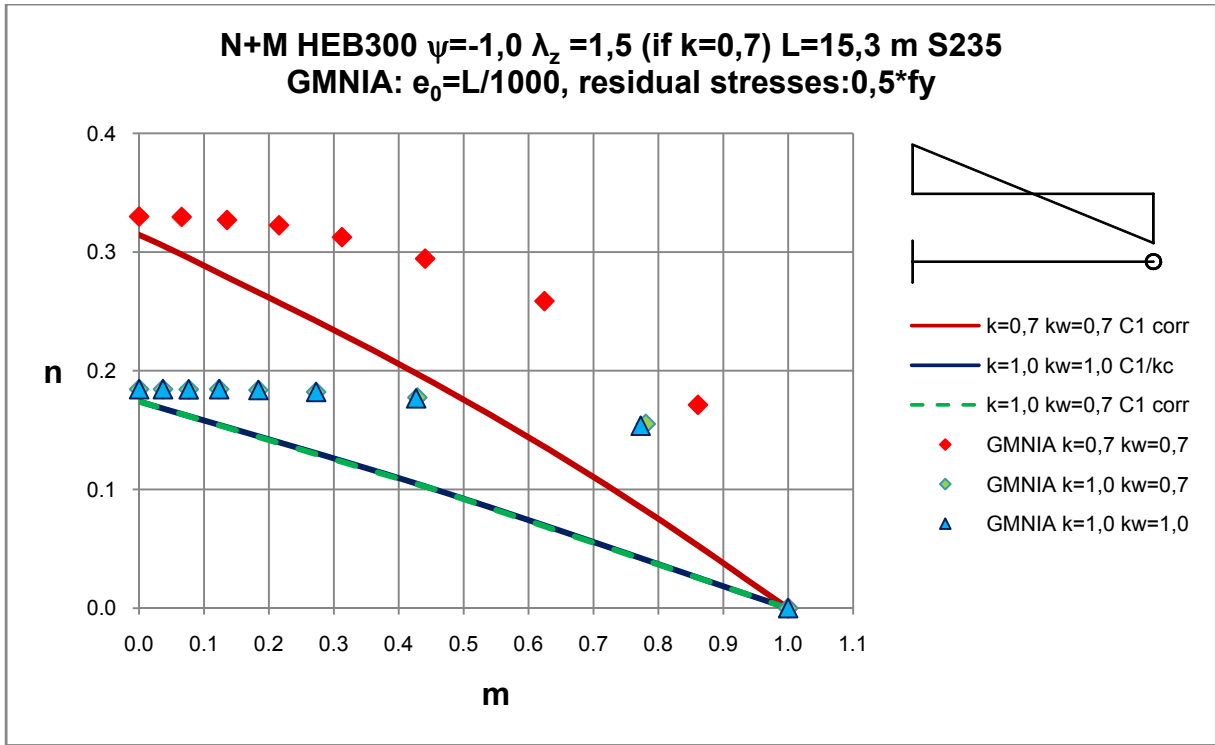


Fig. 73

6.5. Conclusions

The following conclusions can be drawn from the GMNIA analyses for beam-columns described in this chapter of the thesis:

- Under support condition $k=0,7$ $k_w=0,7$ the interaction curves according to EC3 are on the safe side and could therefore be used for practical design if warping and rotational fixations are present at the member ends, because the GMNIA analyses have shown higher values of resistance than the EC3. The “correct” calculation of the slenderness for LTB by a FEM program (for example LTBeam) is highly recommended.
- The beneficial effect of the rotational fixation exists in all case with dominant (or pure) compression, because the resistance for flexural buckling is governed by the rotation fixities of the member. Under dominant (or pure) bending the beneficial effect can be gained only in cases, in which the type of failure is an elasto-plastic stability failure and not plastic cross section failure (which depends on the boundary conditions). This last remark would only in theory also be true for the pure compression case, since columns are only very rarely “stockier” than $\bar{\lambda}_z=0,2$, the plateau value for flexural buckling.
- The beneficial effect of the warping fixation does not exist in cases with dominant (or pure) compression, because the resistance for flexural buckling is not influenced by the warping fixities of the member. Under dominant (or pure) bending the beneficial effect can be gained only in cases, in which the type of failure is elasto-plastic stability failure and not plastic cross section failure (which depends on the boundary conditions).
- Under loading condition $\psi=0$ and $\psi=-1$ there are significant (safe-sided) differences between the curves according to EC3 and the GMNIA results for the same support conditions, so the refinement of the interaction curves, for example by a modification of the interaction factor k_{LT} or of the format of the formula itself, are necessary.
- The beneficial effect obtained by rotational and warping fixation is higher in cases for section IPE 500 than in cases for section HEB 300, because sections HEB are less sensitive against LTB.

7. Overall concept (compression and bending, GMNIA)

7.1. Background of the overall concept

The **overall concept** (known in some representations as “general method”, or “generalized slenderness concept”) is a second method for designing beam-columns found in EC3. It is declared there as a “general” method with few limitations to its use; in fact, section 6.3.4 of EN 1993-1-1, which specifically deals with the “general method”, appears to be intended for all cases that are “not the standard cases” of doubly-symmetric sections with end-fork boundary conditions.

The most important feature of the overall concept is that the member slenderness is calculated for a specific, combined loading and support condition, which means the overall slenderness is different for every N+M loading case.

There are two alternatives for the calculation of the **overall slenderness**.

Alternative 1 (MNA based) [20]:

$$\bar{\lambda}_{ov} = \sqrt{\frac{LPF_{MNA}}{LPF_{LBA}}} \quad (7.1)$$

LPF_{MNA} is the load proportionality factor of a N+M load case reached in materially non-linear analysis (MNA) of the member in which no buckling effect and no imperfections are taken into account. Practically MNA leads to the plastic cross sectional resistance for compression and bending in the decisive loaded section of the member. [16]

The MNA load proportionality factor can thus be calculated in two different ways:

1. Simply by the plastic cross sectional resistance according to EC3 (formula)
2. More rigorously by the plastic cross sectional resistance obtained from MNA analyses (ABAQUS)

In subchapters 6.2 and 6.3 these two methods are compared with each other.

LPF_{LBA} is the load proportionality factor of a N+M load case until bifurcation reached. [16]

Alternative 2 ($R_{b,ip}$ based) [20]:

$$\bar{\lambda}_{ov} = \sqrt{\frac{R_{b,ip}}{LPF_{LBA}}} \quad (7.2)$$

In the “general method” as it is defined in section 6.3.4 of EN 1993-1-1, LPF_{MNA} is replaced by $R_{b,ip}$, which means the resistance of the member in terms of a linear amplification of N+M, *including the second-order effects of imperfections and deformation in the main plane of bending (in-plane)* [13].

Practically $R_{b,ip}$ means the value of resistance reached in either an in-plane second-order calculation with equivalent geometric imperfections and cross-sectional resistance checks or (in the most advanced type of calculation) an in-plane GMNIA analysis, where only the failure cases in plane are included and cases out of plane are excluded.

In the following chapters the Alternative 2 is not in focus, because the member slenderness $\bar{\lambda}_y$ for in-plane buckling - particularly for the section IPE 500 - is so low in all studied cases that the resistance $R_{b,ip}$ is very close to the cross sectional resistance (MNA) in the investigated cases. It is therefore considered to be sufficient to analyse the Alternative 1 in order to draw conclusions regarding both Alternatives for the chosen examples.

The “**overall**” **buckling reduction factor** for out-of-plane buckling (χ_{op}) can be calculated in two different ways [16]:

- Taking the minimum of χ_z and χ_{LT} (with using $\bar{\lambda}_{ov}$ instead of $\bar{\lambda}_z$ and $\bar{\lambda}_{LT}$):

$$\chi_{op} = \min(\chi_z; \chi_{LT}) \quad (7.3)$$

- Using an interpolation between χ_z and χ_{LT} on the basis of the cross-sectional utilization of the two components n and m , whereby the factor $\eta_0 = m/n$ is used. [18]

$$\chi_{op} = \frac{(1 + \eta_0) \cdot \chi_z \cdot \chi_{LT}}{\chi_{LT} + \eta_0 \cdot \chi_z} \quad (7.4)$$

In all cases the first method was used.

If Alternative 1 is applied for calculation of the slenderness, **the buckling resistance for out-of-plane buckling (LTB)** according to the overall method is defined as (Fig. 74) [2]:

$$R_{b,op} = \frac{\chi_{op} \cdot LPF_{MNA}}{\gamma_{M1}} \geq 1,0 \quad (7.5)$$

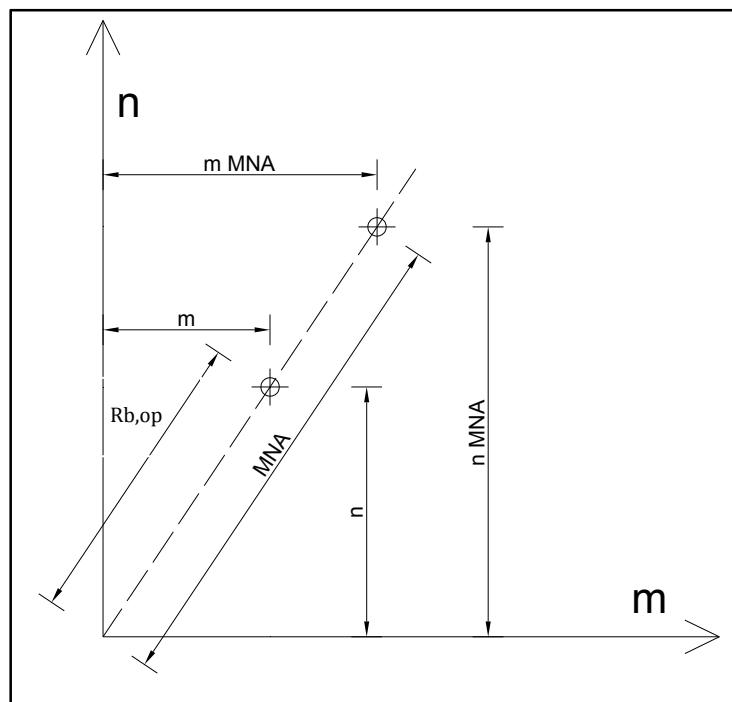


Fig. 74: Calculations of the buckling resistance based on the results of MNA-analyses

7.2. Plastic resistance for N+M according to EC3

If the “Alternativ 1” overall concept based on the pure plastic member/cross-sectional resistance is used and the MNA resistance is simply calculated with the Eurocode cross-sectional resistance formulae for N+M, the following formulae can be used.

The N+M interaction formula according to EC3 for plastic cross section resistance:

$$M_{N,y,Rd} = M_{pl,y,Rd} \cdot \frac{(1-n)}{(1-0,5a)} \quad (7.6)$$

with

$$n = \frac{N_{Ed}}{N_{pl,Rd}} \quad (7.7)$$

$$a = (A - 2bt_{Fl}) / A \leq 0,5 \quad (7.8)$$

Eq. (7.6) can be written into the following term:

$$\frac{M_{N,y,Rd}}{M_{pl,y,Rd}} \cdot (1-0,5a) = 1-n \quad (7.9)$$

$$n + \frac{M_{N,y,Rd}}{M_{pl,y,Rd}} \cdot (1-0,5a) = 1 \quad (7.10)$$

In ULS (at failure):

$$M_{N,y,Rd} = M_{Ed} \quad (7.11)$$

$$n + \frac{M_{Ed}}{M_{pl,y,Rd}} \cdot (1-0,5a) = 1 \quad (7.12)$$

With $\frac{M_{Ed}}{M_{pl,y,Rd}} = m$ and $\eta = \frac{m}{n}$:

$$n + m \cdot (1-0,5a) = 1 \quad (7.13)$$

Eq. (7.13) can be modified by dividing with n into:

$$1 + \frac{m}{n} \cdot (1 - 0,5a) = \frac{1}{n} \quad (7.14)$$

$$1 + \eta \cdot (1 - 0,5a) = \frac{1}{n} \quad (7.15)$$

Finally, the equation of the n-m interaction line (MNA) can be calculated:

$$1 = \frac{1}{n} - \eta \cdot (1 - 0,5a) \text{ and } m \leq 1,0 \quad (7.16)$$

Based on Eq. (7.16) the values of LPF_{MNA} can be calculated for all loading cases, and

The values of LPF_{LBA} were obtained from earlier analyses for N+M; the overall slenderness can be calculated by combining these two results.

With the use of Eq. (7.1) and (7.3) the overall slenderness $\bar{\lambda}_{ov}$ and the buckling reduction factor χ_{op} were calculated. In this way the n-m curves according to the EC3 can be plotted.

In this chapter the goal of calculation according to overall method was the comparison of the values of resistance according to GMNIA results and the overall concept.

Similarly to what was done in the comparisons for the interaction concept, the variables in the parametric studies were again the following:

- cross section: IPE 500 or HEB 300
- slenderness ($k=0,7$): $\bar{\lambda}_z = 1,0$
- load conditions: $\Psi=1,0$; $\Psi=0$ or $\Psi=-1,0$
- support conditions:
 1. $k=0,7$ $k_w=0,7$
 2. $k=0,7$ $k_w=0,7$
 3. $k=1,0$ $k_w=1,0$

In Fig. 75 the GMNIA results are compared to the resistance according to the overall concept for three different cases of support conditions. It can be seen that the values are the same under pure compression, but the general concept indicate higher values, than the GMNIA results as the bending becomes dominant in the load combination. The largest differences are indicated in case of $k=0,7$ $k_w=0,7$.

This result means that the practical design with the use of overall concept can even be unsafe under these circumstances.

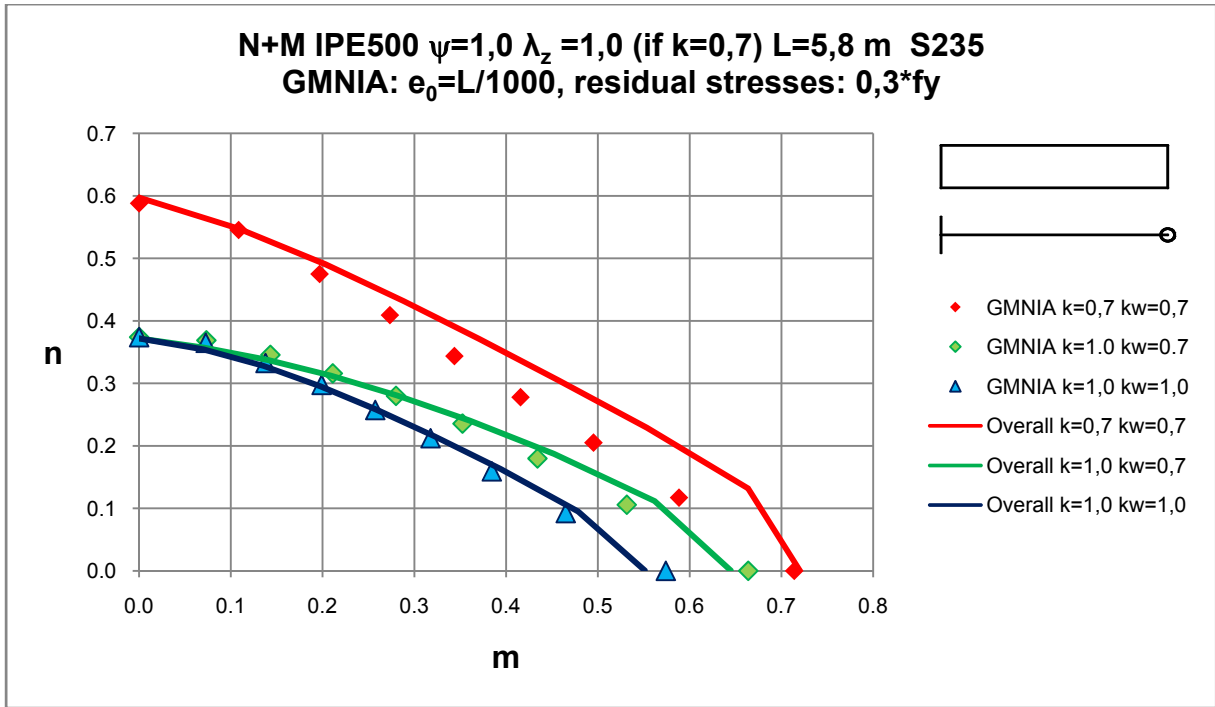


Fig. 75

It shall be noted that the reduction factor χ_{op} was even determined very conservatively by using the lowest of χ_z and χ_{LT} ; the use of the interpolation formula for χ_{op} would lead to even less conservative results for the boundary condition with end fixations.

The advantages and disadvantages of this approach are clearly visible, in particular when the figure is compared to the corresponding figure in chapter 6 (interaction concept). The advantage of the approach is that it manages to reproduce the “upward bend” of the actual (GMNIA) resistance functions better, because it applies the reduction factors to the plastic cross-sectional capacity, which is itself “bent upward” when compared to a straight connection line between N_{pl} and M_{pl} . However, the reduction itself appears not to be sufficient in some cases, as the one shown in Fig. 75 for $k=0,7$ and $k_w=0,7$.

In Fig. 76 to Fig. 77 the comparisons are shown for loading cases $\Psi=0$ and $\Psi=-1$. Based on these result large differences are noted between the overall concept and the GMNIA results, because the buckling resistance was governed by χ_z in all cases and thus the bending moment diagram does not enter the resistance χ_{op} function at all. For these load cases, a clear improvement could be obtained by using the interpolation formula for χ_{op} .

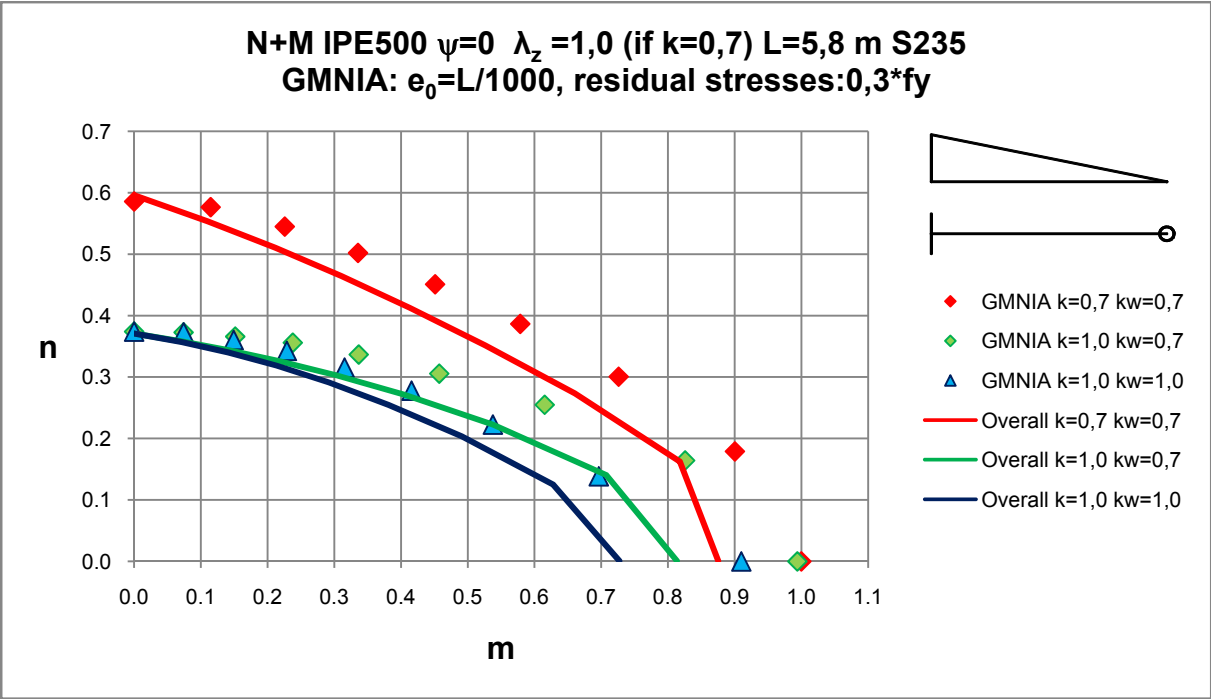


Fig. 76

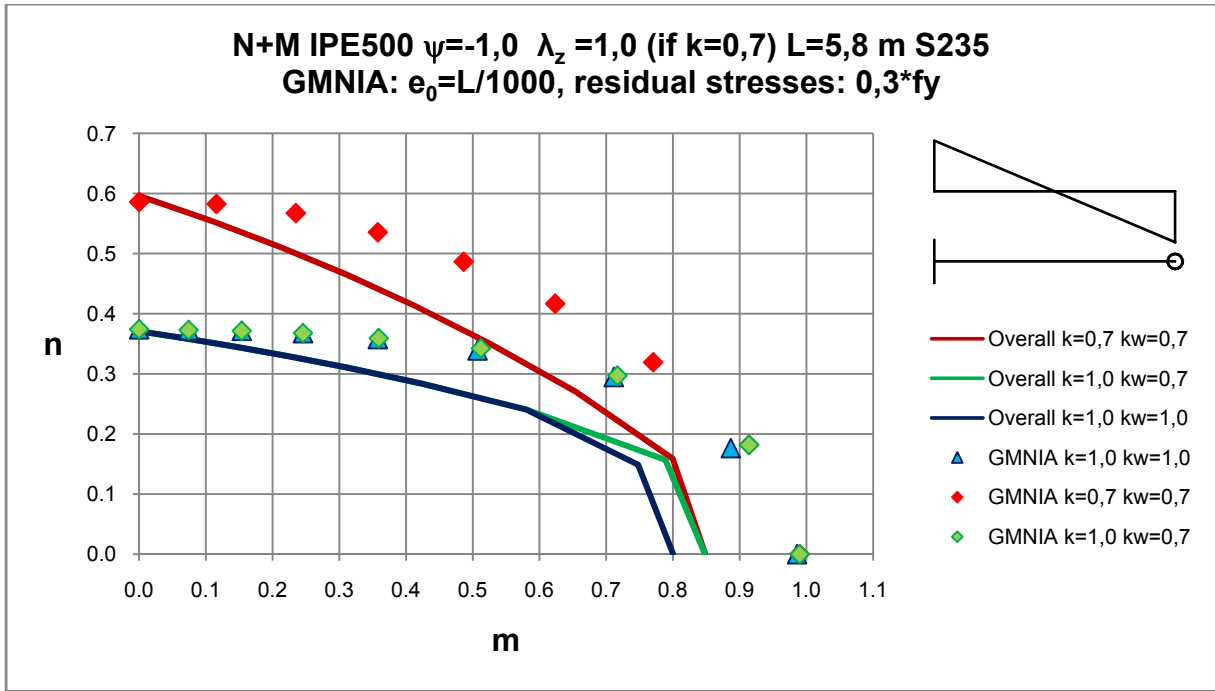


Fig. 77

In Fig. 78 to Fig. 80 the comparisons are represented for section HEB 300. In these cases the differences between GMNIA results and the overall concept were similar as for section IPE 500.

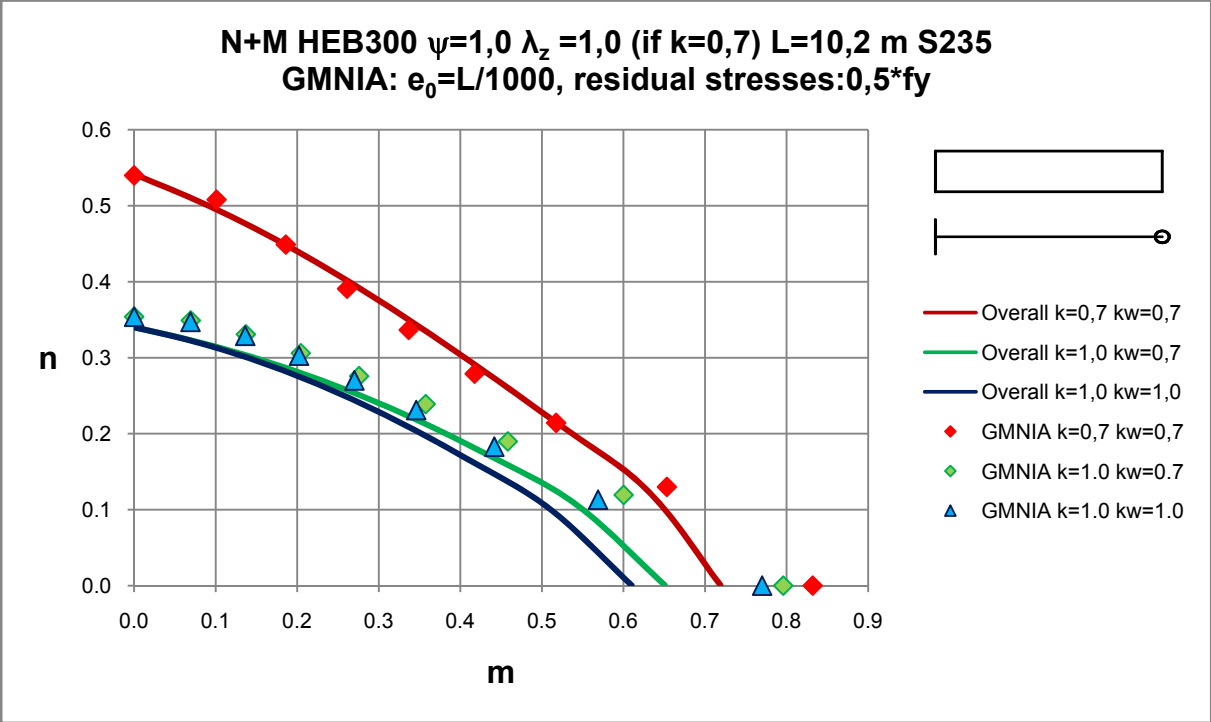


Fig. 78

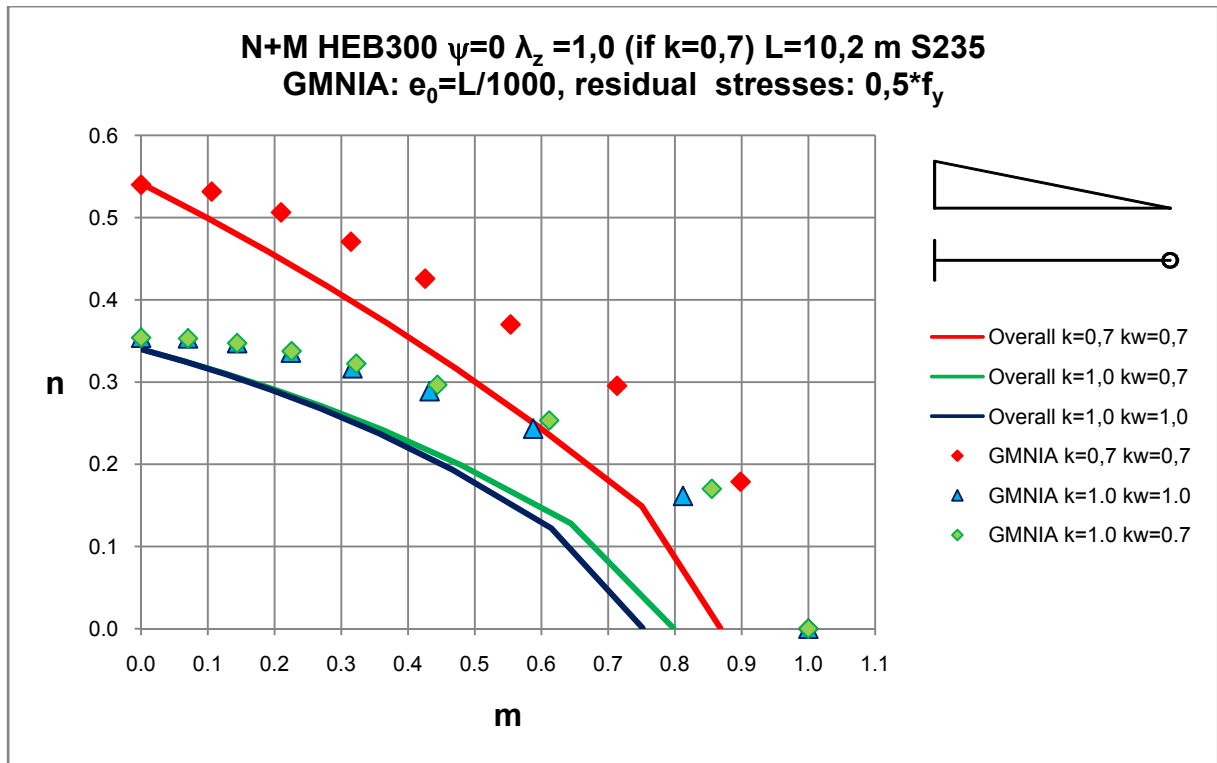


Fig. 79

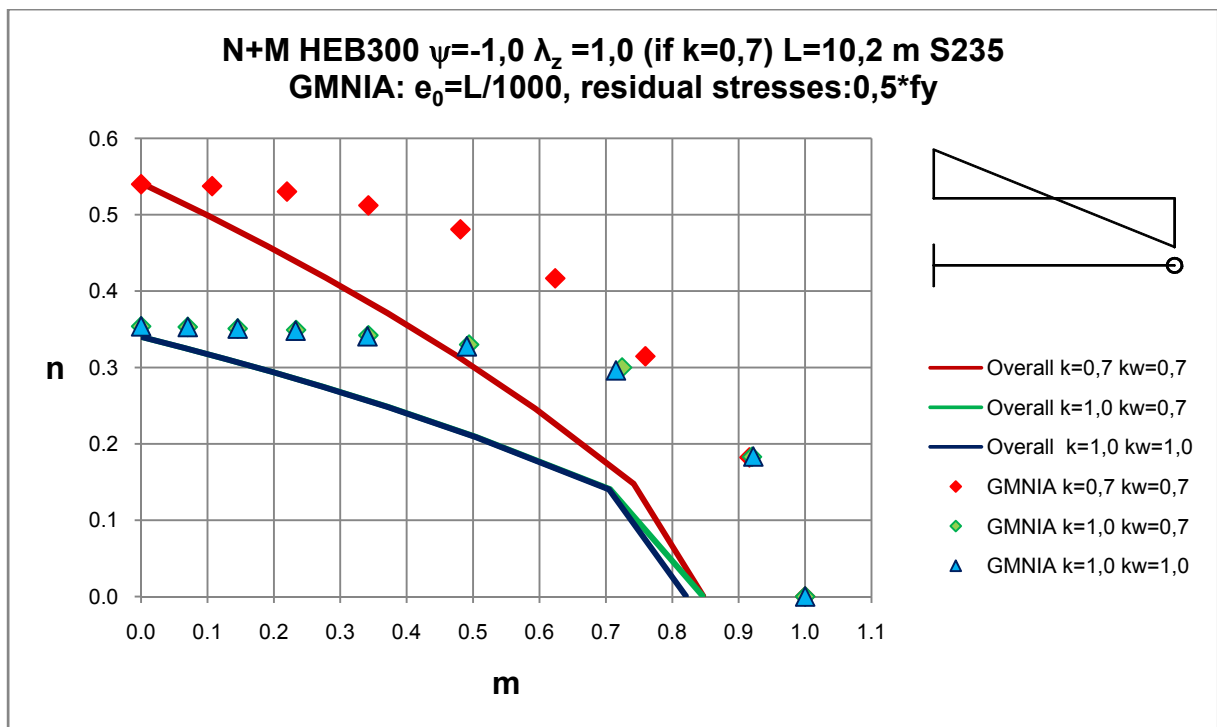


Fig. 80

7.3. Plastic resistance according to MNA analyses

In this subchapter the values of LPF_{MNA} were obtained from MNA analyses in all loading case. The boundary conditions of the parametric studies were the same as in subchapter 7.2, only the MNA-values were calculated “correctly” by a numerical analysis in ABAQUS.

In Fig. 81 to Fig. 86 very similar results are indicated as in Fig. 75 to Fig. 80, which is due to the fact that the EC3 formula accurately describes the plastic cross section resistance for N+M load case.

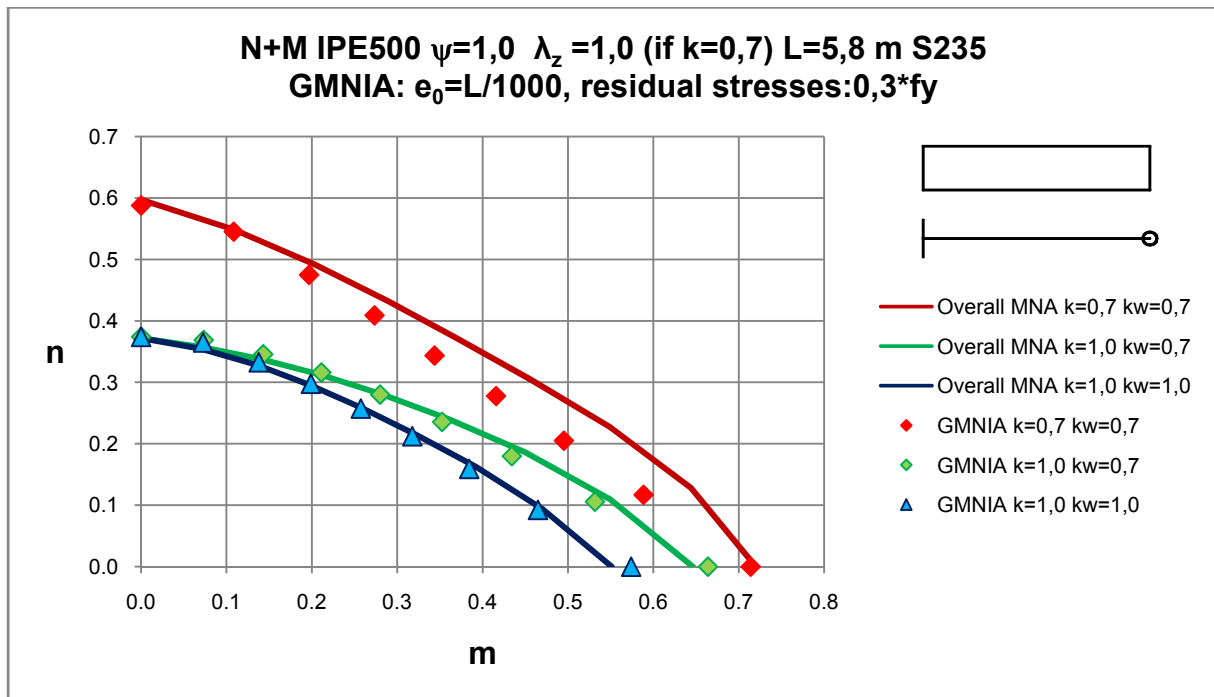


Fig. 81

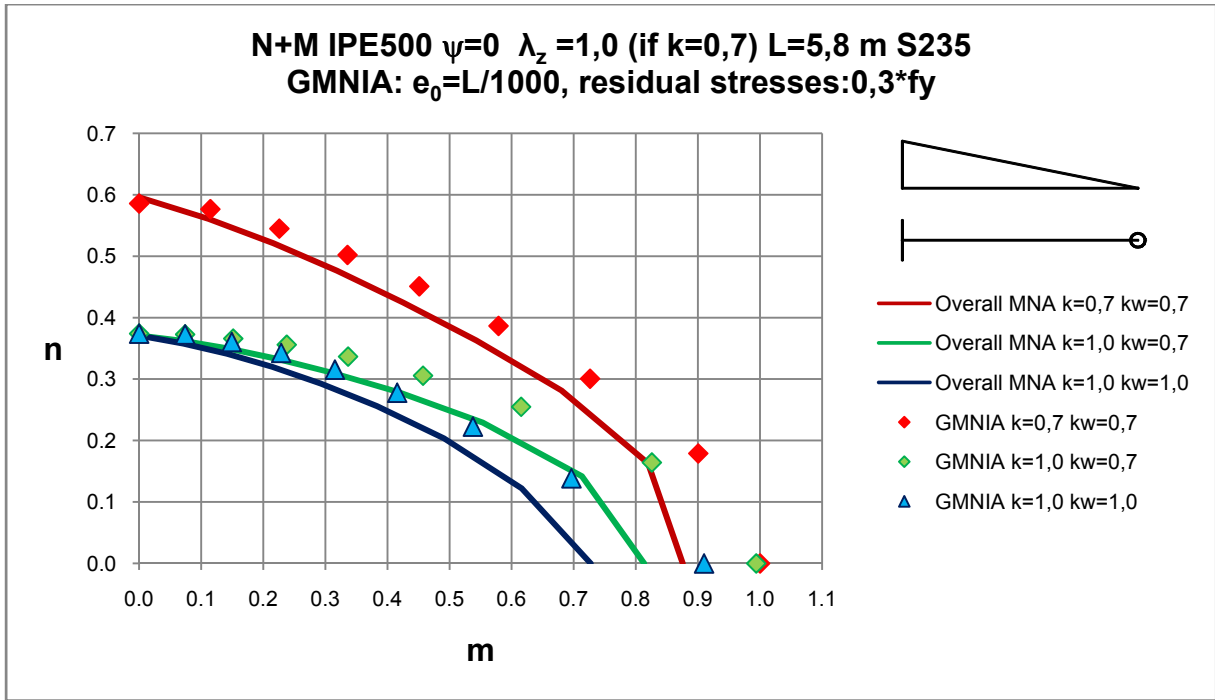


Fig. 82

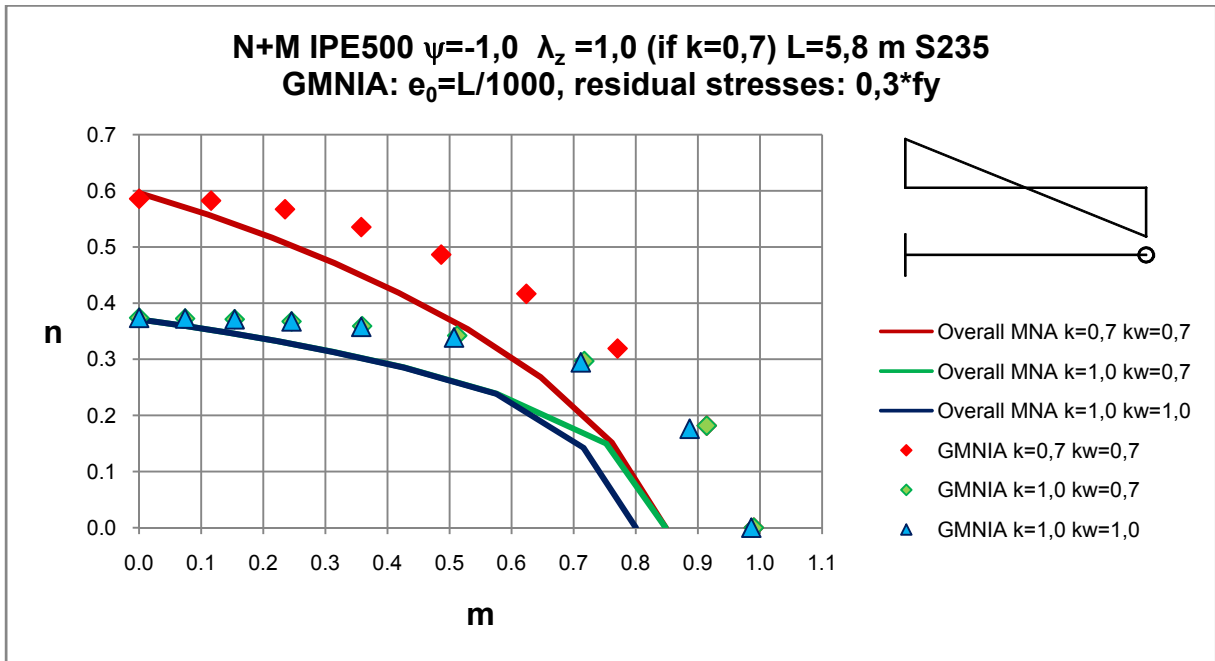


Fig. 83

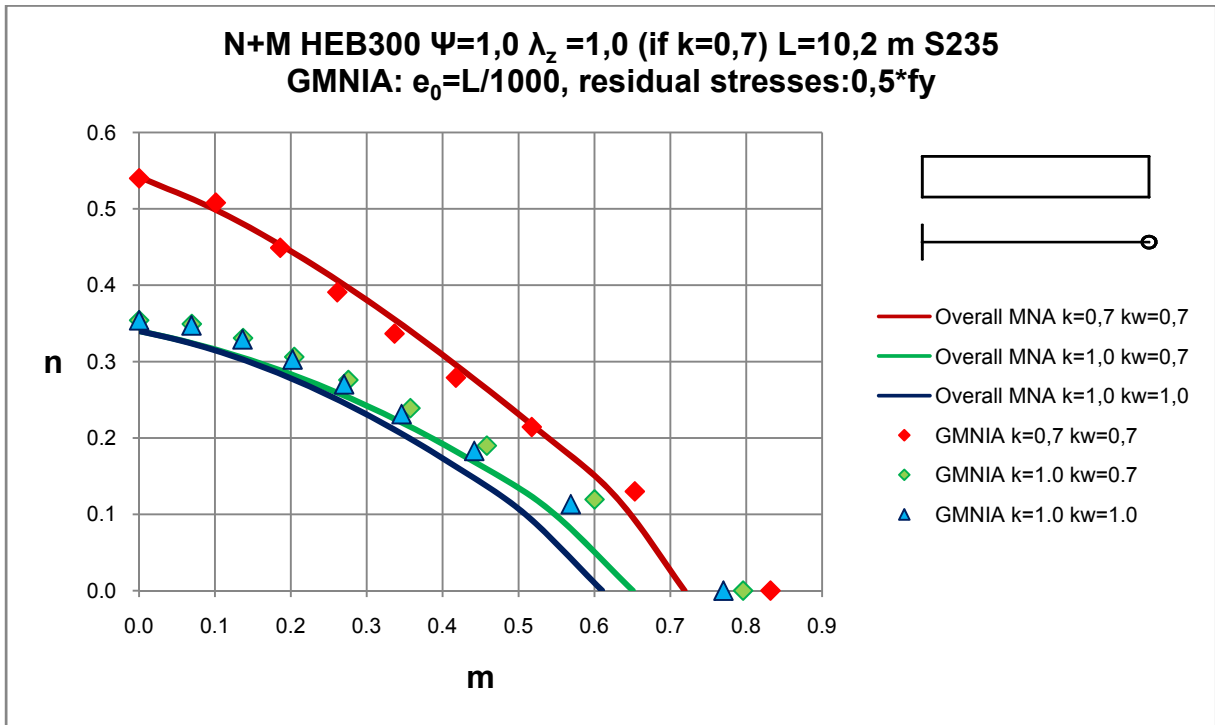


Fig. 84

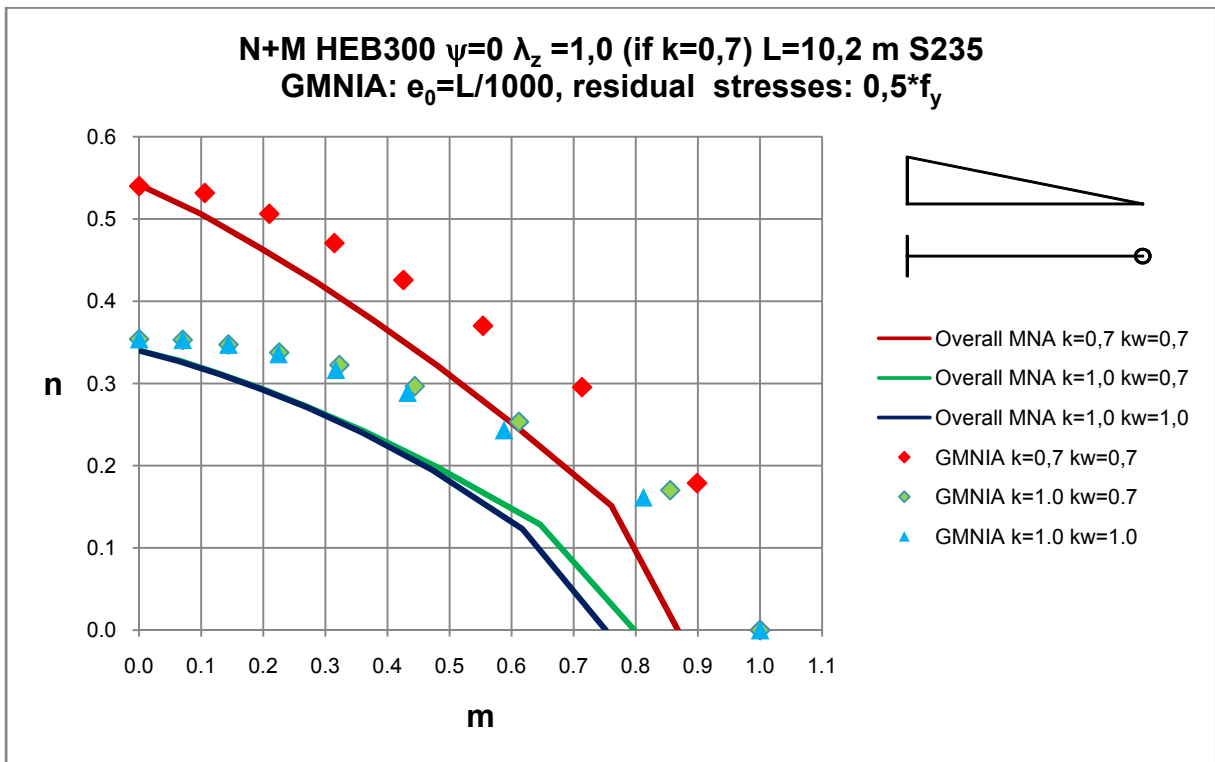


Fig. 85

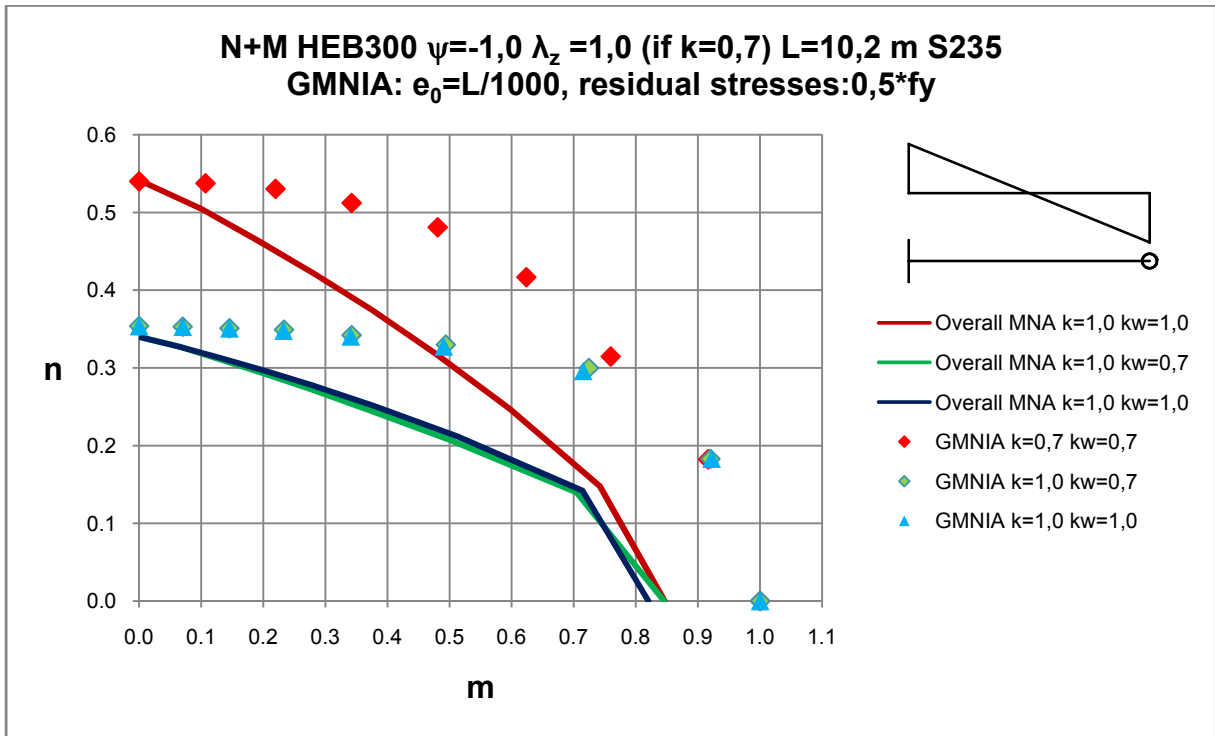


Fig. 86

7.4. Conclusions

In this chapter the following conclusions can be drawn from the FEM results and from the comparisons with EC3:

- The values of resistance calculated according to EC3 were significantly unconservative (unsafe) compared to GMNIA results in the case $k=0,7$ $k_w=0,7$ with $\Psi=1,0$ for section IPE 500, so based on these results the use of the overall concept cannot be recommended for all boundary conditions.
- In most of the cases with non-constant bending moment diagram the buckling resistance was clearly governed by χ_z , which was then in turn used (as the minimum value) as χ_{op} , thus the design resistance for out-of-plane buckling according to the overall concept were more conservative, than according to interaction concept, using this method for the determination of χ_{op} and depending on the support and loading conditions of the case.
- Tab. 29 summarizes how the interaction and the overall method take into account the bending moment diagram. It can be seen that even if the overall diagram is used in combination with an interpolation for χ_{op} (which would make χ_{LT} and thus the f-factor for bending moment diagrams more relevant), the inclusion of the bending moment diagram would still not be “complete”, as it is not present as it is in the factor k_{LT} in the interaction concept.

Tab. 29: Comparison of the interaction and overall concepts

Taking into account the bending moment diagram in...	
<u>Interaction concept</u>	<u>Overall concept</u>
$M_{\text{diagram}} \rightarrow M_{cr} \rightarrow \bar{\lambda}_{LT}$	$M_{\text{diagram}} \rightarrow LPF_{LBA} \rightarrow \bar{\lambda}_{op}$
$M_{\text{diagram}} \rightarrow \chi_{LT}$ (factor f)	$M_{\text{diagram}} \rightarrow (\chi_{LT})$
$k_{LT} \rightarrow C_{m,LT}$	✘

- In order to use the overall method an LBA analysis is needed in all cases for the specific load combination. Based on this fact, the application of overall concept for the practical design is much more difficult than the use of interaction concept, in which no numerical analysis is needed if hand formulae for N_{cr} and especially M_{cr} are applied.
- The formulation of EC3 for plastic cross section resistance for load case N+M describes the MNA failure behaviour very accurately.

8. New Proposal for χ_{LT} for Hot-Rolled Sections

In this chapter a **new design formula proposal**, developed at Graz University of Technology, is investigated from the aspect of LTB resistance of beams (pure bending). [16]

According to the new design formula proposal the case-specific buckling reduction factor χ_S is calculated as follows: [16]

$$\chi_S = \frac{\varphi}{\Phi_S + \sqrt{\Phi_S^2 - \varphi \cdot \bar{\lambda}_S^2}} \leq 1,0 \quad (8.1)$$

and

$$\Phi_S = \frac{1}{2} [1 + \varphi \cdot (\alpha_{0,S} \cdot \alpha_S \cdot (\bar{\lambda}_{e0} - 0,2) + \bar{\lambda}_S^2)] \quad (8.2)$$

where the variables are the following:

- $\bar{\lambda}_S$ normalized slenderness for the specific buckling case
- $\bar{\lambda}_{e0}$ slenderness used for the definition of the generalized imperfection
- α_S generalized imperfection amplitude factor of the specific case
- $\alpha_{0,S}$ case-specific second-order stiffness term
- φ load diagram factor to account for variable loads

If the specific buckling mode of the member is lateral-torsional buckling, then the values and the indexes are the following:

$$\bar{\lambda}_S = \bar{\lambda}_{LT} = \sqrt{\frac{W_{y,pl} \cdot f_y}{M_{cr}}} \quad (8.3)$$

$$\bar{\lambda}_{e0} = \bar{\lambda}_z = \sqrt{\frac{A \cdot f_y}{N_{cr,z}}} \quad (8.4)$$

$$\alpha_S = \begin{cases} \text{hot-rolled } h/b > 1,2: 0,12 \cdot \beta_{LT} \leq 0,34 \\ \text{hot-rolled } h/b \leq 1,2: 0,16 \cdot \beta_{LT} \leq 0,34 \end{cases} \quad (8.5)$$

where:

$$\beta_{LT} = \sqrt{\frac{W_{y,el}}{W_{z,el}}} \quad (8.6)$$

$$\alpha_{0,S} = \left(\frac{\bar{\lambda}_{LT}}{\bar{\lambda}_z} \right)^2 \quad (8.7)$$

And for end-fork conditions and linear bending moment diagrams:

$$\varphi = 1,25 - 0,1 \cdot \psi - 0,15 \cdot \psi^2 \quad (8.8)$$

Finally, in the specific case of lateral torsional buckling the formulation is [16]:

$$\chi_S = \chi_{LT} = \frac{\varphi}{\Phi_{LT} + \sqrt{\Phi_{LT}^2 - \varphi \cdot \bar{\lambda}_{LT}^2}} \quad (8.9)$$

and

$$\Phi_S = \frac{1}{2} [1 + \varphi \cdot (\alpha_{0,S} \cdot \alpha_{LT} \cdot (\bar{\lambda}_z - 0,2) + \bar{\lambda}_{LT}^2)] \quad (8.10)$$

It can be seen that the φ load diagram factor is a new item in the formulation compared to the current EC3. It covers the same effect is similarly covered by the f-factor, which is however a modification of the χ_{LT} factor which is previously determined for a “constant” bending moment diagram and the correct value of M_{cr} .

The other new feature in the proposal is that the buckling reduction factor depends on the slenderness for flexural buckling ($\bar{\lambda}_z$) as well, and not just on the slenderness for LTB ($\bar{\lambda}_{LT}$).

In the calculation of the buckling curves according to the proposal the M_{cr} elastic critical moment was obtained from LTBeam, so the $\bar{\lambda}_{LT}$ slendernesses can be considered as the “correct” values.

In Fig. 87 to Fig. 92 the GMNIA results and the proposal curves are plotted for cases of support condition $k=0,7$ $k_w=0,7$.

Based on the comparisons it can be noted that the new proposal fit very accurately to the GMNIA results in most of the cases, independently of the studied section; it shall be remembered that this was not the case for the current EC3 curves, where the “general case” fit better in one case, and the “specific case” in the other. Fig. 88 and Fig. 91 indicate small differences for the case of a triangular bending moment ($\psi=0,0$) and $k=k_w=0,7$, where the proposal is higher than the GMNIA values, which means it is theoretically unsafe, but these levels of slendernesses refer to very long members (for example >20 m for section HEB 300). Nevertheless, an adaptation of the ϕ values to the most common boundary conditions (similarly to what is done for the C_1 values, see chapter) could be envisaged.

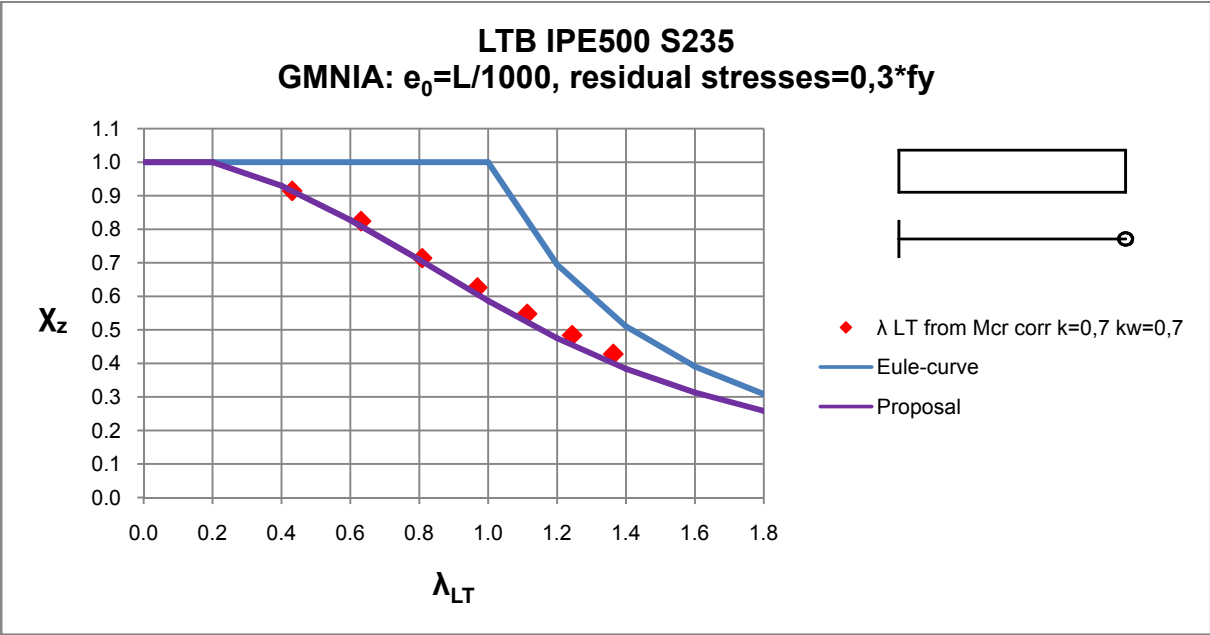


Fig. 87

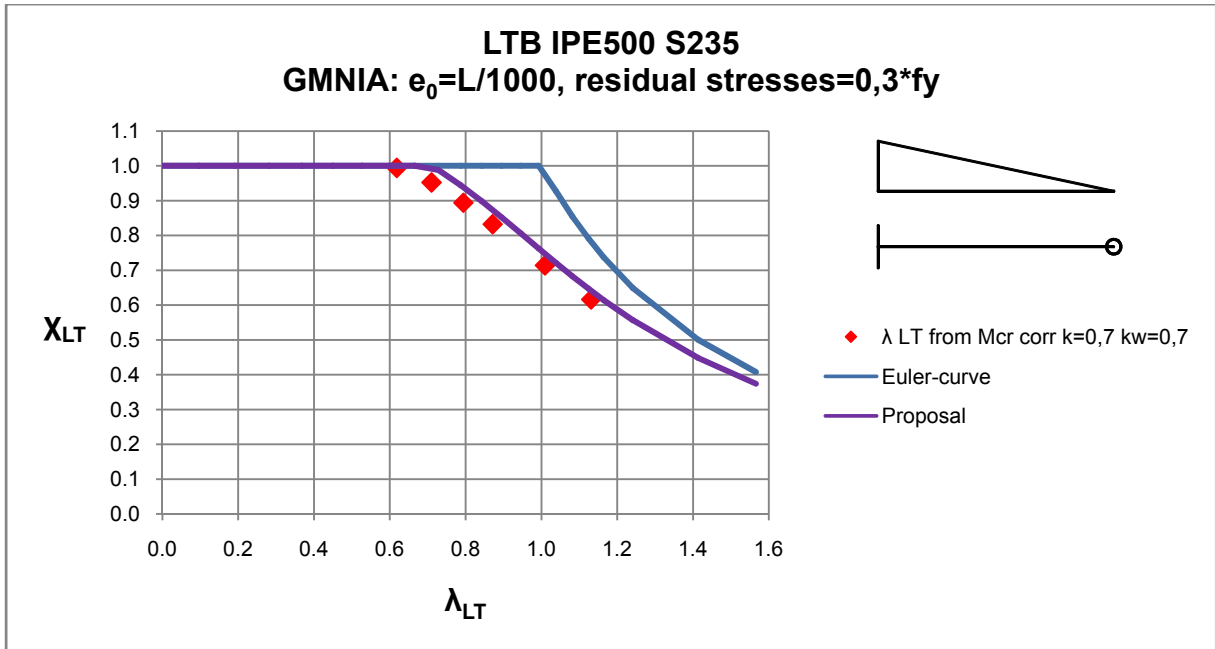


Fig. 88

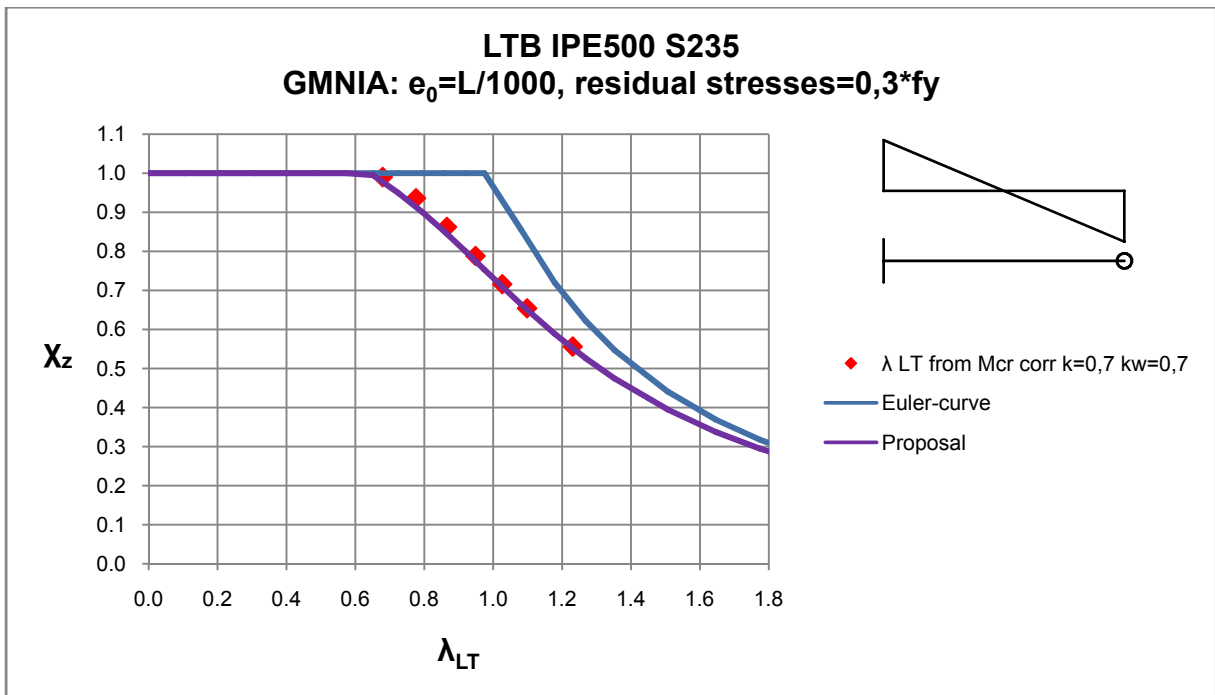


Fig. 89

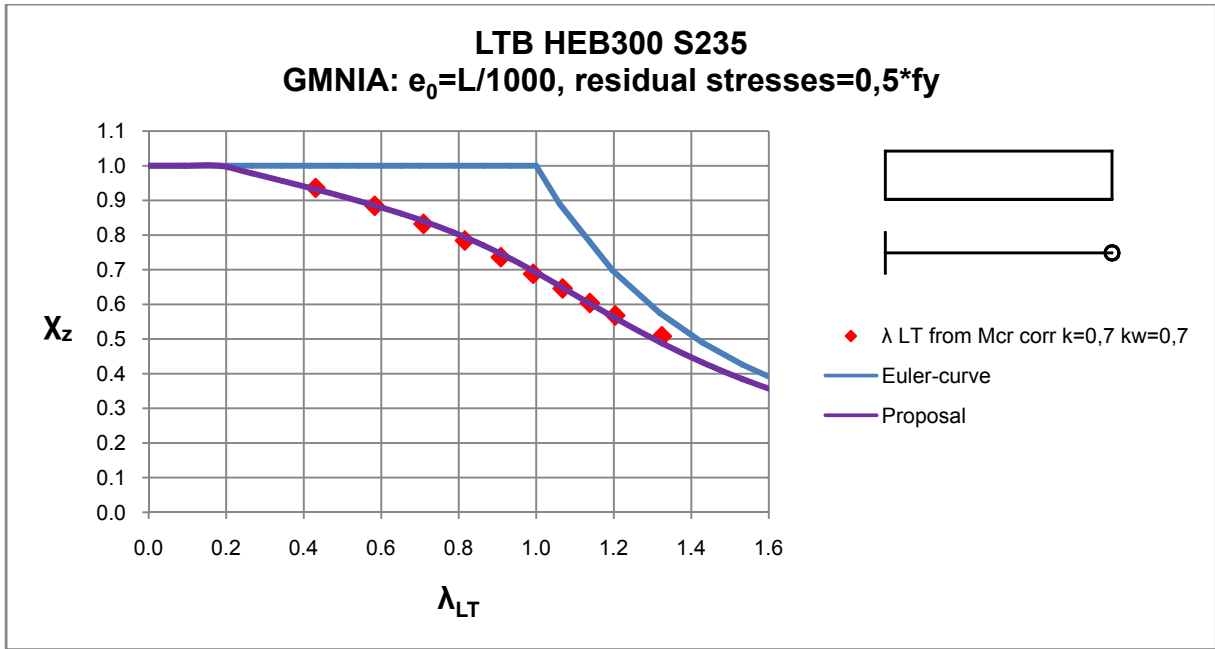


Fig. 90

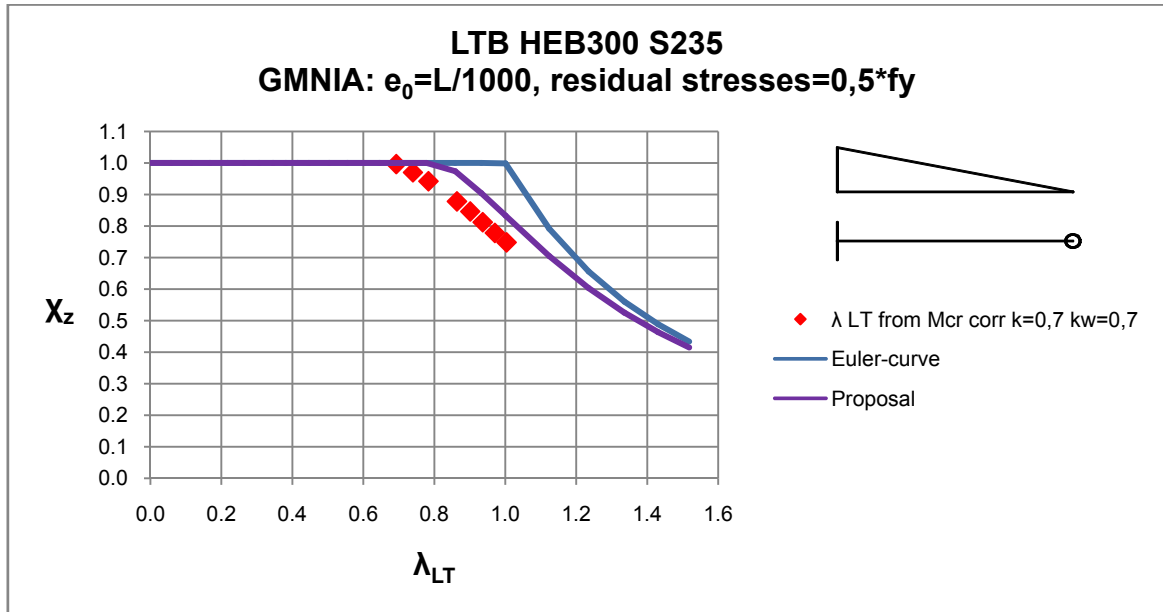


Fig. 91

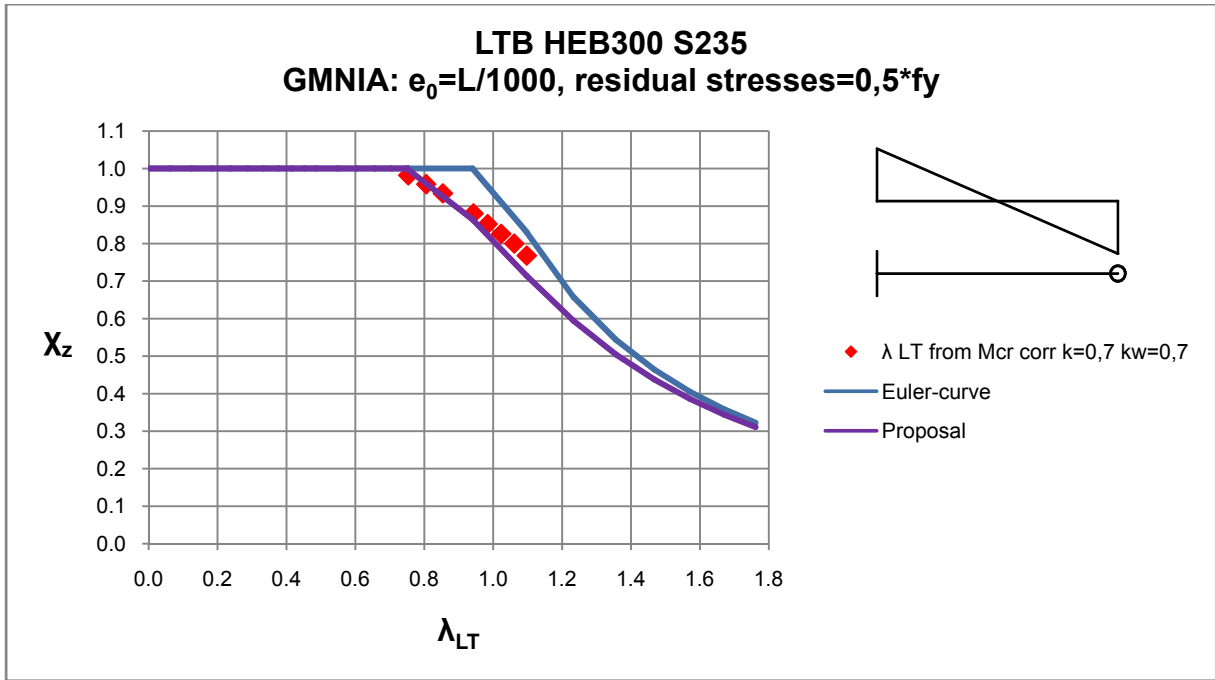


Fig. 92

9. Additional bimoment caused by warping fixation

In this chapter the **normal stress distribution in the flanges** of the section at the member ends is discussed for different support conditions. The importance of these stresses for the correct design of the end joints (if warping and rotational fixities are considered in out-of-plane buckling design) was already discussed in the introduction.

For support condition $k=1,0$ $k_w=1,0$ the end sections are able to rotate and to warp, but for $k=1,0$ $k_w=0,7$ the warping is one-sidedly restrained. In the second case the stresses are higher in the restrained section, because the section is not free to deform.

If the type of failure is LTB (bending moment about the strong axis, deformation about the weak axis), this warping restraint effect causes a **bimoment (M_ω)** about the weak axis as an additional load.

This additional bimoment about the weak axis has an influence on the design of the details end **plate welds by a column**. In this part of the thesis the stress distribution and the additional bending moment is investigated for the following cases:

1. IPE 500; $\psi=1,0$; pure bending; $\bar{\lambda}_z = 1,0$ (if $k=0,7$); $k=1,0$ $k_w=0,7$
2. HEB 300; $\psi=1,0$; pure bending; $\bar{\lambda}_z = 1,0$ (if $k=0,7$); $k=1,0$ $k_w=0,7$

The normal stresses due to $M_{Ed,y}$ at the end section:

$$\sigma_{Ed} = \frac{M_{Ed,y}}{W_{el,y}} = \frac{\chi_{LT} \cdot M_{pl}}{W_{el,y}} \quad (9.1)$$

The correct value of the additional bimoment about the weak axis can be expressed as a weak-axis bending moment per flange and can thus be calculated based on the shell element section forces, which can be imported from the output database file of the model (Fig. 93):

$$M_{z,flange} = \Sigma(\text{Section force (N/mm)} \cdot s \cdot b_{\text{element}}) \quad (9.2)$$

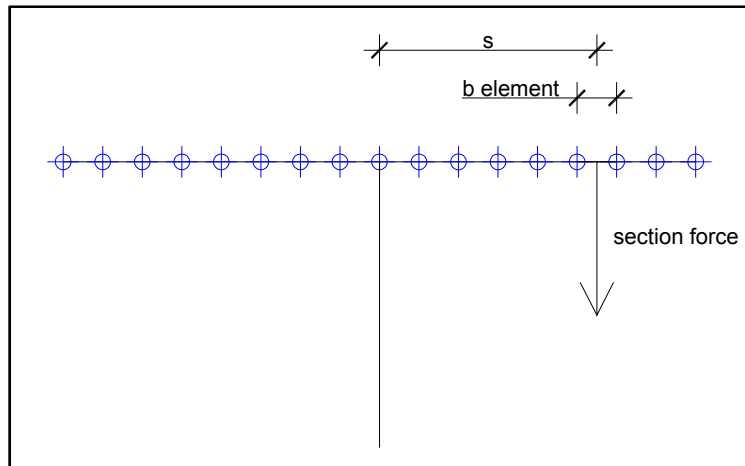


Fig. 93: Calculation of bimoment based on the section forces obtain from modelling results

The plastic resistance of a single flange for bending about the weak axis is:

$$M_{Fl,z,pl} = f_y \cdot t_f \cdot \frac{b^2}{4} \quad (9.3)$$

In order to develop a simple formula for the estimation of the maximum possible end bimoments (“bi-moments”) in the studied sections and load cases, the following considerations can be made:

If a linearized plastic cross sectional interaction verification for $M_y + M_{z,fl}$ is assumed to be valid to the end section, than:

$$\frac{M_{Ed}}{M_{pl}} + \frac{M_{z,fl}}{M_{Fl,z,pl}} \cong 1,0 \quad (9.4)$$

Eq. (9.4) can be modified into:

$$\frac{M_{z,fl}}{M_{Fl,z,pl}} \cong 1,0 - \frac{M_{Ed}}{M_{pl}} = 1,0 - \frac{\chi_{LT} \cdot M_{pl}}{M_{pl}} = 1,0 - \chi_{LT} \quad (9.5)$$

With the use of Eq (9.6) **the additional flange bending moment** can be calculated directly:

$$\frac{M_{z,fl}}{M_{Fl,z,pl}} \cong 1,0 - \chi_{LT} \quad (9.6)$$

Of course, this procedure should always be conservative, as it considers that the failure location corresponds to the end cross-section of the beam in the cases where and fixations are considered.

In Case 1 the following modelling results were studied:

- IPE 500; $\psi=1,0$; pure bending; $\bar{\lambda}_z = 1,0$ (if $k=0,7$); $k=1,0$ $k_w=0,7$

Fig. 94 and Fig. 95 illustrates the normal stress σ_{11} distribution along the upper and the lower flange (x-axis description: 16 elements, y-axis: element centroid values of σ_{11}) of the end section for support condition $k=1,0$ $k_w=0,7$. In the figures the stress level (σ_{Ed}) due to $M_{y,Ed}$ is also indicated, so the asymmetric part of the stresses can be seen. Based on the figures the right side of the flanges have reached the yield stress, so these parts are plastic ($\sigma=235$).

The results of the calculation in order to get the additional flange bending moment $M_{z,Fl}$:

$$\sigma_{Ed} = 178 \text{ N/mm}^2$$

$$M_{z,Fl} = 9134249 \text{ Nmm}$$

$$\frac{M_{z,Fl}}{M_{Fl,z,pl}} = 0,243$$

$$1,0 - \chi_{LT} = 1,0 - 0,664 = 0,336$$

$$0,243 \leq 0,336$$

so the assumption in Eq. (9.6) on the safe side. Note that for an actual design, the above ratio of $M_{z,Fl}$ could still be reduced by a multiplication with the utilization factor (which must be smaller than 1,0) for the LT buckling check.

It shall be noted that there is also a non-linear component in the stresses, which might be attributable to a combination of the residual stresses and some load introduction effect. Nevertheless, it is believed that the essential quantity (the flange bending moment) can be correctly retrieved as a bending moment resultant from these stress distributions.

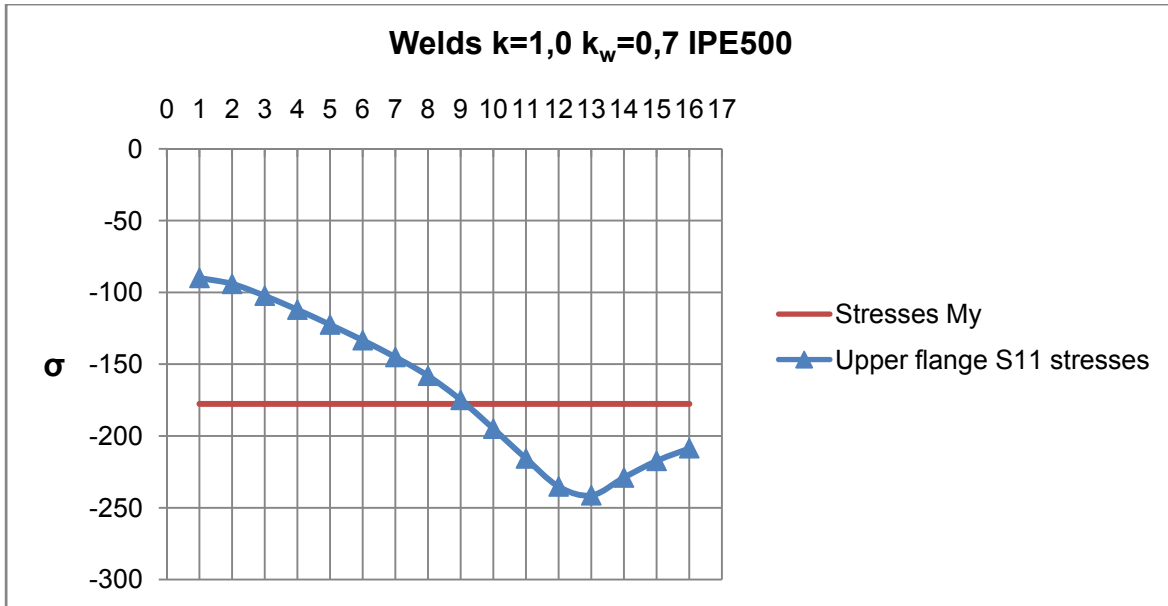


Fig. 94: S11 normal stress distribution of the upper flange under warping restraint (section IPE 500)

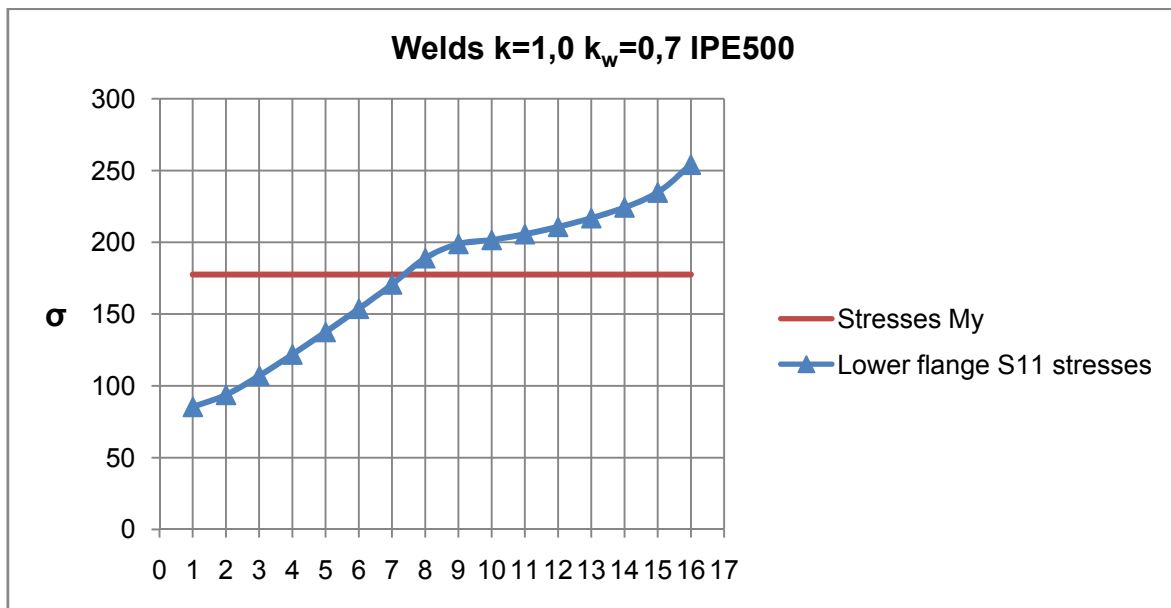


Fig. 95: S11 normal stress distribution of the lower flange under warping restraint (section IPE 500)

In Case 2 the following modelling results were studied:

- HEB 300; $\psi=1,0$; pure bending; $\bar{\lambda}_z = 1,0$ (if $k=0,7$); $k=1,0$ $k_w=0,7$

The normal stress distribution of the flanges is shown in Fig. 96 and Fig. 97 for support condition $k=1,0$ $k_w=0,7$.

The results of the calculation in order to get the additional flange moment $M_{z,Fl}$:

$$\sigma_{Ed} = 208 \text{ N/mm}^2$$

$$M_{z,fl} = 18433909 \text{ Nmm}$$

$$\frac{M_{z,Fl}}{M_{Fl,z,pl}} = 0,183$$

$$1,0 - \chi_{LT} = 1,0 - 0,796 = 0,204$$

$$0,183 \leq 0,204$$

so the assumption in Eq. (9.6) is again on the safe side.

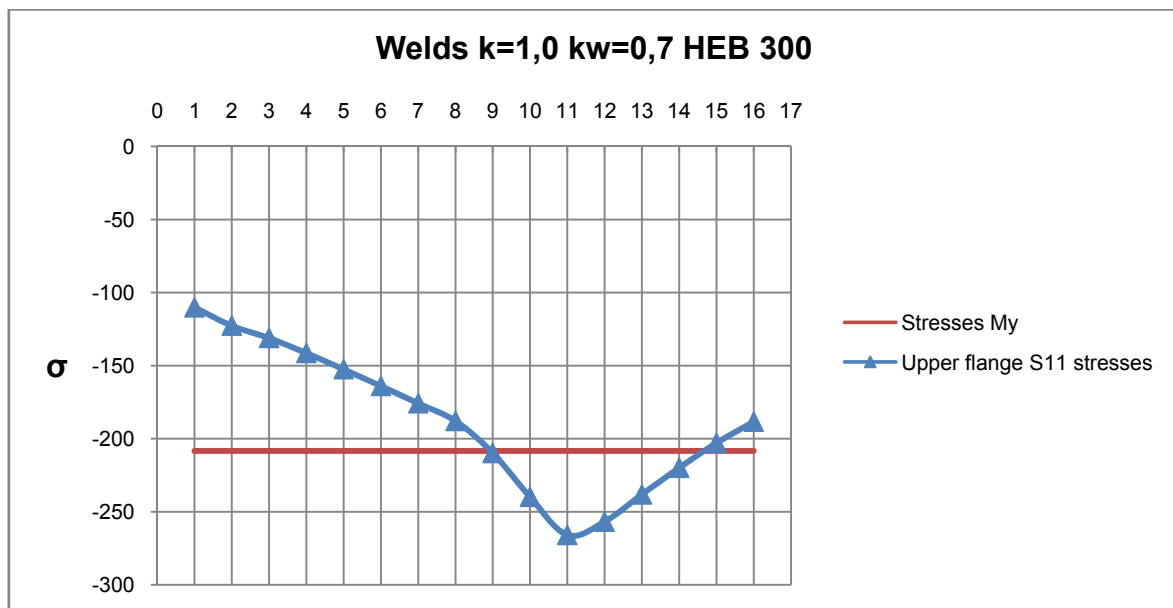


Fig. 96: S11 normal stress distribution of the upper flange under warping restraint (section HEB 300)

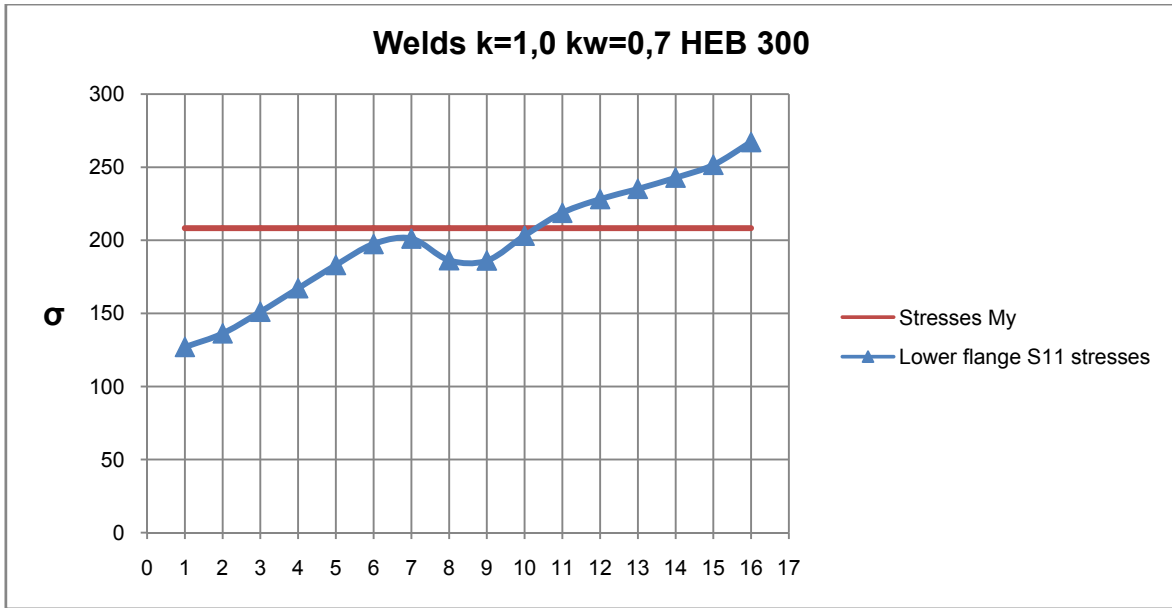


Fig. 97: S11 normal stress distribution of the lower flange under warping restraint (section HEB 300)

10. Summary and conclusions

The present thesis deals with the numerical modelling and analysis -through parametric studies- of the out-of-plane buckling behaviour of steel members (columns, beams and beam-columns) under realistic, non-hinged support conditions. The main objectives are the discussion of the flexural buckling of columns, lateral-torsional buckling of beams and the buckling failure of beam-columns. In every chapter the comparisons are presented between the GMNIA - or LBA- modelling results and the calculations according to the current EC3 design code for steel structures.

The descriptions and the most important conclusions of the chapters are summarized in the following list:

- I. Chapter 1 introduced the motivation of the work and identified the main objectives.
- II. In Chapter 2 the methodology of the numeric modelling and the used ABAQUS discretization are explained.
- III. In Chapter 3 many ways of calculation of the elastic critical moment are demonstrated and discussed. Based on the comparisons the use of simple, dedicated numerical programs - such as LTBeam - is highly recommended, because the warping fixation can be taken into account. The correct value of the critical elastic moment and the slenderness for lateral-torsional buckling gives – in most cases – a beneficial result contrary to the calculation with the factor of C_1 according to the codes.
- IV. Chapter 4 contains two parametric studies about the most simple type of buckling failure, flexural buckling about the weak axis. As result of the studies it can be stated that the EC3 buckling curves are very accurate also for support conditions $k=0,7$, and significant beneficial effect (for example: +30% in case of IPE 500 section) can be obtained in design if the real support conditions are taken into account. The numerical results have confirmed that the warping restraint does not have an influence on the flexural buckling strength.
- V. In the first part of chapter 5 several GMNIA results were compared from the point of view of effects of support and loading conditions on the lateral-torsional buckling behaviour. The restraint of rotation and warping at the end of the member increases the resistance to LTB. The higher the “level” of restraint (k/k_w from 1,0 to 0,5 is more restrained) is the higher the resistance to LTB is. Under non-uniform bending moment loading the resistance to LTB is higher compared to the case of uniform bending moment loading for the same member.

In the second part the EC3 LT-buckling curves were compared to the modelling results in many parametric studies. In most of the cases the modelling results are on the unconservative (safe) side of the buckling curves according to the building code EC3. Based on this results the buckling curves for members with double symmetric I cross-sections – which are valid under “fork conditions” ($k=1,0$ $k_w=1,0$) – can be used in practical design as long as the member slenderness for LTB is calculated “correctly” for the case of support condition $k=0,7$ $k_w=0,7$.

- VI. Chapter 6 focuses on the interaction concept, which is one of the methods for the design of beam-columns.

Under support condition $k=0,7$ $k_w=0,7$ the interaction curves according to EC3 are on the safe side and adaptable for practical design, because the GMNIA analyses have shown higher values for resistance than the EC3 rules would predict.

The magnitude of the beneficial effect of rotational and warping restraints depends on the loading condition (domination of compression or bending) and on the type of the failure (elasto-plastic buckling failure or plastic cross section failure)

The comparisons with EC3 have indicated in many cases that the refinement of the interaction curves, for example by the interaction factor k_{LT} could be necessary.

- VII. The overall concept is treated in Chapter 7, which is the other method for the design of beam-columns.

The values of resistance calculated according to EC3 were significantly unconservative (unsafe) compared to GMNIA results in the case $k=0,7$ $k_w=0,7$ with $\Psi=1,0$ for a more slender section IPE 500, thus based on these results the use of the overall concept/general method cannot generally be recommended for boundary conditions that differ from the end-fork condition.

In most of the cases with non-constant bending moment diagram the buckling resistance was clearly governed by χ_z , which was then in turn used (as the minimum value) as χ_{op} , thus the design resistance for out-of-plane buckling according to the overall concept were more conservative, than according to interaction concept, using the first method for the determination of χ_{op} and depending on the support and loading conditions of the case.

-
- VIII. Chapter 8 explains a new proposal for LT buckling curves for I-sections, developed at TU Graz, It was confirmed that the new formulation is more accurate than the current EC3 curves in describing the behaviour of beams failing in LT-buckling even for non-end-fork boundary conditions, especially for the constant bending moment diagram. For non-constant bending moment diagrams, an adaptation of the factor φ to different boundary conditions could be developed for certain common boundary condition cases, while the factor can always conservatively be set to 1.0 in other cases.
- IX. Finally, in Chapter 9 the additional bimoments in the end cross-sections were investigated in the case of $k=1,0$ $k_w=0,7$ (lateral-torsional buckling). The correct value of bimoment were defined based on the stress distribution of the flanges in the end section. In addition, a simple formula for calculation of bimoment depending on χ_{LT} have been proposed.

10.1. Outlook

The thesis work could represent a starting point for the following ideas and problems possible future research:

- Modelling of real support conditions (rotation and warping) as springs (not purely “rigid”, yet not purely “free”) for construction details (for example: column bases).
- The real buckling behaviour of structures as a part of portal frames could be investigated further, taking into account realistic connection detailing.
- The investigation of buckling behaviour of members with intermediate or continuous lateral restraints on one or both flange and with real support conditions could be combined.
- A refinement of the interaction concept formulae for cases of real support conditions could be considered.
- The development of a simple and/or accurate formulation for the bimoment depending on the real support conditions and load cases should be carried out in order to also safely design the connections at the member ends if the beneficial effects of end fixations is used in out-of-plane buckling design.

11. References

1. **Simoès da Silva, L., Simoes, R. und Gervásio, H.** *Design of Steel Structures; ECCS Eurocode Design Manuals; Part 1-1-General rules and rules for buildings.* Berlin : Ernst und Sohn, 2010.
2. **Eurocode 3, ENV 1993-1-1.** *Eurocode 3. Design of steel structures. General rules and rules for buildings.* Brussels : CEN, 1992.
3. **Nasdala, L.** *FEM-Formelsammlung Statik und Dynamik.* München : Vieweg+Teubner, 2012.
4. **Dassault Systems/, Simulia.** *ABAQUS v. 6.10 Documentation.* Providence RI, USA , 2010.
5. **Graz University of Technology, Institute for Structural Analysis.** *Baustatik 2 Skriptum.* Graz , 2004.
6. **Werkle, H.** *Finite Elemente in der Baustatik.* Konstanz : Vieweg & Sohn, 2008.
7. **Beer, G.** *Introduction to nonlinear finite element analysis.* Graz : Graz University of Technology, Institute for Structural Analysis, 2004.
8. **ECCS.** *Ultimate Limit State Calculations of Sway Frames with Rigid Joints.* Brussels : Editor: Vogel U., European Convention for Constructional Steelwork - TC8, 1984.
9. **ÖNORM B, 1993-1-1.** *Eurocode 3: Design of steel structures - Part 1-1: General structural rules - National specifications concerning ÖNORM EN 1993-1-1, national comments and national supplements.* Wien : Austrian Standards Institute, 2007.
10. **Graz University of Technology, Institute for Steel Structures and Shell Structures.** *Stahlbau GL Skriptum.* Graz : s.n., 2011.
11. **CTICM, Centre Technique Industriel de la Construction Métrallique.** *LTBeam v. 1.0.10 Documentation.* Saint-Aubin, France : CTICM, 2010.
12. **Serna, M. A., et al.** *Equivalent uniform moment factors for lateral-torsional buckling of steel members.* Journal of Constructional Steel Research 62 pp. 566–580 : Elsevier, 2006.
13. **Eurocode 3, EN 1993-1-1.** *Eurocode 3. Design of steel structures. General rules and rules for buildings.* Brussels : CEN, 2005.
14. **Maqoi, R. und Rondal, J.** *Mise en Èquation des Nouvelles Courbes Européenned de Flambement.* Constuction Métrallique, No.1., pp. 17-30. , 1978.

-
15. **Beer, H. und Schultz, G.** *Die Taglast des planmäßig mittig gedrückten Stabes mit Imperfektionen.* VDI-Zeitschrift 21 pp. 1537-1541, 1683-1687, 1767-1772 , 1969.
 16. **Taras, A.** *Contribution to the Development of Consistent Stability Design Rules for Steel Members.* Graz : PhD thesis, Graz University of Technology, Institute for Steel Structures and Shell Structures, 2011.
 17. **Snijder, H.H. und Hoenderkamp, M.C.M.** *Buckling Curves for Lateral-Torsional Buckling of Unrestrained Beams.* Festschrift for René Maquoi, pp. 239-248, Liege , 2008.
 18. **Simoes da Silva, L., Marques, L. und Rebelo, C.** *Numerical validation of the general method in EC3-1-1 for prismatic members.* Journal of Constructional Steel Research 66 pp. 575-590 : Elsevier, 2010.
 19. **Greiner, R. und Lindner, J.** *Interaction formulae for members subjected to bending and axial compression in EUROCODE 3—the Method 2 approach.* Journal of Constructional Steel Research 62 pp. 757-770 : Elsevier, 2005.
 20. **Kaim, P.** *Spatial buckling behaviour of steel members under bending and compression.* Graz : PhD thesis, Graz University of Technology, Institute for Steel Structures and Shell Structures, 2004.
 21. **Petersen, Ch.** *Statik und Stabilität der Baukonstruktionen.* Braunschweig : Vieweg & Sohn, 1982.
 22. **Krüger, U.** *Stahlbau Teil 2- Stabilität und Theorie II. Ordnung.* Berlin : Ernst & Sohn, 2008.
 23. **Graz University of Technology, Institute for Steel Structures and Shell Structures.** *Konstruktionen in Stahl Skriptum.* Graz , 2011.
 24. **Graz University of Technology, Institute for Steel Structures and Shell Structures.** *Stahlbau Skriptum.* Graz , 2011.
 25. **ESDEP, European Steel Design Education Programme.** ESDEP Course. [Online] 1993. [Zitat vom: 05. 03 2012.] <http://www.fgg.uni-lj.si/kmk/esdep/master/toc.htm>.